Balancing Growth in a Warming World

Preliminary

Adrien Bilal* *Stanford University*
Thibault Ingrand† *Stanford University*
Diego R. Känzig‡ *Northwestern University*

March, 2026

Abstract

This paper develops a theory of balanced growth and optimal climate policy in an integrated assessment framework. Climate damages drag down long-run growth in the laissez-faire. Two distinct policy regimes emerge because physical balance equations imply a unit root in carbon accumulation. At low damages, optimal growth coincides with the laissez-faire, and the carbon externality is priced at a constant rate. At high damages, growth is slower in the laissez-faire, and optimal policy prices carbon at an increasing rate that caps temperature growth to prevent escalating losses. We quantify our model with multiple damage functions. Under conventional damage estimates, the economy remains in the low-damage regime. Optimal policy achieves a 1% welfare gain with 3°C of additional warming by 2100. By contrast, under larger estimates exploiting global temperature variation, the economy is in the high-damage regime. Optimal policy raises annual growth by 0.8 percentage points and caps additional warming by 2100 to 0.4°C for a 26% welfare gain. Despite a standard cost-benefit welfare criterion, the combination of economic growth and permanent carbon accumulation delivers a 2100 temperature target of 1.4°C above pre-industrial levels.

JEL classification: E23, H23, O44, Q54, Q56, Q58

Keywords: Climate change, optimal policy, balanced growth, social cost of carbon, integrated assessment

*Stanford University, CEPR and NBER. E-mail: adrienbilal@stanford.edu. Web: www.sites.google.com/site/adrienbilal

†Stanford University. E-mail: ingrand@stanford.edu

‡Northwestern University, CEPR and NBER. E-mail: dkaenzig@northwestern.edu. Web: www.diegokaenzig.com

Introduction

Climate policy is largely built on the presumption that a backstop technology will eventually emerge or that fossil fuels will run out: at some point in the future, cheap and emissions-free energy will replace fossil fuels, carbon capture and storage will become economically viable at scale, or there will be no more fossil fuels to extract. The dominant paradigm in climate economics based on integrated assessment models relies on these assumptions in one form or another to ensure that emissions and temperatures eventually stabilize.

But what if the premise of this argument does not hold? Clean energy may not displace all fossil fuels. Carbon capture may remain costly. Known fossil fuel reserves embed nearly 10°C of additional warming. More reserves may still be discovered. Temperatures may therefore continue to rise for centuries, with possibly escalating climate impacts. Is sustained economic growth even possible in such a continuously warming world? And if so, what do growing economic activity and temperatures imply for policy?

This paper develops a theory of growth and optimal climate policy in an integrated assessment model when both the economy and temperature may increase for the foreseeable future. We show that this possibility fundamentally alters positive and normative implications because greenhouse gas accumulation follows a unit root process and economic losses can escalate. Balanced growth is possible, but climate damages drag it down. Two distinct regimes arise depending on the severity of climate damages. Low damages imply that long-run growth coincides in the laissez-faire and optimal allocations, and optimal policy prices the carbon externality at a constant rate. High damages imply that growth is slower in the laissez-faire, and optimal policy prices carbon at an increasing rate that stabilizes temperature growth to achieve faster economic growth. In our quantitative analysis, we show that existing empirical damage estimates span both regimes. Under lower damages based on local temperature variation, optimal policy leaves the long-run growth rate unchanged and raises welfare by 1%. Under higher damages based on global temperature variation, optimal policy increases long-run growth by 0.8 percentage points (p.p.) annually and raises welfare by 26%. Warming continues in both cases, but seven times slower under higher damages. At large damages, the combination of economic growth and permanent carbon accumulation thus delivers a 2100 temperature target of 1.4°C above pre-industrial levels.

Our analysis starts from the canonical integrated assessment framework (Nordhaus,

1992, 2013; Golosov et al., 2014), which we extend with a multi-sink and multi-layer climate system (Folini et al., 2024). A representative household consumes and saves. A representative firm produces output using capital, labor, and energy. The productivity of the firm has two components: an exogenously growing component reflecting technological progress, and an endogenous component that represents climate impacts and depends on temperatures in possibly all layers, for instance the atmosphere and the upper ocean. A competitive sector extracts energy at a time-varying cost that reflects technological progress or changes in resource scarcity. Energy leads to carbon emissions at a time-varying intensity that reflects improvements in renewables.

The climate system allows for an arbitrary number of carbon sinks and temperature layers as long as they satisfy mass and thermal energy conservation. Carbon emissions are distributed into atmospheric and oceanic sinks, leading to warming in atmospheric and oceanic layers. Our key departure from standard analyses is that we do not impose the existence of a backstop technology. Instead, we allow temperatures to grow for the foreseeable future.

We first characterize balanced growth absent policy intervention. Balanced growth emerges under two conditions that link economic activity and the climate system. First, log output losses are at most linear in temperature, consistent with standard econometric formulations (Dell et al., 2012; Bilal and Känzig, 2025) and canonical integrated assessment models (Nordhaus, 1992, 2013). Second, temperatures depend on log carbon concentrations, consistent with the geoscientific literature and Beer-Lambert saturation (Myhre et al., 1998; Dietz et al., 2021; Barrage and Nordhaus, 2024a; Folini et al., 2024).

When progress in carbon-saving technologies is sufficiently fast relative to productivity growth, temperatures stabilize in the long run and the economy converges asymptotically to an economy with an effective backstop technology. We focus on the opposite region of the parameter space where emissions keep growing over time.

Our analysis uncovers an optimal policy regime switch that depends on the magnitude of climate damages. In each regime, a simple formula links output growth to a small number of parameters, most importantly the parameter governing climate damages. When climate damages are below a critical threshold, long-run economic and temperature growth coincide in the laissez-faire and in the optimal allocation. This threshold is decreasing in productivity growth and in the climate sensitivity, and additionally depends on the rate of time preference, the energy share and the rates of transfer between

carbon sinks and temperature layers. Optimal policy prices carbon at a constant rate that only affects the level of economic activity and emissions, not its growth over time. Despite growing emissions and temperatures that drag down growth, optimal policy in this low damage regime behaves similarly to the case in which temperatures stabilize in the long run.

Once climate damages exceed the critical threshold, optimal policy changes qualitatively. The present value of future losses per unit of energy use is increasing in damages and in the growth rate of emissions: damages depend on the *stock* of atmospheric carbon, which is larger given the current *flow* of emissions when the emissions growth rate is larger. In contrast to the laissez-faire, the planner internalizes this dynamic present value, which can exceed the static marginal product of energy when damages are high and emissions would otherwise grow rapidly.

Thus, at high damages the optimal allocation caps emissions and temperature growth. This choice achieves strictly faster growth than in the laissez-faire because it avoids escalating damages due to the permanent accumulation of carbon in the atmosphere. Pricing carbon at an increasing rate over time decentralizes this optimal allocation.

Our analysis delivers a cap on temperature growth, despite relying on entirely standard cost-benefit tools and without appealing to a precautionary principle. The cap emerges as an optimal policy because carbon is a unit root process whose accumulation leads the dynamic marginal cost of energy use to exceed its static marginal product when emissions grow fast.

How robust are our conclusions to alternative specifications of our framework? We examine a range of variants. First, our results hold for utility functions of the Constant Relative Risk Aversion (CRRA) class, when population grows over time, and regardless of the details of the climate system. Second, they continue to hold when extraction costs are paid in labor units. Third, they hold when energy stocks are dynamically managed as in Hotelling (1931), and exploration is possible at a cost that endogenously rises to reflect scarcity due to past cumulative energy use. Fourth, they hold when we endogenize technological growth through innovation as in Grossman and Helpman (1991) and Aghion and Howitt (1992). Fifth, they hold when we microfound extraction costs and emissions intensity of energy with a bundle of emissions-intensive and renewable sources, with endogenous growth through innovation in renewables. While the exact formulas for long-run growth rates of course differ somewhat across all these specifications, the change of

regime with an emissions and temperature growth cap when damages exceed a threshold is a common and general feature of all these extensions.

The magnitude of climate damages thus determines the properties of optimal policy. But does the *shape* of the damage functions also matter? Our baseline analysis takes place with a log-linear damage function. Yet, many formulations have been proposed in the literature, with varying degrees of nonlinearity and empirical support.

We develop a classification of damage functions to characterize how their degree of nonlinearity affects long run growth. We show that the degree of nonlinearity of the *logarithm* of the damage function is the relevant metric for long run climate impacts on growth—because technological growth is exponential—not the degree of nonlinearity of the *level* of the damage function.

For log-concave damage functions for which proportional losses grow less than linearly with temperature—and that may capture unmodeled adaptation—as in Nordhaus (1992, 2013) and Barrage and Nordhaus (2024a), economic growth and the climate are independent in the long run. For log-convex damage functions for which proportional losses grow faster than linearly with temperature—and that may capture tipping points—as in Acemoglu et al. (2012) and Golosov et al. (2014), damages escalate too fast for balanced growth and the economy grinds to a halt. In this case, optimal policy continues to be split in two regimes, but asymptotic growth rates are independent of the magnitude of damages.

Log-linear damage functions thus offer a conceptual advantage: they deliver an informative intermediate case in which climate impacts depend continuously on damage function parameters. They also offer a practical advantage: they correspond to the majority of formulations that have been estimated in practice. Therefore, we use our baseline log-linear damage function in our quantitative implementation.

We quantify the gains from optimal carbon policy in a parametrization that represents the world economy. We use standard values for the capital and energy shares in production and the capital depreciation rate. We set the rate of time preference to 3% annually. We estimate annual population growth at 1.4% annually. We use the parametrization of the climate system from Folini et al. (2024) that matches Coupled Model Intercomparison Project (CMIP) simulations from large-scale global circulation models at high and low frequencies. We estimate progress in carbon saving technologies and fossil fuel extraction costs from the static equations of the model: we match growth in carbon emissions

relative to energy use and fossil fuel use over the last four decades.

Finally, we estimate exogenous productivity growth by matching output growth over the last four decades. Crucially, the climate system is still far from the balanced growth path, implying that we cannot use balanced growth equations for estimation. Therefore, we initialize the model to 1982 data and search for productivity growth that generates transitional dynamics that reproduce output growth in the data up to 2019. We do so separately for alternative climate damage specifications.

We consider two possibilities for the magnitude of climate damages. We start by considering conventional empirical damage estimates based on local temperature variation (Dell et al., 2012; Burke et al., 2015), without assuming growth effects. We use the local temperature estimates from Bilal and Känzig (2025) that incorporate the empirical degree of persistence, whereby a 1°C increase in atmospheric temperature implies a 3.6% reduction in productivity in the long run. In this case, the economy remains in the low damage regime: laissez-faire and optimal output growth coincide at 3.1%. Optimal carbon pricing temporarily delays emissions without affecting their long-run growth rate, so that 2100 temperatures rise by an additional 1.5°C rather than 2.2°C relative to 2020. Thereafter, temperatures rise by 3°C per century. The optimal policy leads to a 1.2% consumption-equivalent welfare gain, which reflects the modest magnitude of the damage function.

Second, we consider damage estimates based on global temperature variation, whereby a 1°C increase in atmospheric temperature implies a 25% reduction in productivity in the long run (Bilal and Känzig, 2025). In that case, the economy is in the high damage regime. While the economy keeps growing in the laissez-faire, long-run optimal growth is 0.8 percentage point higher, at 3.2% compared with 2.4%. These growth benefits only materialize after the first forty years, during which they are offset by higher energy costs. Optimal carbon pricing permanently caps the growth rate of emissions, leading to slower temperature growth in the short and long run. Thus, warming by 2100 is limited to an additional 0.4°C relative to 2020. Thereafter, temperatures rise by 0.4°C per century. The optimal policy delivers a 26% consumption-equivalent welfare gain that reflects the larger magnitude of climate damages and the resulting externality, together with the qualitatively different policy response that caps temperature growth.

Our results indicate that welfare gains from optimal policy grow more than one-for-one with climate damages: damages based on global temperature are seven times larger than damages based on local temperature, yet the planner achieves welfare gains that

are twenty-two times larger. When damages are low, the laissez-faire is close to the no-damage efficient economy, so that reallocation by the planner delivers only second order gains against first order direct losses. By contrast, when damages are large, reallocation gains become comparable to direct losses. The planner achieves larger relative welfare gains that can offset half of the direct losses from climate change.

Related literature. This paper relates to several strands of the literature. First, it contributes to the integrated assessment literature that studies optimal climate policy (Nordhaus, 1992, 2013; Acemoglu et al., 2012; Golosov et al., 2014; Barrage and Nordhaus, 2024a). Most of this literature assumes that temperatures stabilize in the long run due to some combination of a backstop technology, no technological progress, or scarce fossil fuel reserves. Even if fossil fuel reserves are ultimately finite, from a practical perspective they are effectively infinite once coal is included (Hassler et al., 2016). Temperatures might gradually rise for multiple centuries—longer than the world economy has been sustaining growth for. We characterize the conditions that lead to balanced growth in such a scenario. We uncover an optimal policy regime switch which we link to a small number of parameters.[1]

Second, our analysis reveals that balanced growth arises in the laissez-faire only when certain physical and economic scaling laws hold. We build on Myhre et al. (1998), Dietz et al. (2021), and Folini et al. (2024) to incorporate a rich climate system that matches CMIP simulations at high and low frequencies. It links atmospheric forcing—and thus, temperature—to the log carbon stock due to the Beer-Lambert absorption law. Our damage function takes a standard functional form linking log output losses to the level of temperature that directly maps into existing empirical estimates (Dell et al., 2012; Burke et al., 2015; Nath et al., 2024; Bilal and Känzig, 2025). By contrast, when log output losses are asymptotically log-linear in temperature as assumed in Nordhaus (1992, 2013), growth and the climate are independent in the long run. When log output losses depend linearly on the level of carbon concentrations—or, equivalently, log output losses are exponential in temperature—as in Acemoglu et al. (2012) and Golosov et al. (2014), growth is sub-exponential or is not even possible in the laissez-faire.

[1] Brock and Taylor (2010) characterize balanced growth in a model with emissions but do not incorporate a climate feedback through damages that is central to our analysis.

1 A Model of Growth with Climate Change

1.1 Economic Module

The economic module of our framework is a simple extension of the neoclassical growth model (Koopmans, 1963; Cass, 1965) with energy use, similarly to Golosov et al. (2014). Time is continuous and runs forever.

Preferences. There is a unit continuum of infinitely-lived identical households who populate the world economy. Households have CRRA flow preferences: $U(C) = \frac{C^{1-\gamma}-1}{1-\gamma}$. For ease of exposition, in the main text we focus on logarithmic utility $\gamma = 1$, and report our results under general CRRA utility in the Appendix. Labor supply is exogenous and set to $L_t = 1$. The pure rate of time preference of households is ρ. Intertemporal preferences are given by: $\int_0^\infty e^{-\rho t} U(C_t) dt$.

Final good sector. Firms in the final good sector produce according to a Cobb-Douglas production function. They use capital, labor and energy, with time-dependent TFP Z_t:

$$Y_t = \left(K_t^\alpha (Z_t L_t)^{1-\alpha}\right)^{1-\psi} E_t^\psi \equiv F(Z_t, K_t, L_t, E_t). \tag{1}$$

The path of productivity Z_t is perfectly foreseen and endogenous to the climate module.

Energy sector. Firms in the energy sector extract energy at an exogenous time-varying unit cost χ_t paid in units of the final good. This formulation is isomorphic to one in which energy is produced with the same production function as final goods, with relative total factor productivity χ_t. We show this equivalence in Appendix A.1.

Markets. All factor markets—capital, labor and energy—are perfectly competitive. All goods markets—final good and energy—are perfectly competitive. The final good is the numeraire. Households earn wages w_t from the labor they supply to firms in the final good sector. Households own claims to firms and capital K_t, which they rent out to firms for production at net interest rate r_t. K_0 denotes their initial capital endowment.

Resource and budget constraints. The resource constraint of the economy is: $C_t + \dot{K}_t = Y_t - \delta K_t - \chi_t E_t$. Firms make zero profits given constant returns to scale and perfect competition, implying that profits drop out of the household budget constraint: $C_t + \dot{K}_t = w_t + r_t K_t$.

1.2 Climate Module

Emissions. Energy use E_t generates greenhouse gas emissions E_t^m. For expositional simplicity, we label greenhouse gases "carbon dioxide." Carbon intensity σ_t varies exogenously over time:

$$E_t^m = \sigma_t E_t. \tag{2}$$

In Appendix A.2, we propose a simple microfoundation for time-varying carbon intensity when energy bundles two primary energy sources: emissions-free renewables and emissions-intensive fossil fuels. In that case, technological progress in either or both sectors leads to time-varying emissions intensity. If technology progresses faster in the renewable sector, carbon intensity declines over time.

Carbon cycle. The climate module describes the dynamics of carbon concentration in the environment. We consider a state-of-the-art small-scale climate model with multiple sinks. In our quantitative application, we will use three sinks: the atmosphere, the upper ocean and the lower ocean (Folini et al., 2024). However, our theoretical analysis accommodates any number of sinks $\mathcal{M}$. The carbon cycle ensures that mass is conserved. Carbon emissions first enter the atmosphere and then gradually mix into both ocean layers.

Let $\mathbf{M}$ be the vector of carbon concentrations across the $\mathcal{M}$ sinks. The dynamics of carbon concentrations $\mathbf{M}$ are given by:

$$\dot{\mathbf{M}}_t = \mathbf{A}\mathbf{M}_t + E_t^m \mathbf{m}, \tag{3}$$

where $\mathbf{m}$ is a constant vector that encodes how emissions enter carbon sinks. For instance, in our quantitative application with three sinks, we have: $\mathbf{m} = (1, 0, 0)'$ to ensure that emissions enter through the atmosphere before mixing into the ocean sinks.

The matrix $\mathbf{A}$ encodes the physical features of carbon mixing. Carbon conservation requires: $\sum_j A_{ij} = 0$ for all i. Carbon mixing requires: $A_{ij} \geq 0$ for $i \neq j$ and that $\mathbf{A}$ be irreducible (all sinks are connected at least indirectly). Together, these properties ensure that $\mathbf{A}$ is an irreducible continuous time Markov chain generator: zero is an eigenvalue of $\mathbf{A}$ and all other eigenvalues have strictly negative real parts. Our theoretical analysis only relies on these properties. Appendix A.3 describes the exact structure of the carbon

cycle matrix $\mathbf{A}$ that we use for our quantitative analysis.

Warming. The warming module describes how carbon concentrations map into temperatures. We use a general formulation of the module in Geoffroy et al. (2013). In our quantitative application, we will again follow Folini et al. (2024) and consider two temperature layers: an upper layer consisting of the atmosphere and ocean surfaces, and a lower layer consisting of the deep ocean. However, our theoretical analysis accommodates any number of layers $\mathcal{T} \leq \mathcal{M}$, which need not coincide with carbon sinks.

Let $\mathbf{T}$ be the vector of temperatures across layers. Its dynamics follow:

$$\mathbf{C}\dot{\mathbf{T}}_t = (\mathbf{D} - \mathbf{L})\mathbf{T}_t + \mathbf{F}_{eq} + \mathbf{F}_t. \tag{4}$$

The matrix $\mathbf{C}$ is diagonal, with strictly positive diagonal entries that contain the thermal capacities of each temperature layer. The thermal capacity of a layer measures how much heat it can store, and therefore how much a given temperature difference with adjacent layers warms it. For instance, the thermal capacity of the ocean is larger than that of the atmosphere.

The heat exchange matrix $\mathbf{D}$ ensures that energy is conserved when energy is exchanged between temperature layers, after accounting for their respective thermal capacities, and that all layers are at least indirectly connected. These physical properties require that $\mathbf{D}$ satisfies the same properties as the carbon exchange matrix $\mathbf{A}$: $\sum_j D_{ij} = 0$ for all i, that $D_{ij} \geq 0$ for all $i \neq j$, and that $\mathbf{D}$ is irreducible. Standard results then imply that $\mathbf{D}$ has a single zero eigenvalue, and all other eigenvalues have strictly negative real parts.

The heat loss matrix $\mathbf{L}$ captures that energy is radiated back to outer space. When the entire atmosphere is a layer, then only the atmosphere radiates energy to outer space. Our formulation allows us to disaggregate the atmosphere into multiple regional layers, each potentially radiating energy back to outer space. To encode these properties, $\mathbf{L}$ is diagonal with weakly positive entries, and at least one strictly positive entry.

The vector $\mathbf{F}_{eq} + \mathbf{F}_t$ denotes total radiative forcing—the amount of energy that each layer receives. $\mathbf{F}_{eq}$ represents natural radiative forcing across all layers, for instance in the atmosphere and in the deep ocean.[2] $\mathbf{F}_t$ represents the additional forcing coming from

[2]Deep ocean radiative forcing partly stands in for the thermohaline circulation that cools the deep ocean through the sinking of colder, less saline water at the poles. Appendix A.5 shows that the quantitative properties of our climate module are virtually unchanged once we endogenize the thermohaline circulation

carbon emissions in the atmosphere since the pre-industrial era. Following Myhre et al. (1998), it satisfies:

$$\mathbf{F}_t = \mathbf{H}\Big(\log \mathbf{M}_t - \log \mathbf{M}_{eq}\Big), \tag{5}$$

where $\mathbf{H}$ is a rectangular $\mathcal{T} \times \mathcal{M}$ matrix that encapsulates the greenhouse effect: it contains the semi-elasticity of radiative forcing to carbon emissions. The log function applies element-wise. $\mathbf{M}_{eq}$ denotes the carbon concentration in the atmosphere in the pre-industrial era. In what follows, we refer to the property that forcing scales with the logarithm of carbon concentrations as 'Beer-Lambert' scaling, in reference to the Beer–Lambert law from radiative transfer that underpins equation (5).

Without loss of generality, we order all layers with atmospheric layers first, and then ocean layers. $\mathbf{H}$ is then diagonal-rectangular and captures how much radiative forcing increases following a doubling of carbon dioxide concentrations. We denote by $\mathbf{h}$ the $\mathcal{T} \times 1$ vector that collects the diagonal entries of $\mathbf{H}$ in its left $\mathcal{T} \times \mathcal{T}$ block. For instance, $\mathbf{h}$ has positive entries for each atmospheric layer, and null entries for each deep ocean layer.

We rewrite the warming layer more compactly:

$$\dot{\mathbf{T}}_t = \mathbf{B}\mathbf{T}_t + \mathbf{N}(\mathbf{F}_{eq} + \mathbf{F}_t). \tag{6}$$

with $\mathbf{B} = \mathbf{C}^{-1}(\mathbf{D} - \mathbf{L})$ and $\mathbf{N} = \mathbf{C}^{-1}$. $\mathbf{B}$ is then a Metzler matrix with $\mathbf{D}$ irreducible. Hence all its eigenvalues have strictly negative real parts. $\mathbf{N}$ is diagonal with strictly positive entries. Our theoretical analysis only relies on these properties. Appendix A.4 describes the exact structure of the heat exchange matrix $\mathbf{B}$ and the forcing vector $\mathbf{N}$ that we use for our quantitative analysis.

1.3 Climate damages

The economic module and the climate module are coupled through climate damages. Total factor productivity depends on an exogenous component $\overline{Z}_t$ and an endogenous component that depends on atmospheric temperature relative to its preindustrial level:

$$Z_t = \overline{Z}_t \exp\left(-\boldsymbol{\zeta}'\left(\mathbf{T}_t - \mathbf{T}_{eq}\right)\right). \tag{7}$$

and recalibrate our system to match CMIP simulations as in Folini et al. (2024).

The structural damage function $\boldsymbol{\zeta} \in \mathbb{R}^{\mathcal{T}\times 1}$ governs the sensitivity of productivity to temperature across all layers. Our formulation is consistent with empirical evidence that it features 'level effects' (Bilal and Känzig, 2025). Although damages operate through level effects and do not permanently reduce the growth rate, they generate widening output losses over time in a growing economy.

In our quantitative application, we use a formulation of the damage function that incorporates persistent level effects: $Z_t = \overline{Z}_t \exp\left(-\int_0^t \boldsymbol{\zeta}_s'(\mathbf{T}_{t-s} - \mathbf{T}_{eq})ds\right)$. Our theoretical results extend immediately to this case provided we formulate them using the cumulative damage function. However, this extension comes at the cost of additional notation, which we abstract from for clarity of exposition in the main text.

1.4 Population Growth

We specify our baseline framework with a fixed population for expositional simplicity. However, it immediately accommodates population growth. Suppose that instead of staying constant, population L_t grows at rate n, so that $L_t = e^{nt}$. Appendix A.6 shows how to rescale the economy with population growth so that it is isomorphic to our baseline economy in per capita variables.

Including population growth requires three modifications to the per capita framework. First, we shift the rate of time preference to $\rho - n$: larger future population makes dynasties effectively more patient. Second, we shift the capital depreciation rate to $\delta + n$: population growth dilutes capital per capita.

To describe the third modification, denote by g_σ the rate of progress in the emissions intensity of energy in the economy with a growing population, $\sigma_t = e^{-g_\sigma t}$. The third modification is to shift this rate of progress to $g_\sigma - n$ for per capita emissions: population growth increases total emissions intensity of per capita emissions. With these three modifications, population growth leaves our entire analysis unchanged.

2 Balanced Growth in a Warming World

We now analyze whether balanced growth is possible and efficient in the presence of climate change. We start our analysis with the laissez-faire, before moving the planner's allocation.

2.1 Laissez-Faire

In the laissez-faire (decentralized equilibrium), households maximize the present value of discounted utility from consumption taking prices $\{r_t, w_t\}_t$ as given:

$$\max_{\{C_t, K_t\}_t} \int_0^\infty e^{-\rho t} U(C_t) dt \qquad \text{subject to} \qquad C_t + \dot{K}_t = r_t K_t + w_t,$$

with K_0 given. Firms in the final good sector maximize profits taking productivity $\{Z_t\}_t$ and prices $\{r_t, w_t, p_t\}_t$ as given:

$$\max_{K_t^D, L_t^D, E_t} F(Z_t, K_t^D, L_t^D, E_t) - (r_t + \delta) K_t^D - w_t L_t^D - p_t E_t.$$

Firms in the energy sector extract energy competitively, implying that the price of energy satisfies $p_t = \chi_t$. Capital and labor markets clear: $K_t^D = K_t$ and $L_t^D = 1$.

Emissions E_t^m are related to energy use according to (2). Carbon concentrations $\mathbf{M}_t$ evolve according to (3), temperatures $\mathbf{T}_t$ evolve according to (6) and forcing F_t follows (5). Productivity Z_t evolves according to (7).

The equilibrium conditions in the laissez-faire are standard. The Euler equation writes: $\gamma C_t / C_t = F_K(Z_t, K_t, L_t, E_t) - \delta - \rho$, where we denote partial derivatives with subscripts, for instance: $F_K \equiv \partial F / \partial K$. Together with perfect competition and market clearing, capital and labor demand from the final good firms implies: $r_t + \delta = F_K(Z_t, K_t, L_t, E_t)$ and $w_t = F_L(Z_t, K_t, L_t, E_t)$.

The central equilibrium condition in the laissez-faire is energy demand:

$$F_E(Z_t, K_t, L_t, E_t) = \chi_t. \tag{8}$$

Firms do not internalize that energy demand today affects productivity today and in the future due to carbon emissions and climate damages. They only take the current energy price into account. This is the only condition that will differ from the social planning allocation.

We now impose that the technology grows at rate g: $\overline{Z}_t = Z_0 e^{gt}$; that extraction costs χ_t grow at constant rate g_χ: $\chi_t = \chi_0 e^{g_\chi t}$; and that emissions intensity of emissions grows at rate g_σ: $\sigma_t = \sigma_0 e^{g_\sigma t}$. These growth rates can be positive or negative. Before stating our main results, we define a few useful concepts for reference.

Asymptotic Constant Growth Path. In an asymptotic constant growth path, all variables except temperatures asymptotically grow at constant exponential rates. An asymptotic constant growth path is unique if the growth rates do not depend on initial conditions.

Balanced Growth Path. A balanced growth path is an asymptotic constant growth path in which the ratios K_t/Y_t, $\chi_t E_t/Y_t$ are constant over time.

We exclude temperatures from our definition of an asymptotic growth path because their dynamics will differ substantially across cases.

We are interested in how this balanced growth path depends on the parameters that govern the economy and the climate system. We can summarize these comparative statics with four key objects.

The first object is the energy share adjusted by the value-added share, defined as:

$$\pi = \frac{\psi}{(1-\alpha)(1-\psi)}.$$

The larger π, the more important energy is in production relative to labor, which is the scarce factor.

The second object is the growth rate of carbon savings, defined as:

$$\omega = g_\sigma + (1+\pi)g_\chi.$$

ω is higher if there is faster growth in carbon-saving technologies g_σ. It is also higher if there is faster growth in energy extraction costs g_χ, which lowers the carbon intensity of production as mediated by the energy share π.

The third object is the long-run elasticity of climate damages to emissions, defined as:

$$\Delta = \boldsymbol{\zeta}'(\mathbf{L}-\mathbf{D})^{-1}\mathbf{h} > 0. \tag{9}$$

To gain intuition, consider a unidimensional climate system $\mathcal{M} = \mathcal{T} = 1$ with an instantaneous damage function (a Dirac mass at $s = 0$). In that case, $\mathbf{D} \equiv 0$, and $\mathbf{L} \equiv \lambda > 0$ is a scalar that captures energy losses to outer space. We then obtain: $\Delta = \frac{\zeta h}{\lambda}$. With the damage functions we consider in our calibration together with the climate system calibration from Folini et al. (2024), $\Delta = 0.14 - 1.03$.

In the unidimensional case, the long-run elasticity of damages to emissions depends

on three parameters. The first object is the cumulative damage function, ζ. When it is larger, a given temperature has larger economic impacts. The second object is the semi-elasticity of radiative forcing to atmospheric carbon concentrations, h. When it is larger, a given amount of atmospheric carbon leads to higher radiative forcing. The third parameter λ represents relative energy losses to outer space. When energy losses to outer space λ are larger, a given amount of forcing leads to lower atmospheric temperatures because more energy is radiated back to outer space.

The fourth object is the discounted long-run elasticity of climate damages to emissions, defined as:

$$\overline{\Delta} = \boldsymbol{\zeta}'(\rho\mathbf{C} + \mathbf{L} - \mathbf{D})^{-1}\mathbf{h} > 0. \tag{10}$$

With the damage functions we consider in our calibration together with the climate system calibration from Folini et al. (2024), $\overline{\Delta} = 0.13 - 0.93$.

Equation (9) generalizes this logic to a climate module of any dimensionality. Δ is strictly positive because $\mathbf{L} - \mathbf{D}$ is an irreducible non-singular M-matrix and therefore has a strictly positive inverse.

Proposition 1 (Growth in the Laissez-Faire)**.** *The laissez-faire admits a unique asymptotic constant growth path, which is also a balanced growth path. It satisfies:*

(i) If carbon savings grow faster than technology $g < \omega$:

Emissions fall $g_m = g - \omega < 0$, temperatures are constant, productivity grows at rate $g_Z = g$, and output grows at rate $g_Y = g - \pi g_\chi$.

(ii) If carbon savings grow as fast as technology $g = \omega$:

Emissions are constant $g_m = 0$, temperatures increase log-linearly, productivity grows at rate $g_Z = g$, and output grows at rate $g_Y = g - \pi g_\chi$.

(iii) If carbon savings grow slower than technology $g > \omega$:

Emissions grow at rate $g_m = \frac{g-\omega}{1+\Delta} > 0$, temperatures grow linearly with slopes $g_m\boldsymbol{\theta}$, $\boldsymbol{\theta} = (\mathbf{L} - \mathbf{D})^{-1}\mathbf{h} \geq 0$ with at least one strictly positive entry, productivity grows at rate $g_Z = g - \Delta g_m$, and output grows at rate $g_Y = \frac{g+(\Delta-\pi)g_\chi+\Delta g_\sigma}{1+\Delta}$. In addition, output growth g_Y is decreasing in damages Δ, is positive if $g_\chi + g_\sigma > 0$, and is negative if $g_\chi + g_\sigma < 0$ and $\Delta > \left|\frac{g-\omega}{g_\chi+g_\sigma}\right| - 1$.

Proof. See Appendix B.1. □

Proposition 1 continues to hold as such under any CRRA utility function. The first case in Proposition 1 arises when carbon savings grow faster than production technology. Even though the economy would demand more energy over time because of higher productivity all else equal, two forces blunt the effect of rising energy demand on emissions. The first is reductions in emissions intensity that mechanically reduce atmospheric carbon. The second consists of a rising extraction cost—and thus, energy price—over time, which lowers energy demand enough if the energy share is high.

This first case is the asymptotic equivalent of the assumption of an exogenous backstop technology. Under these assumptions, the carbon intensity of production falls to zero, so that emissions fall over time. As a result, the atmospheric carbon converges to a constant, implying that temperatures stabilize. As a result, output growth is independent from climate damages. This case serves as a useful benchmark as our setting nests the case of a backstop technology, asymptotically.

The second case in Proposition 1 is the knife-edge situation in which carbon savings grow exactly as fast as production technology. Emissions are constant, and so temperatures increase log-linearly over time. This increase is too weak to accumulate and is dominated by exogenous productivity growth in the long run. From an economic perspective, this case resembles the first one, as climate damages do not affect long run economic activity.

These conclusions fail when carbon savings grow more slowly than exogenous productivity $\omega < g$. Over time, production requires more energy. The price of energy is not rising fast enough to blunt energy demand, and the emission intensity of energy is growing too slowly. As a result, emissions keep rising over time, implying that atmospheric carbon grows exponentially. Beer-Lambert scaling induces temperature to grow linearly.

Given the damage function, linearly rising temperatures drag down productivity growth proportionally to the long-run elasticity of damages to emissions, Δ, and to the growth rate of emissions. This drag on productivity growth feeds back to output growth, which is now weaker if damages Δ are larger.

In fact, Proposition 1 reveals that the economy does not need to always grow. When extraction costs rise and emissions intensity improves over time, emissions accumulate sufficiently slowly that output growth is positive.

However, the carbon externality can cause immiserizing growth. When extraction

costs fall rapidly over time, output would grow faster absent the carbon externality—as in the benchmark case. With the carbon externality, declines in energy costs can lead to an adverse feedback loop. Demand for energy grows so fast that carbon accumulates rapidly in the atmosphere. When damages Δ are large relative to technological progress, the economic impact of rising temperatures dominates and degrowth emerges.

We now turn to the social planning allocation.

2.2 Social Planner Allocation

In contrast to the laissez-faire, the social planner internalizes the global carbon externality and how it affects productivity. They solve:

$$\max_{\{C_t, K_t, E_t\}_t} \int_0^\infty e^{-\rho t} U(C_t) dt$$
$$\text{subject to } C_t + \dot{K}_t = F(Z_t, K_t, L_t, E_t) - \chi_t E_t$$
$$\text{and to equations (2), (3), (6), (5), (7).}$$

As we show in Appendix B.2, the only difference between the decentralized equilibrium and the planner's allocation arises in energy use. The planner's allocation satisfies:

$$F_E(Z_t, K_t, L_t, E_t) = \chi_t + \tau_t \qquad \tau_t = \frac{\sigma_t \boldsymbol{\mu}_t' \mathbf{m}}{u'(C_t)}. \tag{11}$$

The planner internalizes how energy use today affects productivity today and in the future through the climate system and climate damages. The social cost of energy τ_t depends on three objects. It rises with the carbon intensity of emissions: higher carbon intensity implies larger future damages from energy use today. The shadow cost falls with the marginal utility from consumption: lower marginal utility implies a lower valuation of output losses. Finally, the shadow cost increases with the planner's shadow value of an additional unit of carbon in each sink, $\boldsymbol{\mu}_t$.

The social cost of energy τ_t is related to the well-known concept of the social cost of carbon. The social cost of carbon evaluates the marginal damage from emitting one ton of carbon, and therefore adjusts the social cost of energy for its carbon content $\mathcal{S}_t = \tau_t / \sigma_t = \frac{\boldsymbol{\mu}_t' \mathbf{m}}{u'(C_t)}$. Efficient energy demand (11) immediately implies that τ_t is the energy tax that decentralizes the efficient allocation.

The dynamics of the planner's solution can differ qualitatively from the laissez-faire because of the social cost of energy τ_t. In general, τ_t can grow faster or more slowly than the extraction cost χ_t. Depending on which component dominates, energy use and climate dynamics differ in the long run, which feed back differently to the economy.

Proposition 2 (Efficient Growth)**.** *The solution to the planner's problem admits a unique asymptotic constant growth path. There exists a threshold $\overline{g}_m \in (0, +\infty]$ which is finite if and only if $\overline{\Delta} > \pi$, such that on the asymptotic constant growth path:*

(i) If carbon savings grow faster than technology net of damages $g \leq \omega + (1+\Delta)\overline{g}_m$:

Growth rates coincide with those in the laissez-faire from Proposition 1, and the allocation is a balanced growth path. On the growth path, the optimal energy tax that decentralizes the efficient allocation is a constant proportion of extraction costs.

(ii) If carbon savings grow more slowly than technology net damages $g > \omega + (1+\Delta)\overline{g}_m$:

Emissions grow at rate $\overline{g}_m$, temperatures grow linearly with slopes $\overline{g}_m \boldsymbol{\theta}$, $\boldsymbol{\theta} = (\mathbf{L} - \mathbf{D})^{-1}\mathbf{h} \geq 0$ with at least one strictly positive entry, productivity grows at rate $g_Z = g - \Delta\overline{g}_m$, and output grows at rate $g_Y = \frac{g+(\pi-\Delta)\overline{g}_m+\pi g_\sigma}{1+\pi}$. Output growth is higher in the planner's allocation than in the laissez-faire. On the growth path, the optimal energy tax that decentralizes the efficient allocation grows relative to the extraction cost.

Proof. See Appendix B.2. □

Proposition 4 in Appendix B.2 extends Proposition 2 to the CRRA case. Proposition 2 reveals that the structure of efficient growth paths is fundamentally different in the efficient allocation. When emissions fall over time, growth rates do coincide with the laissez-faire. This region of the parameter space is the analogue of a backstop technology, in which temperature stabilizes on its own in the long run. In that case, optimal policy only corrects the level of emissions, but not its long run growth rate.

In the intermediate region, emissions grow moderately over time: $\omega < g < \omega + (1 + \Delta)\overline{g}_m$. Long run growth rates continue to coincide with the laissez-faire. Despite climate change dragging down growth, the planner continues to solely correct the level of energy use. Carbon is not accumulating fast enough for temperature to rise rapidly enough to justify altering the long-run path of the economy.

However, an entirely different growth regime emerges in configurations in which emissions grow rapidly in the laissez-faire: $g > \omega + (1+\Delta)\overline{g}_m$. To understand why, consider a unidimensional climate system $\mathcal{M} = \mathcal{T} = 1$. In that case, on a constant growth path, the social cost of energy satisfies:

$$\tau_t = \frac{\zeta \nu h}{\rho + \lambda \nu} \frac{g_m}{\rho + g_m} \frac{Y_t}{E_t}, \tag{12}$$

where ν is the inverse thermal capacity and λ energy outflow. When the climate system is higher-dimensional, the social cost of energy continues to be proportional to output per unit of energy Y_t/E_t, and the proportionality factor aggregates the multidimensional climate dynamics and is given in equation (17), Appendix B.2.

The cost of energy increases with the damage function. It falls with thermal capacity ν, as higher ability to absorb forcing reduces warming. The cost of energy is a present value over the stream of future damages, and thus depends inversely on the rate of time preference ρ. When more heat radiates outward—a higher lambda λ—long-run temperature associated with emissions is lower, which leads to additional discounting. When the forcing is more sensitive to atmospheric carbon—a higher h—the social cost of energy is higher. Just as the marginal benefit from energy use, the social cost of energy scales with current economic activity relative to energy use.

The social cost of energy in equation (12) is reminiscent of the formula in Golosov et al. (2014), but features three important differences. The first difference is that our formula holds without additional assumptions on the savings rate, as the savings rate is always constant along the balanced growth path.

The second difference is that the social cost of energy is a constant proportion of output per unit of energy Y_t/E_t, rather than a constant proportion of output. This difference arises because our damage function is specified as a function of temperature instead of the carbon stock, and because temperature rises log-linearly with carbon in the long run due to Beer-Lambert scaling, not linearly: $T_t = h \log S_t + o(\log S_t)$. A linear relationship can be a valid approximation for small short-run changes in carbon concentrations. However, Beer-Lambert scaling corresponds to physical laws for larger changes such as a doubling of concentrations over the long run.

The structure of our damage function is consistent with empirical specifications used in the literature (Dell et al., 2012; Burke et al., 2015; Bilal and Känzig, 2025). By contrast and given Beer-Lambert scaling, the specification in Golosov et al. (2014) would be

equivalent to a super-exponential damage function: $Z_t = \exp\left(gt - \zeta \exp(T_t)\right)$. This specification implicitly imposes substantially more convex damages than existing empirical estimates and, as we discuss below, is incompatible with long-run growth.

This second difference due to Beer-Lambert scaling is key for the long run behavior of optimal carbon and energy pricing. Energy demand (11) immediately implies that, in the regime in which laissez-faire growth coincides with the planner's, the optimal energy tax is a constant fraction of extraction costs. By contrast, the super-exponential specification of Golosov et al. (2014) would imply that the energy tax becomes arbitrarily large relative to extraction costs.

The third and critical difference is that the social cost of energy is increasing in the growth rate of emissions through the ratio $\frac{g_m}{\rho+g_m}$. Faster emissions growth has two effects. First, it causes carbon—and thus, economic losses—to accumulate faster relative to current energy use. The marginal damage from a marginal unit of energy today is decreasing in the carbon stock M_t due to Beer-Lambert scaling, but is then more damaging relative to total energy use E_t. We express the social cost of energy τ_t with respect to energy use E_t rather than the carbon stock M_t because it corresponds to the relevant units for the marginal product of energy $F_E = \psi \frac{Y_t}{E_t}$. The numerator g_m encodes this force.

Second, faster emissions growth lowers the marginal warming potential of future emissions, again through Beer-Lambert scaling. Because this channel operates intertemporally on yet future emissions, it is additionally discounted: the denominator adds $\rho + g_m$.

On net, the social cost of energy is increasing in the growth rate of emissions g_m. When emissions growth is fast enough, the first effect—faster damage accumulation relative to current energy use—dominates, and the social cost of energy accounts for the entire marginal product of energy F_E. In that case, extraction costs become negligible in the long run relative to the social cost of energy.

In this qualitatively different regime, the growth rate of emissions is capped by the constraint $g_m = \overline{g}_m$, where $\overline{g}_m$ is such that the proportionality factor in the social cost of energy equals the energy elasticity of production. In the unidimensional climate system:

$$\pi = \frac{\zeta \nu h}{\rho + \lambda \nu} \frac{\overline{g}_m}{\rho + \overline{g}_m}. \tag{13}$$

Of course, equation (13) may not always have a solution if π is large. Whether there exists

a solution corresponds to the condition $\overline{\Delta} - \pi > 0$. Folini et al. (2024) suggest $\nu = 0.14$, $h = 4.98$ and $\lambda = 1.06$. In our calibration, we consider $\rho = 0.015$, $\zeta = 0.03 - 0.22$ and $\psi = 0.05$. In the one-dimensional climate system, the left-hand-side takes values $0.05 - 0.86$ and thus the condition is satisfied.

To assess whether the emissions growth cap is tight or loose relative to the data, we solve equation (13) and express the cap as:

$$\overline{g}_m = \frac{\rho}{\frac{\overline{\zeta}\nu h}{\psi(\rho+\lambda\nu)} - 1}. \tag{14}$$

Given the values discussed above, we obtain: $\overline{g}_m = 0.031 - 0.002$. In the data, the annual growth rate of emissions is close to 0.01. Thus, when damages are estimated from local temperature variation $\zeta = 0.03$, the emissions growth cap unlikely to bind, and long-run growth coincides in the laissez-faire and the efficient allocation. When damages are estimated from global temperature variation $\zeta = 0.22$, the emissions growth rate cap binds, and long run growth diverges between the laissez-faire and the efficient allocation.

2.3 Alternative Formulations

How specific are these results to our particular setup? We have shown that they do not depend on the details of the climate system as long as carbon and temperature dynamics are linear, and radiative forcing is log-linear in carbon concentrations. In this section we show that our results continue to hold when we consider three additional departures from our setup: extraction costs in labor units; dynamic energy resource management as in Hotelling (1931); and endogenous technological growth as in Grossman and Helpman (1991) and Aghion and Howitt (1992).

Extraction cost in labor units. So far we assumed that producing energy requires the same bundle of inputs as production of the final good. This assumption is a natural benchmark. Nevertheless, we also explore a more demanding formulation in which energy production only requires labor: $\chi_t E_t = L_t^E$, with $L_t = L_t^Y + L_t^E$. Because labor is the scarce factor, this formulation implies that the cost of energy rises faster than in our benchmark specification. Even then, our results continue to apply. The only modification is that emissions growth is given by $g_m = -(g_\chi + g_\sigma)$ in the laissez-faire, leaving the change of regime possible, albeit less likely.

Corollary 1 (Growth with Labor-Intensive Energy Production)**.** *Propositions 1 and 2 apply when energy production only requires labor, with the following modifications: the regime distinction is solely based on* $g_m = \min\{-(g_\chi + g_\sigma), \overline{g}_m\}$ *instead of* ω*, and* $g_Y = \frac{g - \pi g_\chi - \Delta \max\{g_m, 0\}}{1+\pi}$.

Proof. See Appendices B.1 and B.2. □

Appendices B.1 and B.2 extend 1 to CRRA utility.

Exhaustible resource management with exploration. So far we have abstracted from the dynamic management of energy stocks—for instance, fossil fuels. The optimal decision to extract or not affects the dynamics of energy prices, which may alter our conclusions. Of course, if there is a tight upper limit on how much energy can be extracted, carbon stocks and temperature eventually stabilize, and long run growth in the laissez-faire coincides with the efficient allocation. However, if potential energy sources are unbounded and exploration is possible, temperature may grow without bound.

We show that incorporating the dynamic management of an existing stock of energy resources as in Hotelling (1931) together with exploration leaves our results unchanged. We sketch the main elements in the main text, and relegate a complete description to Appendix B.3. Energy reserves R_t now evolve according to the difference between exploration X_t and energy use E_t: $\dot{R}_t = X_t - E_t$. Exploration comes at a cost that reflects the scarcity of energy: $\frac{\chi(S_t)}{2}\left(X_t/R_t\right)^2 R_t$, where S_t represents cumulative extraction and satisfies $\dot{S}_t = E_t$, and where $\chi(S_t) = \overline{\chi} S_t^\eta$.

To focus on the carbon externality, we require that households internalize that cumulative extraction affects exploration costs. A simple microfoundation is that each household owns energy fields and understands that more extraction implies higher costs. The rest of the economy is unchanged.

To avoid a lengthy discussion of cases, in the main text we require three mild restrictions that are consistent with the data. First, there is some progress in carbon intensity over time, $g_\sigma \geq 0$. Second, extraction costs are convex in cumulative extraction and output growth is positive, which we show can be ensured by $1 < \eta < \frac{1}{1-\pi}$. With these conditions in hand—which we relax in Corollary 5, Appendix B.3, including CRRA utility—we show that our results remain qualitatively unaffected by the dynamic management of energy stocks and exploration.

Corollary 2 (Growth with Energy Stock Management)**.** *The solution of the exhaustible resource model* (18) *admits a unique asymptotic growth path, which is also a balanced growth path.*

Propositions 1 and 2 apply, with the following modifications: $g_\chi = 0$, $\omega = \frac{1+\pi\theta}{1-\theta} g_\sigma$, *and when growth rates coincide* $g_Y = \frac{g+\overline{\Delta} g_\sigma}{1+\pi\theta+\overline{\Delta}(1-\theta)}$, *where* $\overline{\Delta} = \Delta \mathbb{1}\{g > \omega\}$ *and* $\theta = \frac{\eta}{1-\eta}$.

Proof. See Appendix B.3 □

Endogenous technological growth. So far we have assumed that technological growth was exogenous. If technological growth is the result of private innovation decisions, optimal policy must also intervene to align them with the social optimum. This change in the long run growth rate feeds back into emissions and may affect long run carbon policy.

To assess whether these forces alter our conclusions, we enrich our framework with endogenous growth. Instead of exogenous technological growth g, in this section we microfound the creative destruction process through innovation as in Grossman and Helpman (1991) and Aghion and Howitt (1992). We sketch the main elements in the main text, and relegate a complete description to Appendix B.4.

A Cobb-Douglas aggregator of varieties now constitutes aggregate output. Each variety is produced with the production function (1) subject to a variety-specific productivity. Within varieties, there is perfect competition. At any given point in time for any variety, a leader enjoys a productivity advantage $\lambda > 1$ over its competitors, leading to limit pricing. Firms use labor to innovate over the leader, with one unit of labor leading to a success rate of η. Labor is perfectly mobile between production and innovation.

The only difference from our baseline specification is that the allocation of scarce labor between innovation and production determines the growth rate of technology g. The relationship $g_Z = g - \Delta \max\{g_m, 0\}$ continues to hold, where g is a function of parameters given in Appendix B.4: the rate of time preference ρ, the innovation step size λ, the labor cost of innovation η and the labor elasticity of production.

The technological growth rate g differ between the laissez-faire and the efficient allocation, which we denote with superscripts LF and SP. Therefore, we continue to obtain the same classification of growth paths within the laissez-faire, and within the efficient allocation. In particular, the result that the planner places a cap on emissions growth when technological growth is sufficiently high continues to hold. The only difference with our baseline results is that growth rates are generally shifted in the planner allocation because of innovation externalities—business stealing and market size—that are unrelated to the carbon externality.

Corollary 3 (Endogenous Technological Growth)**.** *Proposition 1 and 2 apply to the endogenous growth model, with the following modifications in regimes without the emissions cap:* $g_Y^i = \frac{g^i + (\overline{\Delta}^i - \pi) g_\chi + \overline{\Delta}^i g_\sigma}{1 + \Delta^i}$*, where* $\overline{\Delta}^i = \Delta \mathbb{1}\{g^i > \omega\}$*, for* $i = LF, SP$*.*

Proof. See Appendix B.4 □

Corollary 6 in Appendix B.4 extends Corollary 3 to the CRRA case.

Endogenous progress in renewables. So far we have assumed that progress in renewable energy was exogenous. If progress in carbon-free energy is the result of endogenous innovation decisions, directing innovation to reduce the carbon intensity of production may complement, or even dominate, rising carbon pricing over time when emissions would otherwise escalate.

To assess whether these forces affect our conclusions, we enrich our framework with endogenous growth in renewables. Instead of exogenous growth in χ_t and σ_t, in this section we introduce innovation in renewables in the tradition of Grossman and Helpman (1991) and Aghion and Howitt (1992), similarly to above when we introduced it for general technological growth. We use a formulation in which energy is a bundle of carbon-free and carbon-intensive sources with a unit elasticity of substitution, as in Appendix A.1. We sketch the main elements in the main text, and relegate a complete description to Appendix B.5.

The only difference from our baseline specification is that the allocation of scarce labor between innovation in renewables and production determines the growth rate of productivity of renewables. We denote $\overline{g}_\chi, \overline{g}_\sigma$ the exogenous growth rate of extraction costs and emissions intensity if renewables had constant productivity, and let g_χ, g_σ denote the endogenous growth rate of extraction costs and emissions intensity.

Innovation endogenizes g_χ and g_σ through market forces. As above however, g_χ and g_σ are entirely determined by parameters that reflect the rate of time preference, the innovation step size, the labor cost of innovation, and output elasticities. These rates now differ between the laissez-faire and the efficient allocation, which we denote with superscripts LF and SP.

Despite the fact that the planner now has the possibility to endogenously increase progress in carbon-free energy production, we continue to obtain the same classification of growth paths within the laissez-faire, and within the efficient allocation. In particular, the result that the planner places a cap on emissions growth when technological growth

is sufficiently high continues to hold. This conclusion may partly reflect the unit elasticity of substitution between fossil fuels and renewables. The only significant difference with our baseline results is that growth rates are generally shifted in the planner allocation because of innovation externalities that are unrelated to the carbon externality.

Corollary 4 (Endogenous Progress in Renewable Energy)**.** *Proposition 1 and 2 apply to the model with innovation in renewables, with the following modifications in regimes without the emissions cap:* $\omega^i = \overline{\omega} + \pi(g^i_\chi - \overline{g}_\chi)$ *and* $g^i_Y = \frac{g+(\overline{\Delta}^i-\pi)g^i_\chi+\overline{\Delta}^i\overline{g}_\sigma+\overline{\Delta}^i(g^i_\chi-\overline{g}_\chi)}{1+\overline{\Delta}^i}$*, where* $\overline{\Delta}^i = \Delta\mathbb{1}\{g > \omega^i\}$ *for* $i = LF, SP$*, and* $\overline{\omega} = (1+\pi)\overline{g}_\chi + \overline{g}_\sigma$*.*

Proof. See Appendix B.5 □

Corollary 7 in Appendix B.5 extends Corollary 4 to CRRA utility.

2.4 Nonlinear Climate Damages

Our damage function (7) imposes a log-linear relationship between productivity and temperature. This formulation is consistent with econometric specifications that estimate ζ using temperature variation (Dell et al., 2012; Burke et al., 2015; Bilal and Känzig, 2025). However, a wide range of damage function specifications have been proposed in the literature. If damages are strongly concave in temperature—perhaps because of unmodeled adaptation—they might not affect long run growth. If damages are highly convex—perhaps because of tipping points—they might have more dramatic effects on growth.

To understand the role of the shape of the damage function, we propose a simple classification. For expositional simplicity in this section, we focus on a unidimensional climate system $\mathcal{M} = \mathcal{T} = 1$ and consider damage functions $\mathcal{D}(T)$ that are decreasing in temperature T, and such that $Z_t = \overline{Z}_t\mathcal{D}(T_t)$. For every damage function $\mathcal{D}(T)$, we denote $D(T) = -\log \mathcal{D}(T)$.

We say that a damage function $\mathcal{D}(T)$ is asymptotically *log-linear* in temperature if there exists a constant $\zeta > 0$ such that associated log damages D satisfy: $D'(T) \to \zeta$ as T grows large. This formulation is the one we use in (7) and is the one most commonly adopted in empirical studies of climate impacts, and in structural models such as Bilal and Känzig (2025). Because the logarithm of output is linear in temperature, this damage function embeds nonlinearity in output levels.

We say that a damage function $D(T)$ is asymptotically *log-concave* in temperature if $D'(T) \to 0$ as T grows large. This formulation implies that damages grow much more slowly than log-linearly as temperature grows. Crucially, it includes the specifications across a wide range of integrated assessment models (Nordhaus, 1992; Barrage and Nordhaus, 2024b). In these studies, the level of the damage function is specified as nonlinear in temperature, for instance $\mathcal{D}(T) = \frac{1}{1+\zeta T^d}$ for $\zeta, d > 0$. While this specification allows for *nonlinearities in levels*, it is sublinear in logs, and, in fact, *log-concave*: $D(T) \sim -d \log T$. Therefore, the log-concave damage functions in (Nordhaus, 1992; Barrage and Nordhaus, 2024b) impose less nonlinearities that our baseline (7).

We say that a damage function $D(T)$ is asymptotically *log-convex* in temperature if $D'(T) \to +\infty$ as T grows large. This formulation implies that damages grow much faster than log-linearly as temperature grows. It includes the specification in Golosov et al. (2014), who specify log damages as a function of the level of carbon stock M_t. Given Beer-Lambert scaling, this specification is equivalent to a log damage function $D(T) = \zeta e^{dT}$ for $\zeta, d > 0$. Thus, the level of such a damage function is effectively super-exponential: $\mathcal{D}(T) = e^{-\zeta e^{dT}}$. The log-convex damage function in (Golosov et al., 2014) imposes more nonlinearities that our baseline (7).

Equipped with this classification of damage functions, we characterize how our results change when the damage function has different shapes. It is useful to define the combination of parameters that corresponds to a determinant of temperature growth in one of the cases: $\vartheta = \frac{\psi\rho(\rho+\lambda\nu)}{\nu\lambda}$

Proposition 3 (Growth with a Nonlinear Damage Function)**.**

(i) If the damage function is asymptotically log-linear, Propositions 1 and 2 apply.

(ii) If the damage function is asymptotically log-concave, long run growth rates are independent from the climate and coincide in the laissez-faire (LF) and social planner (SP) allocations, and satisfy: $g_m^i = g - \omega$, $g_Y^i = g - \pi g_\chi$, for $i = LF, SP$.

(iii) If the damage function is asymptotically log-convex and if $g < \omega$, Propositions 1 and 2 apply.

(iv) If the damage function is asymptotically log-convex and if $g > \omega$, to leading order:

- *In the laissez-faire: $g_{mt} \to 0$, $g_{Yt} \to g_\chi + g_\sigma$ and $T_t = D^{-1}\big((g-\omega)t\big)$ as $t \to +\infty$.*
- *In the social planner allocation:*

- *If $g < \omega + \vartheta$, long run growth rates of emissions, output and temperature coincide with the laissez-faire*
- *If $g > \omega + \vartheta$, $g_{mt} \to 0$, $g_{Yt} \to g_\chi + g_\sigma + \frac{g-\omega-\vartheta}{1+\pi}$ and $T_t = D^{-1}(\vartheta t)$ as $t \to +\infty$.*

Proof. See Appendix B.6. □

Proposition 3 reveals that log-linear damage functions as in our baseline (7) are the only class of damage functions for which long run growth rates depend continuously on damages, among log-linear, log-concave and log-convex damage functions.

For log-concave damage functions as in Nordhaus (1992) and Barrage and Nordhaus (2024a), climate impacts only affect the level of economic activity. The growth rate of economic activity is independent from the climate, because technological growth outpaces climate damages that grow more slowly. As a result, the laissez-faire and the efficient allocation share the same long run growth rates. This configuration can be interpreted as one in which (unmodeled) adaptation may mute an ever-growing share of direct log-linear damages. The same conclusions arise for log-convex damage functions when carbon savings growth ω is larger than technological progress g so that temperatures stabilize.

For log-convex damage functions as in Golosov et al. (2014) and when $g > \omega$, climate impacts grow so large that the economy grinds to a halt. In the laissez-faire, output growth cannot outpace growth in carbon savings $g_\chi + g_\sigma$. If the latter is negative because energy extraction costs are falling rapidly, immiserizing growth emerges. Carbon emissions grow at an ever smaller rate that converges to zero exactly such that growing climate damages offset technological progress. As a result, the time profile of temperature is fully determined by the damage function: $T_t = D^{-1}((g-\omega)t)$. Our formulas are consistent with sending marginal damages Δ to infinity in Proposition 1, consistent with log-convex damages and growing temperature.

In the efficient allocation, we obtain a similar disjunction of cases to Proposition 2. When technological growth g is below carbon savings plus a threshold $\omega + \vartheta$, growth rates coincide with the laissez-faire.

The second case arises when technological growth g exceeds carbon savings plus the critical determinant of temperature growth, ϑ. The planner then places a cap on emissions growth similarly to Proposition 2. However, instead of enforcing a constant exponential growth rate $\overline{g}_m > 0$ which would lead to exploding damages, the planner controls the rate at which emissions growth g_{mt} converges to zero to equalize marginal benefits and

marginal costs of energy use. This convergence takes place at a different rate than in the laissez-faire.

By engineering this soft landing, the planner ensures damage growth ϑ is capped despite rising temperatures and log-convex damages. Thus, damages do not offset all of technological progress and output growth benefits from technological growth $g - \omega$. In our calibration, $\vartheta = 0.001$, implying that the planner achieves a strictly larger output growth rate than the laissez-faire in most parameter configurations. Temperature growth is once more determined by the damage function: $T_t = D^{-1}(\vartheta t)$.

Taking stock, Proposition 3 indicates the degree of nonlinearity of the *logarithm* of the damage function is the relevant metric for long run climate impacts, not the degree of nonlinearity of the *level* of the damage function. This result follows from the observation that baseline technological growth is log-linear—that is, exponential in levels—and thus dominates climate impacts from any log-concave damage function in the long run. Thus, even highly nonlinear damage functions in levels can imply no long-run climate impacts, while moderately nonlinear damage functions in logs can imply dramatic long-run climate impacts.

While the degree of nonlinearity of the damage function is of course an empirical question, log-linear damage functions have two advantages. The first advantage is conceptual: they deliver an informative intermediate case in which climate impacts depend continuously on damage function parameters. The second advantage is practical: they correspond to the majority of formulations that have been estimated in practice, and the weight of empirical evidence suggests a robustly non-zero log-linear component of the damage function. Therefore, we use our baseline log-linear damage function (7) in our quantitative implementation.

3 Quantification

3.1 Estimation

To assess whether the regime change from Propositions 1 and 2 is quantitatively relevant, we specify the climate system and the parameters of our framework. First, we calibrate a first set of parameters to standard values of the literature. Second, we parametrize the climate system. Third, we parametrize the damage function. Fourth, we estimate internally the key parameters that govern optimal policy—g_σ, g_χ and g—by matching

out-of-balanced growth transitional dynamics between 1982 and 2019. We start in 1982 to capture recent decades and exclude the oil shocks. We stop in 2019 to exclude the pandemic.

Data. We obtain world Gross Domestic Product (GDP) and population data from the World Bank. Global mean temperature anomaly data is from the National Oceanic and Atmospheric Administration (NOAA). Carbon dioxide emissions from energy use are from the Potsdam Real-Time Integrated Model for the probabilistic Assessment of emission Paths (PRIMAP). We obtain world primary energy consumption from the Energy Institute through Our World in Data.

Preferences and population. We set the rate of time preference to $\rho = 0.03$ and use log utility $\gamma = 1$. We use the isomorphic formulation with population growth from Appendix A.6, with population growth set to its world average between 1982 and 2019: $n = 0.014$.

Production. Following standard practice, we set the capital share to $\alpha = 0.3$, the capital depreciation rate to $\delta = 0.08$ and the energy share to its world average of $\psi = 0.05$.

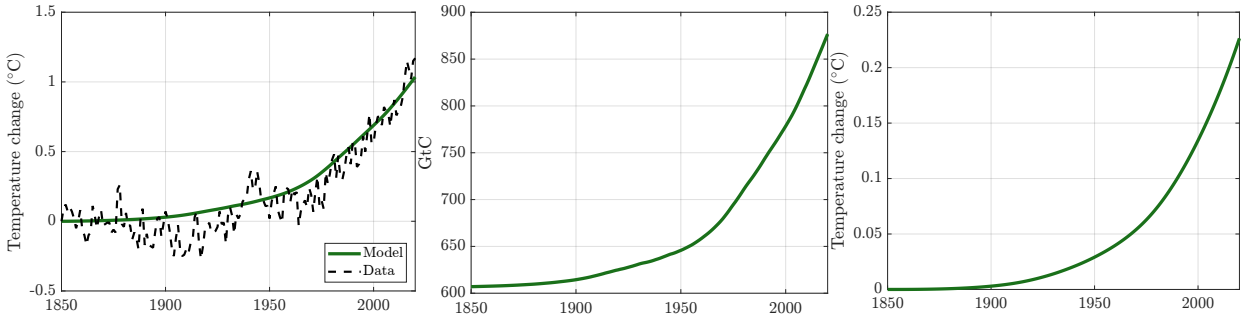
Climate system. We use the quantified climate system from Folini et al. (2024). It includes three carbon sinks: the atmosphere, the upper ocean, and the deep ocean. It features two temperature layers: a combined atmosphere-upper ocean layer and a deep ocean layer. We verify that the parametrization we use matches CMIP5 temperature impulse response functions from large scale climate models. We describe our climate system in more detail in Appendices A.3 and A.4.

We use the parametrized climate system to construct initial conditions for the rest of the estimation in 1982. We take 1850 to be the pre-industrial steady-state of the climate system. Given the parametrized matrices $\mathbf{A}, \mathbf{B}, \mathbf{N}, \mathbf{H}, \mathbf{F}_{eq}$, we calculate the steady-state carbon stocks $\mathbf{M}_{eq}$ in all sinks and temperatures $\mathbf{T}_{eq}$ in all layers. Next, we follow Folini et al. (2024) and input the observed path of emissions between 1850 and 1982. Iterating over the climate system delivers carbon stocks $\mathbf{M}_{1982}$ and temperatures $\mathbf{T}_{1982}$ that we use as initial conditions for the rest of the emissions. Figure 1 shows that this procedure delivers a path of global mean temperatures that aligns with the data—up to natural climate variability that we do not directly model in this paper.

Damage function. We use an asymptotically log-linear damage function with persistent level effects that loads on temperature in the combined atmosphere-upper ocean layer with temperature T^A: $Z_t = \overline{Z}_t \exp\left(-\int_0^t \zeta_s \left(T^A_{t-s} - T^A_{eq}\right) ds\right)$. We use two damage

Figure 1: Climate Dynamics Between 1850 and 1982.

(a) Temperature Change in Atmosphere and Upper Ocean (b) Carbon in Atmosphere (c) Temperature Change in Deep Ocean



Note: Solid green line: outcome of climate model given observed path of emissions. Dashed black line: data. Temperatures normalized to zero in 1850.

functions from Bilal and Känzig (2025) in our exercises, as their empirical strategy applies directly to our framework.

The first damage function ζ_s^{local} is estimated using annual variation in local, country-level temperature as in Dell et al. (2012) and Burke et al. (2015). This approach leads to a damage function with cumulative impact $\int_0^\infty \zeta_s^{\text{local}} ds = 0.036$.

The second damage function ζ_s^{global} is estimated using annual variation in global temperature directly—itself driven by phenomena such as solar cycles, El Niño or volcanic eruptions—and is a closer counterpart of the damage function in the framework. This approach leads to a damage function with cumulative impact $\int_0^\infty \zeta_s^{\text{global}} ds = 0.25$. It is seven times larger because global temperature fluctuations capture damaging extreme weather events such as extreme rain, wind and droughts that are not strongly correlated with idiosyncratic local temperature realizations.

Emissions intensity and extraction cost growth rates. In our framework, the growth rate of emissions to energy use, E_t^m / E_t is equal to the growth rate of emissions intensity σ_t. Similarly, the growth rate of the extraction cost χ_t is equal to the growth rate of output per unit of energy Y_t / E_t. Crucially, these relationships also hold away from a growth path. Thus, we can directly target these average growth rates in the data between 1982 and 2019. Despite progress in less carbon-intensive energy generation, we estimate a relatively low value $g_\sigma = 0.003$ which, combined with population growth, is necessary to rationalize rising emissions over time. Similarly, we estimate $g_\chi = 0.012$. These estimates let us construct $\omega = (1 + \pi) g_\chi + g_\sigma$. To characterize the growth regime, we must now

estimate g.

Technological growth rate. Estimating technological growth g is more challenging. If the economy was on a constant growth path in the data, Proposition 1 and 2 would let us read off g from output growth g_Y. However, the climate system is still far from a constant growth path. Oceans take centuries to fully catch up to atmospheric temperatures, while emissions have been growing at current rates for only a few decades. Thus, the rate of warming is still below what it would be on a constant growth path in which oceanic temperatures have caught up. As a result, economic damages are growing at an increasing rate over time, and the entire economy is away from constant growth.

We address this challenge with a simulated method of moments. For each technological growth rate g, we solve the nonlinear transition of the model from its initial conditions in 1982—including the initial conditions of the climate system that we obtained above—to its long run constant growth path. We search for the rate of technological growth g that allows us to best match the time series of output between 1982 and 2019 to the first 39 years of the transition in the model.[3]

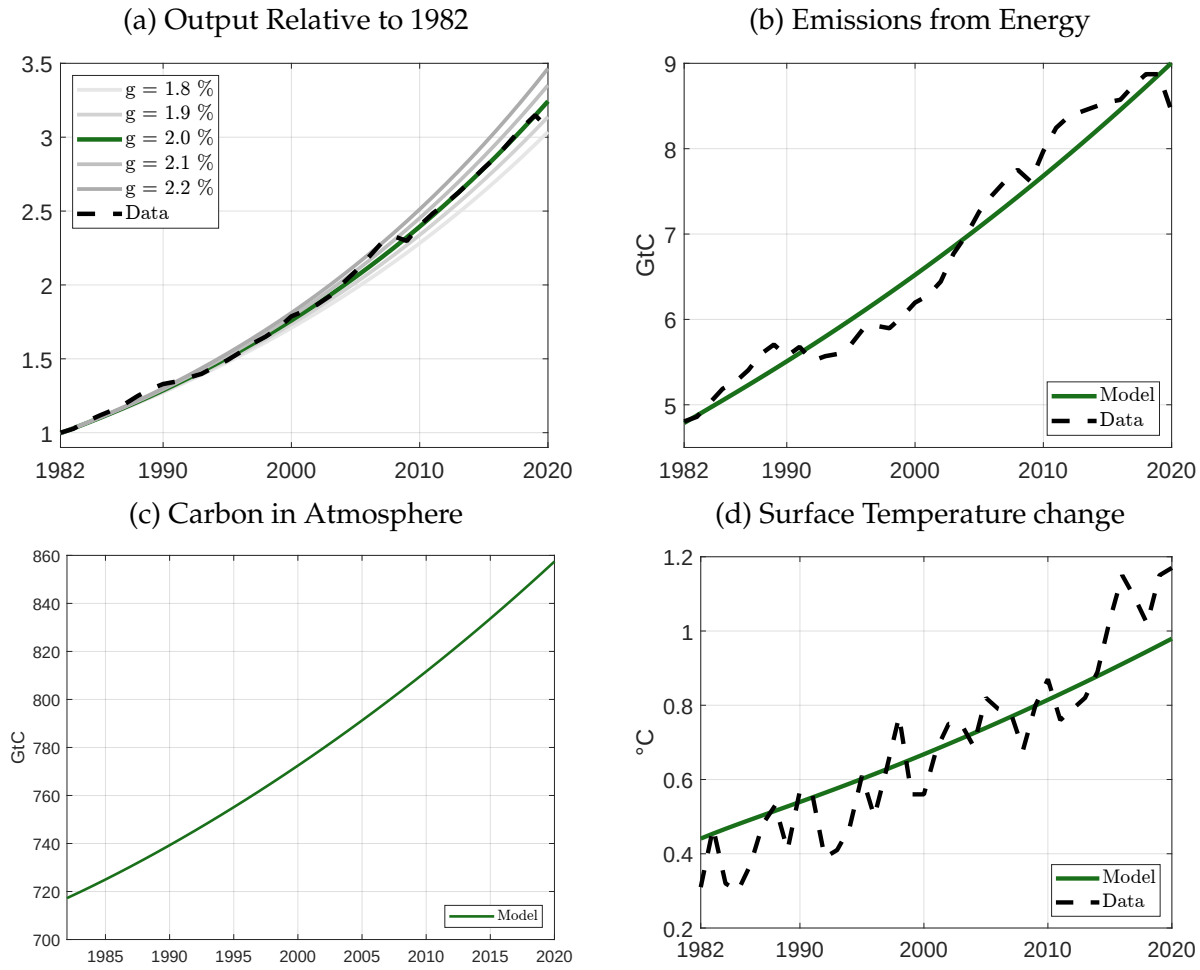
Figure 2 displays the results of the estimation. Panel (a) shows that output growth from 1982 to 2019 identifies technological growth g. As expected, increasing g moves the path of output upward. We infer that technological growth $g = 0.02$ per year. Panels (b), (c) and (d) reveal that the estimated model fits the data well on additional dimensions between 1982 and 2019. Although not surprising because we match the average growth rates of the ratio of emissions to energy, the ratio of energy to output, and the path of output, panel (b) indicates that the path of emissions from energy use in the model is close to the data at all times. Panel (c) displays the path of atmospheric carbon. Panel (d) shows that the path of global mean temperature is also close in the model and in the data between 1982 and 2019.

3.2 Growth and the Climate with Local Temperature Damages

Equipped with the estimated model, we assess the effect of climate change and optimal policy on long-run growth. We start our analysis under a conventional damage function

[3]For now, we estimate g under the damage function ζ^{global}. We plan to repeat the estimation under the damage function ζ^{local}.

Figure 2: Estimation of g and Output and Climate Dynamics Between 1982 and 2019.



Note: Solid green line: model outcomes for estimated g. Dashed black line: data.

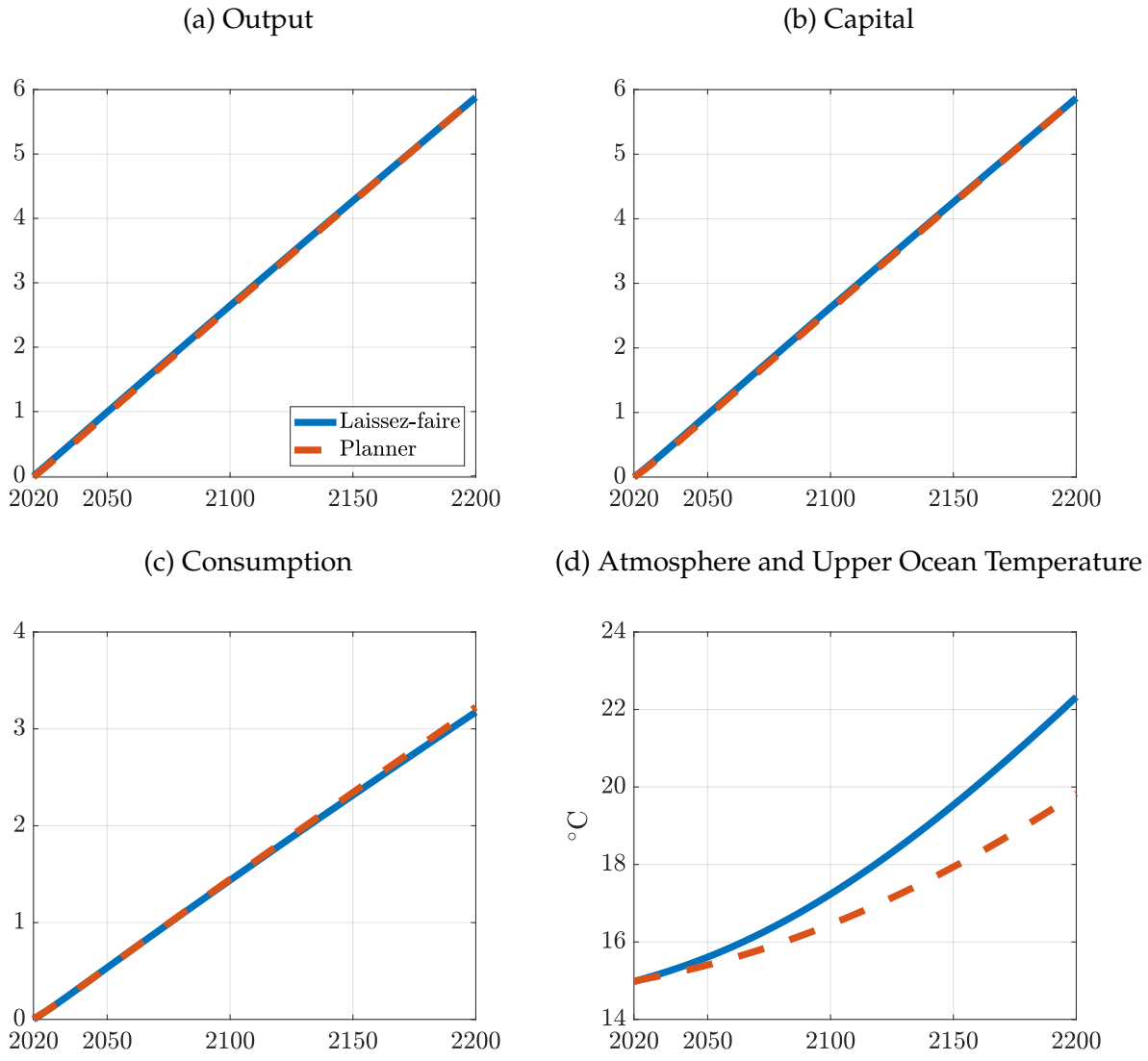
ζ^{local} based on estimates using local temperature variation.[4] We start the economy from initial conditions in 2019 and let it converge to its long-run growth path. We compare the laissez-faire and efficient allocations, and the carbon prices that implement the first-best.

Figure 4 displays transition paths under local damages. Panel 3(a) shows the path of output from 2020 to 2200. In the estimated model, climate damages based on local temperature variation place the economy in the regime in which the planner chooses the same long-run growth rate as in the laissez-faire: $g_Y^{LF} = g_Y^{SP} = 3.1\%$.

Along the transition path, efficient output falls slightly below output in the laissez-faire. This gap arises because the planner internalizes the carbon externality. The planner

[4]Since we estimated the model under ζ^{global}, we rescale exogenous productivity at date $t = 0$ so that initial conditions and output coincide in both specifications, making counterfactuals comparable.

Figure 3: Laissez-Faire and Efficient Transition Paths: Local Damage Function



Note: Transition paths of log output (a), log capital (b), log consumption (c) and upper layer temperature (d). Black dashed line: laissez-faire. Solid green line: efficient allocation. Damage function ζ^{local} estimated with local temperature variation.

chooses to lower energy consumption—or decentralize it with carbon pricing—so that output initially falls below the laissez-faire. Over time, output catches up to the laissez-faire, but this catch-up takes more than a century. Eventually, efficient output exceeds output in the laissez-faire because climate damages are lower.

Panel 3(b) depicts the associated path of capital. Efficient capital also falls below the laissez-faire for multiple decades, because lower energy consumption implies a lower marginal product of capital. Panel 3(c) indicates that despite output falling below the

laissez-faire, the planner maintains consumption above the laissez-faire levels at all times due to lower needs to save. While the consumption gap is initially modest, it eventually opens up more visibly after multiple decades.

The consumption-equivalent welfare gains of moving from the laissez-faire to the efficient allocation is 1.2%. These gains are modest because the consumption gains are themselves moderate and largely back-loaded. This feature in turn follows from relatively minor climate damages. The damage function implies that every permanent increase in temperature implies a 3.6% productivity loss. Given our rate of time preference, background economic growth, and the energy share, the planner can only achieve moderate gains relative to the laissez-faire.

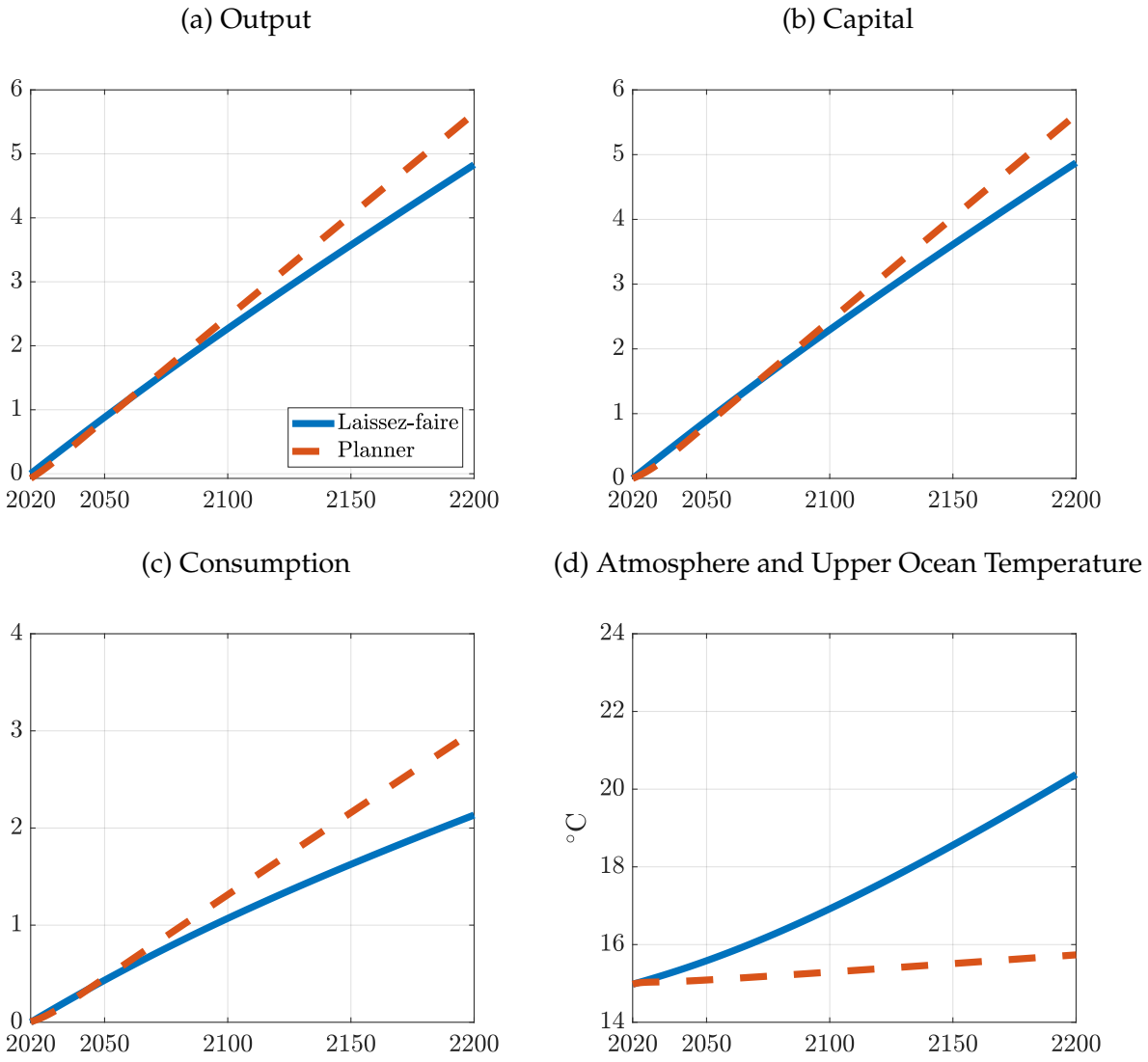
Panel 3(d) reveals that even modest differences in the path of output and energy use can translate into meaningful differences in the temperature path. Under the laissez-faire, global mean temperature rises by an additional 2.2°C by 2100 relative to 2020, or 3.2°C above pre-industrial levels. By 2200, temperature is more than 7°C above 2020 levels, and thus 8°C above pre-industrial levels. By contrast, the efficient allocation reduces 2100 warming to 1.5°C above 2020 levels (2.5°C above pre-industrial levels) and 2200 warming to 4.8°C above 2020 levels (5.8°C above pre-industrial levels).

Propositions 1 and 2 indicate that temperature growth is linear on the constant growth path. While output, capital and consumption grow close to log-linearly along the transition, the temperature path is more convex. Initially, the climate system is still far from the growth path as deep ocean temperature is still lagging behind atmosphere and upper ocean temperature. This initial gap between temperature in the two layers slows down temperature growth in the upper layer. Once the deep ocean temperature growth catches up, temperature growth in the atmosphere and the upper ocean accelerates and reaches its constant growth path speed. This catch-up process closes in the second half of the 22$^{\text{nd}}$ century.

3.3 Growth and the Climate with Global Temperature Damages

We contrast the results from the previous section with those from a damage function ζ^{global} based on estimates using global temperature variation. In that case, the cumulative damage function is nearly seven times larger and is a closer representation of the many manifestations of climate change beyond idiosyncratic, local temperature fluctuations. Propositions 1 and 2 indicate that larger climate damages can place the economy in a

Figure 4: Laissez-Faire and Efficient Transition Paths: Global Damage Function



Note: Transition paths of log output (a), log capital (b), log consumption (c) and upper layer temperature (d). Black dashed line: laissez-faire. Solid green line: efficient allocation. Damage function ζ^{global} estimated with global temperature variation.

regime in which the efficient allocation differs substantially from the laissez-faire. Does the change of regime arise under the larger, global damage function?

Figure 4 displays transition paths under global damages. We find that a damage function based on global temperature variation indeed places the economy in the regime in which the efficient and laissez-faire allocations differ markedly. Panel 4(a) shows the path of output from 2020 to 2200. The long-run growth of output is $g_Y^{\text{LF}} = 2.4\%$ in the laissez-faire. It falls somewhat over time in the laissez-faire, because of slow adjustments in the

climate system that imply that damages accumulate more rapidly later in the transition. By contrast, the efficient allocation achieves a long-run output growth rate a third higher than the laissez-faire, at $g_Y^{\text{SP}} = 3.2\%$.

Along the transition path, efficient output initially falls below laissez-faire output by nearly 10%. As the planner internalizes the carbon externality, they cut back on energy use to limit the accumulation of carbon in the atmosphere. Of course, this decision is intertemporally optimal, as the planner understands that long-run reductions in climate damages are preferable to higher output today. After forty years of reduced output relative to the laissez-faire, efficient output eventually catches up because of lower climate damages. Over time, efficient output outpaces laissez-faire output markedly. In 2100, output is more than 20% larger in the efficient allocation than in the laissez-faire. In 2200, this ratio compounds to 120% due to the permanent gap in growth rates.

Panel 4(b) depicts the associated path of capital. Efficient capital also falls below the laissez-faire for fifty years, because lower energy consumption implies a lower marginal product of capital. Panel 4(c) indicates that the initial fall in output leads to short-run consumption losses of a few percent. However, consumption catches up to the laissez-faire by 2050 and eventually substantially exceeds it. By 2200, consumption is more than 140% larger in the efficient allocation than in the laissez-faire. Consumption gains are larger than output gains because lower capital requires less investment.

The consumption-equivalent welfare gains of moving from the laissez-faire to the efficient allocation are markedly larger than under the local temperature damage function. With a global temperature damage function, the welfare gain is 26.3%, or twenty-two times the gains with a local temperature damage function. These gains are larger partly because the damage function is larger, and thus there is more to gain from implementing the optimal policy. Yet, gains are twenty-two times larger, while the cumulative damage function is seven times larger. Thus, the planner achieves larger *relative* gains when the damage function is larger. We unpack this observation in the next section.

Panel 4(d) reveals that the path of global mean temperature differs substantially between the laissez-faire and the efficient allocations. Under the laissez-faire and the global temperature damage function, the rise in global mean temperature is comparable to the rise under the local temperature damage function.[5] The efficient allocation limits 2100

[5]It is slightly lower because larger damages reduce output and therefore emissions. Yet, this difference in the level of flow emissions is quantitatively small compared to the accumulating stock of carbon driven by growing output and emissions.

warming to 0.3°C above 2020 levels (1.3°C above pre-industrial levels) and 2200 warming to 0.8°C above 2020 levels (1.8°C above pre-industrial levels).

Our analysis uncovers that the efficient allocation imposes a warming cap of 0.4°C per century, or 0.04°C per decade. This cap is roughly seven to eight times tighter than the rate of warming in the laissez-faire, which averages 3°C per century, or 0.3°C per decade. This cap arises despite our analysis relying on entirely standard cost-benefit tools and without appealing to a precautionary principle. The cap emerges as an optimal policy because carbon is a unit root process whose accumulation leads the dynamic marginal cost of energy use to exceed its static marginal product when emissions grow fast.

3.4 Welfare Gains and Climate Damages

Why are welfare gains twenty-two times larger when damages are large and based on global temperature variation, while damages themselves are seven times larger? To answer this question, we calculate welfare gains for damage functions that range from no damages at all to global temperature damages, including local temperature damages, by scaling the damage function to change its cumulative impact.[6] We compare welfare gains from moving from the laissez-faire to the optimal allocation, to welfare gains in a scenario in which temperature exogenously stops increasing in 2020. This scenario is infeasible in our framework. It corresponds to the hypothetical emergence of a backstop technology that greens all energy in 2020. Figure 5 displays the result of this comparison.

Panel 5(a) indicates that welfare gains from the optimal policy are increasing with the magnitude of climate impacts. Larger damages imply that there is more to gain from correcting the carbon externality.

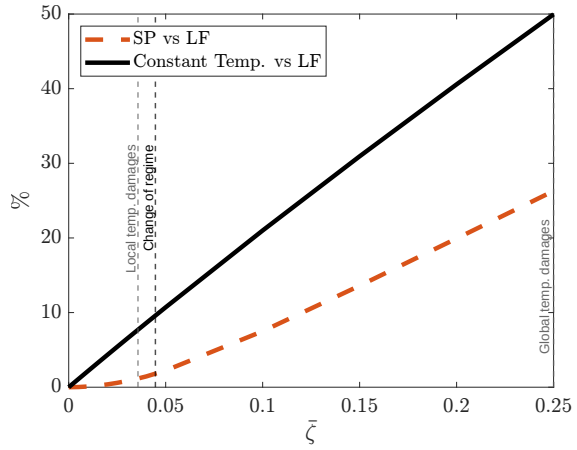
Welfare gains from holding temperatures constant to 2020 values scale nearly proportionally with climate impacts. Climate damages are a constant proportion of output, and thus eliminating them increases output, consumption and welfare by a constant proportion. These gains represent the unconditional losses from the carbon externality.

By contrast, welfare gains from implementing the efficient allocation are convex in climate impacts. At low climate impacts, welfare gains remain close to zero. At large

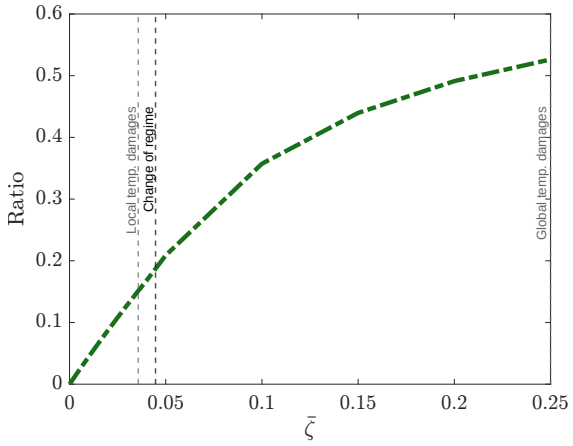
[6]The persistence of the local temperature damage function differs slightly from the persistence of the global temperature damage function. In our comparisons in this section, we refer to the 'local temperature damage function' as the one that features the same persistence as the global temperature damage function, but is scaled so that its cumulative sum coincides with that from the baseline local temperature damage function.

Figure 5: Welfare Gains By Climate Damages

(a) Welfare Gains



(b) Relative Welfare Gains



climate impacts, welfare gains rise nearly linearly. As a result, Panel 5(b) shows that the welfare gains from implementing the optimal policy relative to welfare gains from holding temperatures constant to 2020 values are rising and concave with damages.

Why does the planner recoup only a small proportion of unconditional losses from climate change at low damages, but a larger proportion at high damages? To understand these patterns, recall that the efficient allocation maximizes welfare at all values of damages, including no damages at all. When damages are low, the economy is close to the no-damage efficient allocation. Any reallocation of consumption and energy use leads to second order gains, while direct losses due to damages are first order: the planner has only a limited ability to offset climate change impacts. By contrast, when damages are large, the economy is far away from the no-damage efficient allocation. Second order gains from reallocating consumption and energy use can become comparable to direct losses, and the planner manages to recover close to a constant proportion of climate change impacts.

4 Conclusion

This paper studies long-run growth and optimal climate policy in an integrated assessment framework in which temperatures may continue to increase for the foreseeable future. Because carbon accumulates permanently, climate damages affect long-run growth. Balanced growth remains possible in the laissez-faire, but climate damages drag it down.

Optimal policy is characterized by a regime switch. When damages are below a threshold, the planner corrects levels but not long-run growth rates, and carbon is priced as a constant wedge relative to extraction costs. When damages are above that threshold, the planner places an endogenous cap on emissions growth, which slows temperature growth and raises long-run economic growth relative to laissez-faire.

Quantitatively, this regime switch is first-order for welfare and for the long-run trajectory of the economy. Under conventional damage estimates based on local temperature variation, optimal policy delivers modest welfare gains and largely preserves laissez-faire growth, even though it lowers the temperature path. Under larger damage estimates based on global temperature variation, optimal policy induces a qualitatively different transition: it front-loads mitigation, compresses long-run warming, and increases long-run growth by limiting escalating productivity losses from cumulative carbon. As a result, welfare gains rise more than proportionally with damages. The model therefore rationalizes how standard cost-benefit analysis can imply tight temperature targets without invoking the precautionary principle.

References

Acemoglu, Daron, Philippe Aghion, Leonardo Bursztyn, and David Hemous (2012). "The Environment and Directed Technical Change". *American Economic Review* 102.1, 131–66.

Aghion, Philippe and Peter Howitt (1992). "A Model of Growth through Creative Destruction". *Econometrica* 60.2, pp. 323–351.

Barrage, Lint and William D. Nordhaus (2024a). "Policies, projections, and the social cost of carbon: Results from the DICE-2023 model". *Proceedings of the National Academy of Sciences of the United States of America* 121.13, e2312030121.

— (2024b). "Policies, projections, and the social cost of carbon: Results from the DICE-2023 model". *Proceedings of the National Academy of Sciences of the United States of America* 121.13, e2312030121.

Bilal, Adrien and Diego R. Känzig (2025). "The Macroeconomic Impact of Climate Change: Global vs. Local Temperature". *Working Paper*.

Brock, William A. and M. Scott Taylor (2010). "The Green Solow model". *Journal of Economic Growth* 15.2, pp. 127–153.

Burke, Marshall, Solomon M. Hsiang, and Edward Miguel (2015). "Global non-linear effect of temperature on economic production". *Nature* 527.7577, pp. 235–239.

Cass, David (1965). "Optimum growth in an aggregative model of capital accumulation". *The Review of Economic Studies* 32.3, pp. 233–240.

Dell, Melissa, Benjamin F. Jones, and Benjamin A. Olken (2012). "Temperature shocks and economic growth: Evidence from the last half century". *American Economic Journal: Macroeconomics* 4.3, pp. 66–95.

Dietz, Simon, Frederick van der Ploeg, Armon Rezai, and Frank Venmans (2021). "Are Economists Getting Climate Dynamics Right and Does It Matter?" *Journal of the Association of Environmental and Resource Economists* 8.5, pp. 895–921.

Folini, Doris, Aleksandra Friedl, Felix Kübler, and Simon Scheidegger (2024). "The Climate in Climate Economics". *The Review of Economic Studies*.

Geoffroy, Olivier, David Saint-Martin, Dirk J.L. Olivié, Aurore Voldoire, Gilles Bellon, and Sophie Tytéca (2013). "Transient climate response in a two-layer energy-balance

model. Part I: Analytical solution and parameter calibration using CMIP5 AOGCM experiments". *Journal of climate* 26.6, pp. 1841–1857.

Golosov, Mikhail, John Hassler, Per Krusell, and Aleh Tsyvinski (2014). "Optimal Taxes on Fossil Fuel in General Equilibrium". *Econometrica* 82.1, pp. 41–88.

Grossman, Gene M and Elhanan Helpman (1991). "Trade, knowledge spillovers, and growth". *European Economic Review* 35.2-3, pp. 517–526.

Hassler, John, Per Krusell, and Anthony A Smith Jr (2016). "Environmental macroeconomics". *Handbook of macroeconomics*. Vol. 2. Elsevier, pp. 1893–2008.

Held, Isaac M., Michael Winton, Ken Takahashi, Thomas Delworth, Fanrong Zeng, and Geoffrey K. Vallis (2010). "Probing the fast and slow components of global warming by returning abruptly to preindustrial forcing". *Journal of Climate* 23.9, pp. 2418–2427.

Hotelling, Harold (1931). "The economics of exhaustible resources". *Journal of Political Economy* 39.2, pp. 137–175.

Koopmans, Tjalling C. (1963). "On the concept of optimal economic growth".

Manabe, Syukaro, Ronald J. Stouffer, Michael J. Spelman, and Kirk Bryan (1991). "Transient responses of a coupled ocean–atmosphere model to gradual changes of atmospheric CO2. Part I. Annual mean response". *Journal of Climate* 4.8, pp. 785–818.

Myhre, Gunnar, Eleanor J. Highwood, Keith P. Shine, and Frode Stordal (1998). "New estimates of radiative forcing due to well mixed greenhouse gases". *Geophysical Research Letters* 25.14, pp. 2715–2718.

Nath, Ishan B., Valerie A. Ramey, and Peter J. Klenow (2024). "How Much Will Global Warming Cool Global Growth?" *National Bureau of Economic Research Working Paper Series 32761*.

Nordhaus, William D. (1992). "An optimal transition path for controlling greenhouse gases". *Science* 258.5086, pp. 1315–1319.

— (2013). "Integrated economic and climate modeling". *Handbook of Computable General Equilibrium Modeling*. Vol. 1. Elsevier, pp. 1069–1131.

Winton, Michael, Ken Takahashi, and Isaac M. Held (2010). "Importance of ocean heat uptake efficacy to transient climate change". *Journal of Climate* 23.9, pp. 2333–2344.

A Model Setup

A.1 Energy cost

In this section we show the equivalence between an energy cost denominated in units of the final good—as in the main text—and energy production using the same production function as for the final good.

Suppose that energy is produced according to: $E_t = \chi_t^{-1} F(Z_t, K_t^E, L_t^E, E_t^E)$, where E superscripts denote inputs into the production of energy, and χ_t now indexes relative total factor productivity in the energy sector. We use Y superscripts to denote inputs into production of the final good. Similarly, we have: $Y_t = F(Z_t, K_t^Y, L_t^Y, E_t^Y)$. Finally: $E_t = E_t^E + E_t^Y$.

In the laissez-faire and in the planning allocation, the marginal product of inputs are equalized across sectors because of factor mobility. Let $\kappa_t^S = K_t^S/(Z_t L_t^S)$ and $\varepsilon_t^S = E_t^S/(Z_t L_t^S)$ denote input ratios for sector S. We obtain: $F_I(1, \kappa_t^Y, 1, \varepsilon_t^Y) = F_I(1, \kappa_t^E, 1, \varepsilon_t^E)$ for each input I. Given constant returns, these conditions imply that input ratios $\kappa_t^S \equiv \kappa_t$ and $\varepsilon_t^S \equiv \varepsilon_t$ are equalized across sectors $S = Y, E$. Therefore, we define: $F_t^* = F(Z_t, \kappa_t Z_t, 1, \varepsilon_t Z_t)$ so that $Y_t = L_t^Y F_t^*$ and $E_t = L_t^E F_t^*$.

The resource constraint becomes:

$$C_t + \dot{K}_t + \delta K_t = Y_t = L_t^Y F_t^* = (L_t - L_t^E) F_t^* = \overline{Y}_t - \chi_t E_t,$$

where $\overline{Y}_t = F(Z_t, K_t, L_t, E_t)$ since input ratios are common across sectors, so that they are also equal to aggregate input ratios: $K_t/(Z_t L_t) = \kappa_t$ and $E_t/(Z_t L_t)$. Therefore $\overline{Y}_t$ corresponds to output as if all resources were allocated to the final good. This resource constraint coincides with the one in the main text.

The household budget constraint becomes: $C_t + \dot{K}_t = r_t K_t + w_t$. By constant returns and factor mobility, the final good and energy firm problems lead to: $Y_t = (r_t + \delta) K_t^Y + w_t L_t^Y + p_t E_t^Y$ and $E_t = \chi_t^{-1}[(r_t + \delta) K_t^E + w_t L_t^E + p_t E_t^E]$. Therefore: $r_t K_t + w_t = \overline{Y}_t - p_t E_t$ as in the main text.

A.2 Microfoundation of Time-Varying Carbon Intensity

Assume that energy is Cobb-Douglas aggregator of two energy sources: fossil fuels B_t that are emissions-intensive and renewables G_t that are emissions-free.

$$E_t = B_t^{1-\beta} G_t^{\beta}.$$

Production of fossil fuels and of renewables requires χ_t^B and χ_t^G units of the final good, respectively. Competitive markets implies that production of the energy bundle costs:

$$\mathcal{C}(E_t) = E_t \left(\frac{p_t^B}{\beta}\right)^{1-\beta} \left(\frac{p_t^G}{1-\beta}\right)^{\beta} = \Theta E_t (\chi_t^B)^{1-\beta} (\chi_t^G)^{\beta} = E_t \chi_t,$$

where $\Theta = \beta^{-\beta}(1-\beta)^{1-\beta}$ and we define $\chi_t = \Theta(\chi_t^B)^{1-\beta}(\chi_t^G)^{\beta}$. This expression coincides with the one we use in the main text and relates the energy bundle extraction cost to the extraction cost of fossil fuels and renewables.

Expressing fossil-fuel use in the same units as emissions, we have:

$$E_t^m = B_t = (1-\beta)\frac{p_t^E}{p_t^B} E_t = (1-\beta)\Theta \left(\frac{p_t^G}{p_t^B}\right)^{\beta} E_t = (1-\beta)\Theta \left(\frac{\chi_t^G}{\chi_t^B}\right)^{\beta} E_t = \sigma_t E_t,$$

where the second equality uses optimal demand of fossil fuels by the intermediaries that bundle fossil fuels and renewables, and where we defined: $\sigma_t = (1-\beta)\Theta \left(\frac{\chi_t^G}{\chi_t^B}\right)^{\beta}$.

Finally, with our convention of a negative sign on g_σ:

$$g_\chi = (1-\beta) g_{\chi B} + \gamma g_{\chi G} \qquad g_\sigma = \beta g_{\chi B} - \beta g_{\chi G} \qquad g_\chi + g_\sigma = g_{\chi B}.$$

With a Cobb-Douglas energy bundle, technical progress in renewables leads to higher fossil fuel demand because of the unit elasticity of substitution. As a result, $g_\chi + g_\sigma = g_{\chi B}$ is entirely determined by technological progress in fossil fuels.

A.3 Carbon Cycle

We parametrize the carbon cycle matrix $\mathbf{A}$ as in Folini et al. (2024):

$$\mathbf{A} = \begin{pmatrix} -a_1 & r_1 a_1 & 0 \\ a_1 & -(r_1 a + a_2) & r_2 a_2 \\ 0 & a_2 & -r_2 a_2 \end{pmatrix}. \tag{15}$$

Quantitatively, we use the calibration from Folini et al. (2024): $a_1 = 0.054$, $a_2 = 0.0082$, $r_1 = \frac{M^A_{eq}}{M^U_{eq}}$, $r_2 = \frac{M^U_{eq}}{M^L_{eq}}$ and $M_{eq} = (607, 489, 1281)$, where M_{eq} is the pre-industrial equilibrium before any anthropogenic carbon emissions.

A.4 Warming

We follow Folini et al. (2024) for the calibration of the matrices $\mathbf{B}$ and $\mathbf{N}$:

$$\mathbf{B} = \begin{pmatrix} -\nu b_1 - \nu\lambda & \nu b_1 \\ b_2 & -b_2 \end{pmatrix} \quad \mathbf{N} = \begin{pmatrix} \nu & 0 \\ 0 & 1 \end{pmatrix},$$

with the following calibration: $\nu = 0.137$, $b_1 = 0.73$, $b_2 = 0.00689$, $\lambda = 1.06$, $F_{2XCO2} = 3.45$.

Equivalently, define T_{eq} as the equilibrium temperature vector when $F_t = 0$, and $\widehat{T}^X_t = T^X_t - T^X_{eq}$. The dynamics of the deviations from pre-industrial temperatures are given by :

$$\dot{\widehat{T}}^U_t = \nu \cdot \left(-\lambda \widehat{T}^U_t + b_1(\widehat{T}^L_t - \widehat{T}^U_t) + F_t \right) \qquad \dot{\widehat{T}}^L_t = b_2(\widehat{T}^U_t - \widehat{T}^L_t).$$

Since we specify the model in levels rather than in deviations from steady-state, we also need to calibrate the constant forcing terms in the two layers by targeting temperature levels in the two layers (in Kelvin degrees). Specifically, we choose F^U_{eq} and F^L_{eq} to target $T^U_{eq} = 288.15K$ (15C) and $T^L_{eq} = 278.15K$ (5C), by solving:

$$F^U_{eq} = \lambda\, T^U_{eq} + b_1 \left(T^U_{eq} - T^L_{eq} \right) \quad F^L_{eq} = -b_2 \left(T^U_{eq} - T^L_{eq} \right).$$

We obtain:

$$F^U_{eq} = 312.7390 \quad F^L_{eq} = -0.0689.$$

A.5 Thermohaline Circulation

The warming module from Folini et al. (2024) is specified in deviations from pre-industrial values. Once specified in levels, it is isomorphic to our specification with exogenous forcing in the deep oceans. This exogenous forcing is necessary to ensure that, in equilibrium, the deep oceans are colder than the upper ocean and atmospheric layer as in the data.

In practice, the colder temperature of deep oceans is in part caused by the thermohaline circulation (the "global conveyor belt"). The thermohaline circulation is caused by spatial heterogeneity in atmospheric temperatures and upper ocean temperatures together with salinity. Water cools at the poles where the atmosphere is colder (and local radiative forcing is weaker). It also mixes with ice melt which has lower salinity. Both factors increase water density, which sinks to the bottom of the ocean floor, where it is gradually moved by deep ocean currents. This convective channel implies that there is additional heat exchange between the atmosphere and the oceans, in a way that maintains a constant temperature differential between the two.

In this subsection, we show that incorporating this channel into our warming block leaves the quantitative predictions of our climate module virtually identical once properly recalibrated. To do so in a disciplined way, we propose the following modification to the warming module from Geoffroy et al. (2013) that underlies Folini et al. (2024):

$$\begin{aligned} C^U \dot{T}_t^U &= F_t - \lambda T_t^U + \varepsilon\gamma(T_t^L - T_t^U) + \omega(T_t^L - \phi T_t^U) \\ C^L \dot{T}_t^L &= \gamma(T_t^U - T_t^L) + \omega(\phi T_t^U - T_t^L). \end{aligned}$$

C^U, C^L denote the heat capacity of the atmosphere and the ocean, respectively. Importantly, the heat flow $\gamma(T_t^L - T_t^U)$ that enters the atmosphere temperature equation is the same as the one that enters the ocean temperature equation. Geoffroy et al. (2013) note that this heat flow is best adjusted by an additional coefficient ε possibly different from one to incorporate some effects of the thermohaline circulation (Manabe et al., 1991; Winton et al., 2010; Held et al., 2010). However, the adjustment by ε does not resolve the problem that ocean and atmosphere temperatures must equalize in the long run.

Our proposed modification includes an additional term $\omega(T_t^L - \phi T_t^U)$. This adjustment captures the idea that convective exchange between the ocean and the atmosphere depends on polar temperatures in the upper ocean, which are lower than average temper-

atures in the upper ocean. We then also impose that heat inflows and outflows between the two layers due to thermohaline circulation are identical.

We now discuss how to calibrate the additional parameters ω, ϕ. We start by renormalizing the system into a similar format to the one in Folini et al. (2024):

$$\dot{T}_t^U = \nu\Big(F_t - \lambda T_t^U + b_1(T_t^L - T_t^U)\Big) + c_1(T_t^L - \phi T_t^U)$$
$$\dot{T}_t^L = b_2(T_t^U - T_t^L) + c_2(\phi T_t^U - T_t^L),$$

with $c_1 = \omega/C^U$, $c_2 = \omega/C^L$, $\nu = 1/C_A$, $\varepsilon\gamma = b_1$ and $b_2 = \gamma/C^L$. The corresponding transition matrix writes:

$$\mathbf{B} = \begin{pmatrix} -\nu(b_1 + \lambda) - c_1 & \nu b_1 + c_1 \\ b_2 + c_2\phi & -(b_2 + c_2) \end{pmatrix}.$$

Geoffroy et al. (2013) use $C^U = 8$ W yr m^{-2} K^{-1} and $C^L = 100$ W yr m^{-2} K^{-1}, so that: $c_1/c_2 = 8/100 = 0.08$. Next, we posit that in the initial steady-state ϕT^U is approximately 0C, and T^U is approximately 15C.

We specify our warming module in Kelvin because it represents the relevant absolute unit in which to measure heat exchange. Kelvin degrees are a constant shift relative to Celsius degrees. Therefore, in the original Geoffroy et al. (2013) and Folini et al. (2024) specifications, switching between Kelvin and Celsius degrees drops out. With our proposed modification, it is isomorphic to a constant shift in exogenous forcing.

We now verify whether this new climate module with a thermohaline circulation adjustment delivers similar predictions to the one without the thermohaline circulation adjustment. Starting from steady-state, we will consider three distinct shocks that mirror the exercises in Folini et al. (2024): one in which the atmospheric carbon content exogenously quadruples at time 0, one in which it exogenously doubles at time 0, and one in which the carbon content of the atmosphere grows at 1% per year so that it quadruples over 200 years.

Parameters in the baseline warming module have been chosen to best match the temperature paths that follow from these two shocks in large-scale climate models—CMIP5 simulations. Therefore, we also recalibrate the parameters in the module with the thermohaline circulation adjustment to match the same CMIP5 simulations.

We proceed as follows. At any point in time: $\phi = \frac{\text{Polar temperature}}{T^U}$. We use the current

level of this ratio to calibrate ϕ. That is: $\phi = \frac{273.15}{288.15} = 0.948$. In steady-state: $c_2 = b_2 \frac{1-\tau}{\tau-\phi}$, where $\tau = \frac{T^L}{T^U}$. We use the pre-industrial steady-state ratio to calibrate: $\tau = \frac{278.15}{288.15} = 0.9653$. In steady-state: $(b_2 + c_2\phi)T^U = (b_2 + c_2)T^L$, implying: $\frac{T^L}{T^U} = \frac{b_2+c_2\phi}{b_2+c_2} < 1$. We invert this relationship to obtain c_2: $c_2 = b_2 \frac{1-\tau}{\tau-\phi}$ and $c_1 = 0.08 \cdot c_2$.

In our recalibration exercise, we keep ν and λ at their original values, as they are radiative parameters calibrated on the long-run climate response after the quadrupling of atmospheric carbon concentration, which should be invariant to the model structure. We then choose b_1 and b_2 to minimize the maximum distance between the temperature paths from the baseline Folini et al. (2024) module and our adjusted module in the quadrupling exercise. We use the instantaneous doubling and gradual increases exercises as an over-identification check.

Figure 6 shows the fit of our recalibration exercise. Figures 7, 8 and 9 display the results of our over-identification exercises. Across all exercises, both models behave very similarly.

Figure 6: Quadrupling carbon dioxide concentrations at time 0.

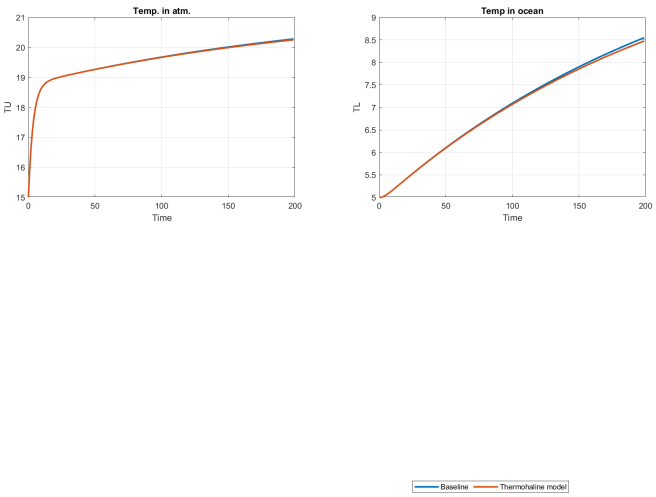


Figure 7: Doubling carbon dioxide concentrations at time 0.

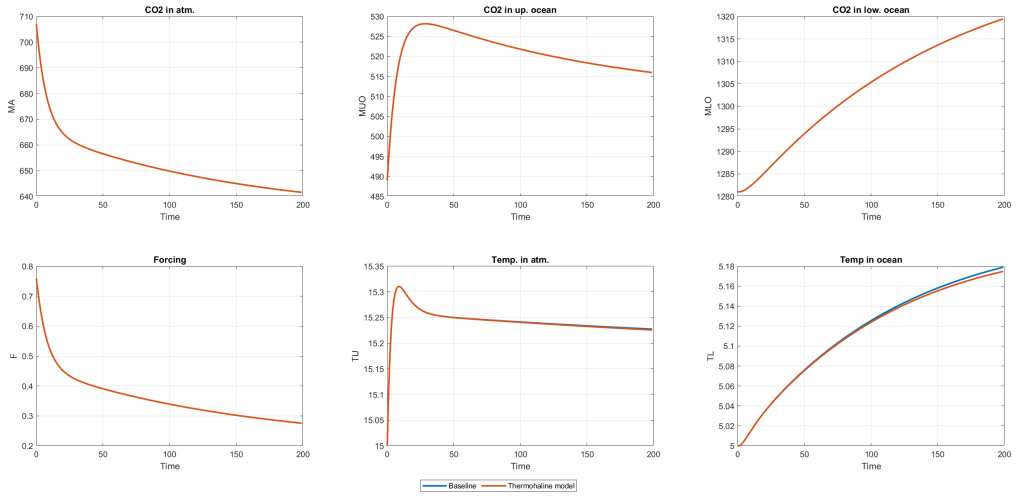


Figure 8: Constant increase in carbon dioxide concentrations at 1% a year.

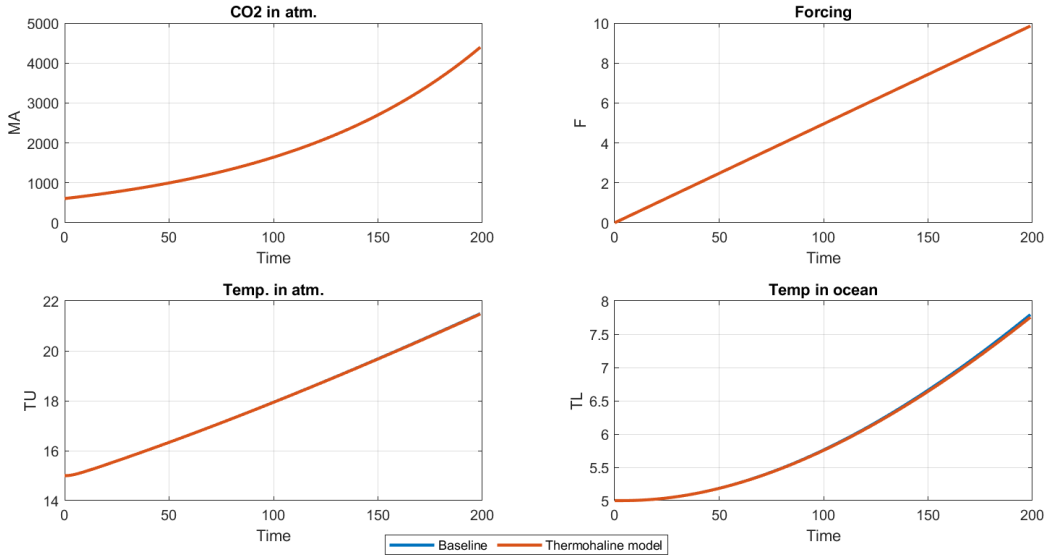
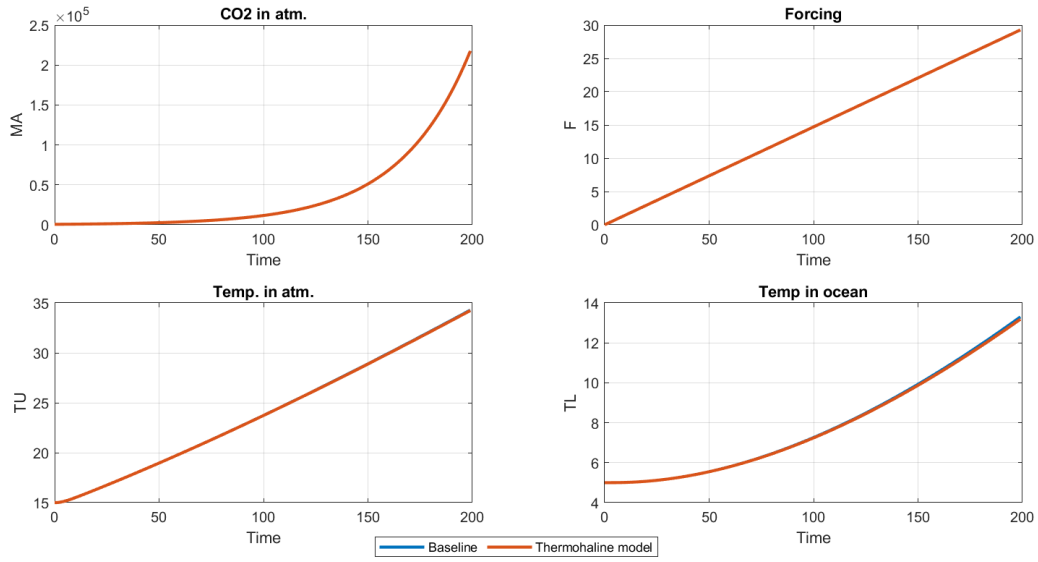


Figure 9: Constant increase in carbon dioxide concentrations at 3% a year.



A.6 Population Growth

In this section we show that our model can be rescaled to accommodate population growth. Assume that population L_t grows at rate n: $L_t = e^{nt}$. We denote per capita variables as before, and aggregate variables with a bar. Dynastic preferences are then:

$$\int_0^\infty e^{-\rho t} L_t U(C_t) dt = \int_0^\infty e^{-(\rho - n)t} U(C_t) dt.$$

Thus, we need to shift the rate of time preference to $\rho - n$.

The production function implies that aggregate output $\overline{Y}_t$ satisfies:

$$\overline{Y}_t = \left((L_t Z_t)^{1-\alpha} \overline{K}_t^{\alpha} \right)^{1-\psi} \overline{E}_t^{\psi} = L_t \left(Z_t^{1-\alpha} K_t^{\alpha} \right)^{1-\psi} E_t^{\psi} = L_t Y_t = L_t F(Z_t, K_t, 1, E_t).$$

The resource constraint is:

$$\overline{C}_t + \dot{\overline{K}}_t = \overline{Y}_t - \delta \overline{K}_t.$$

Using that $\dot{\overline{K}}_t = \dot{K}_t L_t + K_t L_t n$, we obtain the per capita resource constraint:

$$C_t + K_t = Y_t - (\delta + n) K_t.$$

Thus, we need to shift the capital depreciation rate to $\delta + n$.

The budget constraint of the representative dynasty is:

$$\overline{C}_t + \dot{\overline{K}}_t = r_t \overline{K}_t + w_t.$$

As for the resource constraint:

$$C_t + \dot{K}_t = (r_t - n)K_t + w_t.$$

Thus, we need to shift the interest rate to $r_t - n$.

Emissions are:

$$\overline{E}_t^m = \overline{\sigma}_t L_t E_t = \sigma_t E_t,$$

where the growth rate of σ_t is now $g_\sigma - n$.

The firm's optimality conditions are:

$$r_t + \delta = \alpha(1-\psi)\frac{\overline{Y}_t}{\overline{K}_t} = \alpha(1-\psi)\frac{Y_t}{K_t} \qquad w_t = (1-\alpha)(1-\psi)\frac{Y_t}{L_t} \qquad p_t = \psi\frac{Y_t}{E_t}.$$

We can rewrite the capital demand equation:

$$(r_t - n) + (\delta + n) = \alpha(1-\psi)\frac{Y_t}{K_t},$$

which is then consistent with our rescaling above.

B Proofs

B.1 Proof of Proposition 1

B.1.1 Economic module

Consider an asymptotic growth path. Let g_Z be the asymptotic growth rate of productivity. The resource constraint requires that the growth rates of output, consumption and capital are equal: $g_Y = g_C = g_K$. The Cobb-Douglas production function implies a constant energy share, and thus: $g_\chi + g_E = g_Y$. The structure of the production function then

requires: $g_Y = \alpha(1-\psi)g_Y + (1-\alpha)(1-\psi)g_Z + \psi g_E$, which we rewrite: $(1+\pi)g_Y = g_Z + \pi g_E$. Substituting out g_E and solving for g_Y yields: $g_Y = g_Z - \pi g_\chi$. From the definition of emissions, they grow asymptotically at rate: $g_m = g_E - g_\sigma = g_Y - g_\chi - g_\sigma$, where we choose the convention: $\sigma_t = \sigma_0 e^{-g_\sigma t}$.

B.1.2 Climate module

We now turn to the asymptotic behavior of the climate module. We divide the analysis into three different cases, corresponding to three different emissions regimes.

Case 1: Growing emissions $g_m > 0$. We start from $E_t^m = \overline{m} e^{g_m t} + \mathcal{O}(1)$. The asymptotic behavior of the carbon cycle is given by:

$$\dot{\mathbf{M}}_t = \mathbf{A}\mathbf{M}_t + \overline{m} e^{g_m t} \int_0^t e^{s(\mathbf{A} - g_m \mathbf{I})} ds \, \mathbf{m} + \mathcal{O}(1),$$

where $\mathbf{I}$ denotes the identity matrix. The explicit solution is $\mathbf{M}_t = \mathbf{M}_0 e^{t\mathbf{A}} + \overline{m} e^{g_m t} \int_0^t e^{s(\mathbf{A} - g_m \mathbf{I})\tau} ds \, \mathbf{m}$. Since $\mathbf{A}$ has a single zero eigenvalue and all other eigenvalues have strictly negative real parts, and $g_m > 0$, the homogeneous component $\mathbf{M}_0 e^{t\mathbf{A}}$ converges exponentially to a constant, and the integral $\int_0^t e^{s(\mathbf{A} - g_m \mathbf{I})} ds$ converges exponentially to a constant as well. Therefore, $\mathbf{M}_t$ grows at rate g_m asymptotically.

Since forcing is log-linear in atmospheric CO2, which (asymptotically) grows at a constant rate, forcing must (asymptotically) grow linearly with a constant slope $\mathbf{a_F} = g_m \mathbf{h}$: $\mathbf{F}_t = t\mathbf{a_F} + \mathcal{O}(1)$. Therefore, temperature dynamics are asymptotically given by:

$$\dot{\mathbf{T}}_t = \mathbf{B}\mathbf{T}_t + t\mathbf{N}\mathbf{a_F} + \mathcal{O}(1).$$

Solving for $\mathbf{T}_t$:

$$\mathbf{T}_t = e^{t\mathbf{B}}\mathbf{T}_0 + \int_0^t e^{(t-s)\mathbf{B}} s \, \mathbf{N}\mathbf{a_F} ds + \mathcal{O}\left(\int_0^t e^{(t-s)\mathbf{B}} ds \right)$$

$\mathbf{B}$ has eigenvalues with strictly negative real parts, implying that $e^{t\mathbf{B}}\mathbf{T}_0$ converges exponentially to zero. Similarly $\int_0^t e^{(t-s)\mathbf{B}} ds$ converges exponentially to a constant. Integrating by parts since B is invertible implies that: $\int_0^t e^{(t-s)\mathbf{B}} s \, \mathbf{N} ds = -t\mathbf{B}^{-1}\mathbf{N} + \mathcal{O}(1)$. Therefore:

$$\mathbf{T}_t = -t g_m \mathbf{B}^{-1}\mathbf{N}\mathbf{h} + \mathcal{O}(1) = t g_m (\mathbf{L} - \mathbf{D})^{-1}\mathbf{h} + \mathcal{O}(1) = t g_m \boldsymbol{\theta} + \mathcal{O}(1),$$

where the thermal capacity matrix cancels out in the $\mathbf{B}$ inverse and the definition of $\mathbf{N}$. Since $\mathbf{L} - \mathbf{D}$ is a nonsingular M-matrix, its inverse is a positive matrix, in that it maps vectors with positive entries into themselves. Thus, $\boldsymbol{\theta} \geq 0$ with at least some strictly positive entries.

Finally, we turn to the asymptotic dynamics of Z_t and check that asymptotically linear temperature delivers constant growth. $\log Z_t = \log Z_0 + gt - \boldsymbol{\zeta}'\big(\mathbf{T}_t - \mathbf{T}_{eq}\big)ds$.

$$\log Z_t = \log Z_0 + gt - \Delta g_m t + \mathcal{O}(1),$$

where $\Delta = \boldsymbol{\zeta}'\boldsymbol{\theta}$.

Using the expression for g_Y and g_m, we obtain $g_Y = g - \Delta(g_Y - g_\chi - g_\sigma) - \pi g_\chi$. Rearranging: $(1+\Delta)g_Y = g - \omega + (1+\Delta)(g_\chi + g_\sigma)$, which delivers the expression in Proposition 1. The condition $g_m > 0$ then becomes $g - \omega > 0$.

Case 2: Falling emissions $g_m < 0$. The derivations in Case 2 mirror those from Case 1. Emissions are asymptotically equal to zero. By mass conservation, carbon masses in all sinks are asymptotically constant. Radiative forcing is therefore also asymptotically constant. With constant forcing, temperature is asymptotically constant, and so are damages. Hence, Z_t grows asymptotic at constant rate g. Using the expression for g_Y as a function of g_Z, the growth rate of output is simply: $g_Y = g - \pi g_\chi$. Using the expression for g_m as a function of g_Y, the condition that $g_m < 0$ is thus equivalent to: $g < \omega$.

Case 3: Constant emissions $g_m = 0$. The derivations in Case 3 mirror those from Case 1. Carbon grows asymptotically linearly in time since the dominant term in $\int_0^t e^{s\mathbf{A}}ds$ corresponds to the zero eigenvalue. As a consequence, radiative forcing grows log-linearly in time: $\mathbf{F}_t = \mathbf{h}\log t + \mathcal{O}(1)$. Similar calculation to those above then imply that temperatures grow asymptotically log-linearly: $\mathbf{T}_t = \boldsymbol{\theta}\log t + \mathcal{O}(1)$. This property implies that Z_t asymptotically grows at a constant rate g, and economic variables grow as in Case 1. $g_m = \omega$ then corresponds to $g = \omega$.

B.1.3 Energy Costs in Labor Units

Now suppose that energy production only uses labor instead of the final good: $E_t = \chi_t^{-1} L_t^E$. An asymptotic growth path requires that the marginal product of capital is stable over time. The marginal product of capital depends on $L_t^Y = 1 - \chi_t E_t$. Therefore, $\chi_t E_t$ must stay constant or shrink over time, implying: $g_\chi + g_E \leq 0$.

Energy demand implies: $F_E = w_t \chi_t$. The household budget constraint requires that w_t grows at g_Y. Therefore: that $g_E = g_Y - g_Y - \gamma_\chi = -g_\chi$, so that $\chi_t E_t$ is exactly constant. We next obtain: $g_m = -g_\chi - g_\sigma$, which now only depends on parameters. The same distinction of cases—as when energy uses final goods—arises, where we obtain instead: $g_Y = \frac{g - \pi g_\chi - \Delta \max\{-g_\chi - g_\sigma, 0\}}{1+\pi}$.

B.2 Proof of Propositions 2 and 4

In this section we prove Proposition 2 under log utility, and we prove its variant under general CRRA utility, that we state below.

Away from logarithmic utility, the classification of efficient growth paths is richer than under log utility, although it retains the same overall structure. We provide a partial characterization below.

Proposition 4 (Efficient Growth With CRRA Utility)**.** *There exists a threshold $\overline{\rho}$ such that, if $\rho < \overline{\rho}$ and $\gamma \neq 1$:*

- *If $\gamma > 1$ and $\pi < \Delta$, or if $1 - \frac{(1+\pi)\rho}{g + \pi g_\sigma} < \gamma < 1$ and $\pi > \Delta$: the efficient allocation admits a unique asymptotic constant growth path. There exists a unique threshold $\overline{g}_m$ such that the results from Proposition 2 applies.*
- *In all other cases, any asymptotic growth path admits the structure from Proposition 2(i) or (ii).*

B.2.1 Optimality conditions

The current-value Hamiltonian of the planner's problem is:

$$\begin{aligned}\mathcal{H} = U(C_t) + \lambda_t \Big(F\big(Z(\mathbf{T}_t), K_t, 1, E_t\big) - \chi_t E_t - C_t - \delta K_t \Big) \\ + \boldsymbol{\mu}_t' \Big(\mathbf{A}\mathbf{M}_t + \sigma_t E_t \mathbf{m} \Big) + \boldsymbol{\nu}_t' \Big(\mathbf{B}\mathbf{T}_t + \mathbf{N}\mathbf{F}_{eq} + \mathbf{N}\mathbf{H}\big(\log \mathbf{M}_t - \log \mathbf{M}_{eq} \big) \Big).\end{aligned}$$

The optimality condition and co-state equation for capital accumulation lead to the Euler equation: $\gamma C_t / C_t = F_K(Z_t, K_t, 1, E_t) - \delta - \rho$ and $\lambda_t = u'(C_t)$. The optimality condition with respect to energy is:

$$\chi_t = \psi \frac{Y_t}{E_t} + \frac{\sigma_t}{u'(C_t)} \boldsymbol{\mu}_t' \mathbf{m}.$$

The co-state equations for carbon and temperature are:

$$\rho\boldsymbol{\mu}_t - \dot{\boldsymbol{\mu}}_t = \mathbf{A}'\boldsymbol{\mu}_t + \mathcal{D}(\mathbf{M}_t)^{-1}\mathbf{P}\boldsymbol{\nu}_t \qquad \rho\boldsymbol{\nu}_t - \dot{\boldsymbol{\nu}}_t = -u'(C_t)Y_t\overline{\boldsymbol{\zeta}} + \mathbf{B}'\boldsymbol{\nu}_t$$

where we denote $\mathcal{D}(\mathbf{M}) = \mathbf{diag}((\mathbf{M}_i)_i)$ the diagonal matrix with the vector $\mathbf{M}$ on the diagonal, $\mathbf{P} = (\mathbf{NH})'$, and $\overline{\boldsymbol{\zeta}} \equiv (1-\alpha)(1-\psi)\boldsymbol{\zeta}$.

The transversality conditions are:

$$e^{-\rho t}u'(C_t)K_t \to 0 \qquad e^{-\rho t}\boldsymbol{\mu}_t \circ \mathbf{M}_t \to 0 \qquad e^{-\rho t}\boldsymbol{\nu}_t \circ \mathbf{T}_t \to 0,$$

where $\circ$ denotes the element-wise product.

B.2.2 Constant growth path

Economic module. The economic module behaves as in the laissez-faire, except for energy demand. Consider an asymptotic growth path. Let g_Z be the asymptotic growth rate of productivity. The resource constraint requires that the growth rates of output, consumption and capital are equal: $g_Y = g_C = g_K$. The structure of the production function then requires: $g_Y = \alpha(1-\psi)g_Y + (1-\alpha)(1-\psi)g_Z + \psi g_E$. The capital transversality condition implies: $(1-\gamma)g_Y < \rho$. However, energy demand now depends on whether the extraction cost or the shadow value of emissions grows faster in the long run. To determine it, we turn to the climate module.

Climate module. We now turn to the asymptotic behavior of the climate module. We divide the analysis into three different cases, corresponding to three different emissions regimes.

We first solve for $\boldsymbol{\nu}_t$. To accurately account for long-run stability, we solve forward. To leading order:

$$\begin{aligned}
\boldsymbol{\nu}_t &= e^{t\overline{\mathbf{B}}}\boldsymbol{\nu}_0 + C_0^{-\gamma}Y_0 e^{(1-\gamma)g_Y t}\int_0^t e^{s[\overline{\mathbf{B}}-(1-\gamma)g_Y\mathbf{I}]}\overline{\boldsymbol{\zeta}}ds \\
&= e^{t\overline{\mathbf{B}}}\boldsymbol{\nu}_0 + C_0^{-\gamma}Y_0 e^{(1-\gamma)g_Y t}e^{t[\overline{\mathbf{B}}-(1-\gamma)g_Y]}[\overline{\mathbf{B}}-(1-\gamma)g_Y\mathbf{I}]^{-1}\overline{\boldsymbol{\zeta}} \\
&- C_0^{-\gamma}Y_0 e^{(1-\gamma)g_Y t}[\overline{\mathbf{B}}-(1-\gamma)g_Y\mathbf{I}]^{-1}\overline{\boldsymbol{\zeta}} \\
&= e^{t\overline{\mathbf{B}}}\left\{\boldsymbol{\nu}_0 + C_0^{-\gamma}Y_0[\overline{\mathbf{B}}-(1-\gamma)g_Y\mathbf{I}]^{-1}\overline{\boldsymbol{\zeta}}\right\} - C_t^{-\gamma}Y_t[\overline{\mathbf{B}}-(1-\gamma)g_Y\mathbf{I}]^{-1}\overline{\boldsymbol{\zeta}}
\end{aligned}$$

where $\overline{\mathbf{B}} = \rho\mathbf{I} - \mathbf{B}'$. $\overline{\mathbf{B}}$ has eigenvalues with strictly positive real part. From the capital

transversality condition, so does $\overline{\mathbf{B}} - (1-\gamma)g_Y\mathbf{I}$. Therefore, the first component grows at rate ρ unless ν_0 is such that the bracket is equal to zero. Since temperature is weakly increasing over time, growth in the first component at rate ρ violates the temperature transversality condition. Therefore, ν_0 is such that the first component is zero, and to leading order:

$$\boldsymbol{\nu}_t = -C_t^{-\gamma} Y_t \overline{\boldsymbol{\nu}}.$$

where $\overline{\nu} = [\overline{\mathbf{B}} - (1-\gamma)g_Y\mathbf{I}]^{-1}\overline{\boldsymbol{\zeta}}$. From the capital transversality condition, $\overline{\mathbf{B}} - (1-\gamma)g_Y\mathbf{I}$ has strictly positive eigenvalues. Therefore, it is a positive matrix, and $\boldsymbol{\nu} < 0$ if $\boldsymbol{\zeta} > 0$.

Let g_M denote the exponential growth rate of carbon stocks.[7] Substituting the expression for $\boldsymbol{\nu}_t$ into the equation for $\boldsymbol{\mu}_t$ and solving forward to leading order:

$$\begin{aligned}
\boldsymbol{\mu}_t &= e^{t\overline{\mathbf{A}}}\boldsymbol{\mu}_0 + C_0^{-\gamma} Y_0 e^{[(1-\gamma)g_Y - g_M]t} \int_0^t e^{s[\overline{\mathbf{A}} - (1-\gamma)g_Y + g_M]} \cdot \mathcal{D}(\mathbf{M}_0)^{-1}\mathbf{P}\overline{\boldsymbol{\nu}} ds \\
&= e^{t\overline{\mathbf{A}}}\boldsymbol{\mu}_0 + C_0^{-\gamma} Y_0 e^{[(1-\gamma)g_Y - g_M]t} e^{t[\overline{\mathbf{A}} - (1-\gamma)g_Y + g_M]} [\overline{\mathbf{A}} - g_M\mathbf{I} + (1-\gamma)g_Y\mathbf{I}]^{-1}\mathcal{D}(\mathbf{M}_0)^{-1}\mathbf{P}\overline{\boldsymbol{\nu}} \\
&- C_0^{-\gamma} Y_0 e^{[(1-\gamma)g_Y - g_M]t} [\overline{\mathbf{A}} - (1-\gamma)g_Y\mathbf{I} + g_M\mathbf{I}]^{-1}\mathcal{D}(\mathbf{M}_0)^{-1}\mathbf{P}\overline{\boldsymbol{\nu}}
\end{aligned}$$

where $\overline{\mathbf{A}} = \rho\mathbf{I} - \mathbf{A}'$. Since $\mathbf{A}$ has eigenvalues with strictly positive real part, the first component converges to zero, and the second component is dominated by the third one. Therefore:

$$\boldsymbol{\mu}_t = -\frac{Y_t}{C_t^{\gamma} M_t}\overline{\boldsymbol{\mu}}$$

where $\overline{\boldsymbol{\mu}} = [\overline{\mathbf{A}} - (1-\gamma)g_Y\mathbf{I} + g_M\mathbf{I}]^{-1}\mathcal{D}(\mathbf{M}_0/M_0)^{-1}\mathbf{P}[\overline{\mathbf{B}} - (1-\gamma)g_Y\mathbf{I}]^{-1}\overline{\boldsymbol{\zeta}}$, and M_t denotes an arbitrary but fixed entry of the carbon sink vector.

Energy use. We are now ready to return to energy use, which satisfies to leading order:

$$\left(\psi - \phi\frac{E_t^m}{M_t}\right)\frac{Y_t}{\chi_t E_t} = 1. \tag{16}$$

where $\phi = \overline{\boldsymbol{\mu}}'\mathbf{m}$. There are two possibilities: either $\psi > \phi\frac{E_t^m}{M_t}$, or $\psi = \phi\frac{E_t^m}{M_t}$. $\psi < \phi\frac{E_t^m}{M_t}$ would lead to a contradiction.

[7] For now we abstract from the knife-edge condition under which emissions are exactly constant and therefore carbon stocks grow linearly.

Case 1: $g_m < 0$. Carbon stocks are constant over time. E_t^m / M_t converges to zero. Temperature and damages are asymptotically constant, so that $g_Z = g$. Energy use then mirrors the laissez-faire, with $g_Y = g_\chi + g_E$ and so $g_Y = g - \pi g_\chi$. The condition $g_m < 0$ becomes $g < \omega$.

Case 2: $g_m = 0$. Carbon stocks grow linearly over time. Temperature and damages grow log-linearly, so that $g_Z = g$. E_t^m / M_t converges to zero. As in the laissez-faire, we obtain $g_Y = g - \pi g_\chi$. The condition $g_m = 0$ becomes $g = \omega$.

Case 3: $g_m > 0$. Solving carbon stocks forward to leading order:

$$\begin{aligned}\mathbf{M}_t &= e^{t\mathbf{A}}\mathbf{M}_0 + E_0^m e^{t g_m} \int_0^t e^{-s[g_m \mathbf{I} - \mathbf{A}]}\mathbf{m} ds \\ &= e^{t\mathbf{A}}\mathbf{M}_0 - E_0^m e^{t\mathbf{A}}[\mathbf{A} - g_m]^{-1}\mathbf{m} + E_t^m [g_m \mathbf{I} - \mathbf{A}]^{-1}\mathbf{m}.\end{aligned}$$

Because $g_m > 0$ and the eigenvalues of $\mathbf{A}$ have weakl negative real parts, the third component dominates the other two. Hence, asymptotically, $g_M = g_m$, and:

$$\mathbf{M}_t = E_t^m [g_m \mathbf{I} - \mathbf{A}]^{-1}\mathbf{m}.$$

Let $\mathbf{e}$ be the vector that selects M_t out of $\mathbf{M}_t$. Then: $M_t = \mathbf{e}'\mathbf{M}_t = E_t^m \mathbf{e}'[g_m \mathbf{I} - \mathbf{A}]^{-1}\mathbf{m}$, and so to leading order:

$$\frac{E_t^m}{M_t} = \frac{1}{\mathbf{e}'[g_m \mathbf{I} - \mathbf{A}]^{-1}\mathbf{m}} \qquad\qquad \frac{\mathbf{M}_0}{M_0} = \frac{[g_m \mathbf{I} - \mathbf{A}]^{-1}\mathbf{m}}{\mathbf{e}'[g_m \mathbf{I} - \mathbf{A}]^{-1}\mathbf{m}}.$$

Recall that $\overline{\boldsymbol{\mu}} = [\overline{\mathbf{A}} - (1-\gamma)g_Y + g_m]^{-1}\mathcal{D}(\mathbf{M}_0/M_0)^{-1}\mathbf{P}[\overline{\mathbf{B}} - (1-\gamma)g_Y \mathbf{I}]^{-1}\overline{\boldsymbol{\zeta}}$. Since $g_m > 0$ and $\rho > (1-\gamma)g_Y$, all the matrices are non-singular irreducible M-matrices and therefore have positive inverses. Then $\overline{\boldsymbol{\mu}} > 0$ if $\boldsymbol{\zeta} > 0$. We obtain:

$$\begin{aligned}\phi \times \frac{E_t^m}{M_t} &= \left\{ \overline{\boldsymbol{\zeta}}'[(\rho - (1-\gamma)g_Y)\mathbf{I} - \mathbf{B}]^{-1}\mathbf{N}\mathbf{H}\mathcal{D}\left(\frac{[g_m \mathbf{I} - \mathbf{A}]^{-1}\mathbf{m}}{\mathbf{e}'[g_m \mathbf{I} - \mathbf{A}]^{-1}\mathbf{m}}\right)^{-1} [(\rho - (1-\gamma)g_Y + g_m)\mathbf{I} - \mathbf{A}]^{-1}\mathbf{m} \right\} \\ &\quad \times \frac{1}{\mathbf{e}'[g_m \mathbf{I} - \mathbf{A}]^{-1}\mathbf{m}} \\ &= \overline{\boldsymbol{\zeta}}'[\eta \mathbf{I} - \mathbf{B}]^{-1}\mathbf{N}\mathbf{H}\mathcal{D}\left([g_m \mathbf{I} - \mathbf{A}]^{-1}\mathbf{m}\right)^{-1} [\eta \mathbf{I} + g_m \mathbf{I} - \mathbf{A}]^{-1}\mathbf{m}\end{aligned}$$

where in the second equality, the second term simplifies with $\mathcal{D}$, and we denoted $\eta = \rho - (1-\gamma)g_Y > 0$.[8] We have thus shown that:

$$\tau_t = \overline{\zeta}'[\eta\mathbf{I} - \mathbf{B}]^{-1}\mathbf{N}\mathbf{H}\mathcal{D}\left([g_m\mathbf{I} - \mathbf{A}]^{-1}\mathbf{m}\right)^{-1}[\eta\mathbf{I} + g_m\mathbf{I} - \mathbf{A}]^{-1}\mathbf{m}\,\frac{Y_t}{E_t} \tag{17}$$

Case 3.1: $\psi > \phi E_t^m / M_t$**.** In that case, energy use mirrors the laissez-faire (third case of Proposition 1), and we obtain the same growth rates. The condition $g_m > 0$ becomes $g > \omega$. However, we will have to verify which parameters lead to $\psi > \phi E_t^m / M_t$.

Case 3.2. $\psi = \phi E_t^m / M_t$ **and** $\gamma = 1$**.** Then:

$$\phi\frac{E_t^m}{M_t} = \overline{\zeta}'[\rho\mathbf{I} - \mathbf{B}]^{-1}\mathbf{N}\mathbf{H}\mathcal{D}\left([g_m\mathbf{I} - \mathbf{A}]^{-1}\mathbf{m}\right)^{-1}[\rho\mathbf{I} + g_m\mathbf{I} - \mathbf{A}]^{-1}\mathbf{m} \equiv f(g_m).$$

Denote $\boldsymbol{\xi}' = \overline{\zeta}'[\rho\mathbf{I} - \mathbf{B}]^{-1}\mathbf{N}\mathbf{H} > 0$. We now prove:

Lemma: f **is continuous, strictly increasing,** $f(0) = 0$ **and** $f(+\infty) = \sum_i \xi_i$**.**

Proof of Lemma. Denote $y(x) = [x\mathbf{I} - \mathbf{A}]^{-1}\mathbf{m}$. We obtain:

$$f(x) = \sum_i \xi_i \frac{y_i(\rho + x)}{y_i(x)}.$$

Going back to valuation formulas, we express: $y_i(x) = \int_0^\infty e^{-xt}v_{it}dt$, where $v_t = e^{t\mathbf{A}}\mathbf{m} > 0$. All the v_{it} are strictly positive for any $t > 0$ because $\mathbf{A}$ is irreducible. We now show that $\log y_i(x)$ is convex. This formulation proves continuity.

In addition, we have:

$$y_i'(x) = -\int_0^\infty te^{-tx}v_{it}dt > 0 \qquad\qquad y_i''(x) = \int_0^\infty t^2e^{-tx}v_{it}dt > 0,$$

[8] We can also re-express this formula. Let $\widetilde{\mathbf{A}} = g_m\mathbf{I} - \mathbf{A}$ and $a = \widetilde{\mathbf{A}}^{-1}\mathbf{m}$. The last two component are equal to:

$$\mathcal{D}(a)^{-1}[\widetilde{\mathbf{A}} + \eta\mathbf{I}]^{-1}\widetilde{\mathbf{A}}a = \mathbf{I} - \eta\mathcal{D}(a)^{-1}(\widetilde{\mathbf{A}} + \eta\mathbf{I})^{-1}a$$

where we have used the resolvent identity: $[\widetilde{\mathbf{A}} + \eta\mathbf{I}]^{-1}\widetilde{\mathbf{A}} = \mathbf{I} - \eta(\widetilde{\mathbf{A}} + \eta\mathbf{I})^{-1}$

Then:

$$y_i(x)y_i''(x) - (y_i'(x))^2 = \iint_0^\infty e^{-x(t+s)} v_{it} v_{is} (s^2 - ts) dt ds = \frac{1}{2} \iint_0^\infty e^{-x(t+s)} v_{it} v_{is} (t-s)^2 dt ds,$$

where the second inequality changed variables to symmetrize the expression. Therefore: $\partial^2 \log y_i(x)/\partial x^2 \geq 0$. Therefore, $\partial \log y_i(x)/\partial x$ is increasing in x. Then:

$$\frac{\partial}{\partial x} \log \frac{y_i(\rho + x)}{y_i(x)} = (\log y_i)'(\rho + x) - (\log y_i)'(x) \geq 0.$$

So $\log \frac{y_i(\rho+x)}{y_i(x)}$ is increasing in x, and so is $\frac{y_i(\rho+x)}{y_i(x)}$. Thus, we have proven strict monotonicity.

Finally, $y_i(0) = +\infty$ because v_t converges to the stationary distribution of $\mathbf{A}$. Therefore, f diverges to plus infinity as x converges to zero. As x becomes arbitrarily large, $y_i(\rho + x)/y_i(x) \to 1$, which concludes the proof of the limits of f. *QED.*

With the Lemma proven, we return to Case 3.2. When $\sum_i \xi_i > \psi$, there is a unique value $\overline{g}_m$ such that $f(\overline{g}_m) = \psi$. This condition immediately rewrites: $\boldsymbol{\zeta}'(\rho \mathbf{I} - \mathbf{B})^{-1} \mathbf{N} \mathbf{h} > \pi$. This value $\overline{g}_m$ only depends on parameters. When $\sum_i \xi_i < \psi$, we define by convention: $\overline{g}_m = +\infty$. We always have $g_m < \overline{g}_m$ in Case 3.1, and $g_m = \overline{g}_m$ in Case 3.2.

In Case 3.1, we have $g_m = \frac{g-\omega}{1+\Delta}$ as in the laissez-faire. Therefore, Case 3.1. arises when $g < \omega + (1+\Delta)\overline{g}_m$ under log utility.

Case 3.2. arises under log utility when $g \geq \omega + (1+\Delta)\overline{g}_m$. We can then solve for $g_E = \overline{g}_m + g_\sigma$. From the production function: $g_Y = \alpha(1-\psi)g_Y + (1-\alpha)(1-\psi)g_Z + \psi g_E$, and so $[1 - \alpha(1-\psi)]g_Y = (1-\alpha)(1-\psi)g_Z + \psi(\overline{g}_m + g_\sigma)$. Noting that $1 - \alpha(1-\psi) = (1-\alpha)(1-\psi)(1+\pi)$, we obtain: $(1+\pi)g_Y = g_Z + \pi g_E = g - \Delta \overline{g}_m + \pi(\overline{g}_m + g_\sigma)$. Rearranging, we obtain:

$$g_Y = \frac{g + (\pi - \Delta)\overline{g}_m + \pi g_\sigma}{1+\pi}.$$

Case 3.3. $\psi = \phi E_t^m / M_t$ **and** $\gamma \neq 1$**.** Define: $z(x) = \overline{\boldsymbol{\zeta}}'[x\mathbf{I} - \mathbf{B}]^{-1}$. Denote by $n_i > 0$ the diagonal elements of $\mathbf{NH}$. Then:

$$\overline{f}(\eta, x) = \sum_{i=1}^{\mathcal{T}} z_i(\eta) n_i \frac{y_i(\eta + x)}{y_i(x)}.$$

By the same arguments as in the Lemma above, $\overline{f}$ is increasing in x, decreasing in η. Given η, $\overline{f}$ limits to 0 and $\sum_i z_i(\eta)n_i$ when x varies between 0 and $+\infty$. Given x, $\overline{f}$ limits to $+\infty$ and 0 when η varies between 0 (its lower bound because of the capital transversality condition) and $+\infty$. Therefore, there exists a unique strictly increasing $X(\eta)$ such that $f(\eta, X(\eta)) = \psi$, which we normalize to being infinite if $\psi > \sum_i z_i(\eta)n_i$. Since z_i is decreasing in η and $z_i(0) = +\infty$, there is always a $\overline{\eta}$ such that $\sum_i n_i z_i(\eta) > \psi$ for $\eta \leq \overline{\eta}$. We also have $X(0) = 0$. Hence X increases from 0 to $+\infty$ for $\eta \in [0, \overline{\eta})$.

In a one-dimensional climate system, $\sum_i n_i z_i(x) = \frac{\zeta \nu h}{x+\nu\lambda}$, and so $\overline{\eta} = \frac{\zeta \nu h}{\psi} - \nu\lambda$. We consider damages between 0.05 and 0.2. ψ is of order 0.05. $\nu = 0.14$, $h \approx 4$ and $\lambda \approx 1$. Therefore, $\overline{\eta}$ is of order 0.35 to 2. To avoid a lengthier discussion of cases below, we therefore impose $\rho < \overline{\eta}$ in what follows. $\overline{\eta}$ is our threshold $\overline{\rho}$.

Substituting into the output growth expression, we obtain:

$$(1+\pi)g_Y = g + (\pi - \Delta)X(\rho - (1-\gamma)g_Y) + \pi g_\sigma.$$

Case 3.3.1. If $\{\gamma < 1 \text{ and } \pi > \Delta\}$, the right-hand-side is decreasing in g_Y and spans $+\infty$ to $g + \pi g_\sigma$ as g_Y spans $\frac{\rho-\overline{\eta}}{1-\gamma} < 0$ to $\frac{\rho}{1-\gamma} > 0$, its lowest and largest possible values. Therefore, if $\frac{(1+\pi)\rho}{1-\gamma} > g + \pi g_\sigma$, there is a unique g_Y that satisfies this equation, and thus $\overline{g}_m = X(\rho - (1-\gamma)g_Y)$. If $\frac{(1+\pi)\rho}{1-\gamma} < g + \pi g_\sigma$, there is no solution g_Y. Hence, we can only be in Case 3.1.

Hence, if $\gamma > 1 - \frac{(1+\pi)\rho}{g+\pi g_\sigma}$, there is a threshold $\overline{g}_m$ and an associated g_Y. If $\gamma < 1 - \frac{(1+\pi)\rho}{g+\pi g_\sigma}$, $\overline{g}_m = +\infty$ and growth rates mirror the laissez-faire.

Case 3.3.2. If $\{\gamma > 1 \text{ and } \pi > \Delta\}$, the right-hand-side is increasing in g_Y and spans $g + \pi g_\sigma > 0$ to $+\infty$ as g_Y spans $-\frac{\rho}{\gamma-1} < 0$ to $\frac{\overline{\eta}-\rho}{\gamma-1} > 0$, its lowest and largest possible values. Hence, there can be no solution, exactly one solution in the knife-edge tangent, or two or more solutions depending on the exact shape of X.

Case 3.3.3. If $\{\gamma < 1 \text{ and } \pi < \Delta\}$, the right-hand-side is increasing in g_Y and spans $-\infty$ to $g + \pi g_\sigma$ as g_Y spans $\frac{\rho-\overline{\eta}}{1-\gamma} < 0$ to $\frac{\rho}{1-\gamma} > 0$, its lowest and largest possible values. Hence, there can be no solution, exactly one solution in the knife-edge tangent, or two or more solutions depending on the exact shape of X.

Case 3.3.4. If $\{\gamma > 1 \text{ and } \pi < \Delta\}$, the right-hand-side is decreasing in g_Y and spans $g + \pi g_\sigma > 0$ to $-\infty$ as g_Y spans $-\frac{\rho}{\gamma-1} < 0$ to $\frac{\overline{\eta}-\rho}{\gamma-1} > 0$, its lowest and largest possible values. Therefore, there is always a unique solution $g_Y > 0$, with an associated threshold $\overline{g}_m$.

The implicit solution g_Y always corresponds to a $\overline{g}_m$ such that $g_Y = \frac{g+(\pi-\Delta)\overline{g}_m+\pi g_\sigma}{1+\pi}$, because this last expression only uses the production function and the definition of emissions.

B.2.3 Comparison of growth rates

We have in the high emissions regime, using the expression of g_Y as a function of g_m in the laissez-faire:

$$g_Y^{\text{SP}} > g_Y^{\text{LF}} \Leftrightarrow \frac{g + (\pi - \Delta)\overline{g}_m + \pi g_\sigma}{1+\pi} > \frac{g + (\pi - \Delta) g_m + \pi g_\sigma}{1+\pi} \Leftrightarrow (\Delta - \pi)(g_m - \overline{g}_m) > 0$$

where $g_m = \frac{g-\omega}{1+\Delta} > \overline{g}_m$. Now, recall that by the properties of M-matrices, $\overline{\Delta} < \Delta$. $\overline{g}_m$ is finite if $\overline{\Delta} > \pi$, and so $\Delta > \pi$. Therefore, $g_Y^{\text{SP}} > g_Y^{\text{LF}}$.

B.2.4 Energy Costs in Labor Units

Now suppose that energy production only uses labor instead of the final good: $E_t = \chi_t^{-1} L_t^E$. An asymptotic growth path requires that the marginal product of capital is stable over time. The marginal product of capital depends on $L_t^Y = 1 - \chi_t E_t$. Therefore, $\chi_t E_t$ must stay constant or shrink over time, implying: $g_\chi + g_E \leq 0$.

Labor optimality implies: $(1-\alpha)(1-\psi)Y_t/L_t^Y = \overline{w}_t$. Hence: $\overline{w}_t$ must grow at g_Y.

Energy demand implies: $F_E = \overline{w}_t \chi_t + \tau_t$, where $\overline{w}_t$ is the planner's multiplier on energy production. Re-arranging as above: $(\psi - \phi E_t^m / M_t)\frac{Y_t}{\overline{w}_t \chi_t E_t} = 1$.

If $\psi > \phi E_t^m / M_t$, $\chi_t E_t$ must be constant. The laissez-faire formulas apply, we need $g_m = -g_\chi - g_\sigma < \overline{g}_m$, where $\overline{g}_m$ is defined as above. If $\psi = \phi E_t^m / M_t$, $g_m = \overline{g}_m$ as above.

B.3 Proof of Corollary 2

In this section we prove Corollary 2 and its CRRA generalization that we state below. We let $\eta = \frac{\theta}{1+\theta}$.

Corollary 5 (Growth with Energy Stock Management). *If $\gamma \geq 1 + 2\theta$, the solution of the exhaustible resource model* (18) *admits a unique asymptotic growth path, which is also a balanced growth path. Propositions 1, 2 and 4 apply, with the following modifications: $g_\chi = 0$, $\omega = \frac{1+\pi\theta}{1-\theta} g_\sigma$, $g_Y = \frac{g+\overline{\Delta} g_\sigma}{1+\pi\theta+\overline{\Delta}(1-\theta)}$ when growth rates coincide, where $\overline{\Delta} = \Delta \mathbb{1}\{g > \omega\}$.*

B.3.1 Setup

Let R_t denote reserves of energy, which evolve according to $\dot{R}_t = X_t - E_t$, where X_t denotes exploration. Exploration comes at a cost that reflects the scarcity of energy: $\frac{\chi(S_t)}{2}\left(\frac{X_t}{R_t}\right)^2 R_t$, where S_t represents cumulative extraction and satisfies $\dot{S}_t = E_t$. We consider an isoelastic specification: $\chi(S_t) = \overline{\chi} S_t^{\frac{\theta}{1+\theta}}$, with $\frac{\theta}{1+\theta} \geq 0$. As before, p_t denotes the price of energy.

In the laissez-faire, households now solve:

$$\max_{\{C_t, K_t, E_t\}_t} \int_0^\infty e^{-\rho t} U(C_t) dt \quad \text{subject to} \quad C_t + \dot{K}_t + \frac{\chi(S_t)}{2}\left(\frac{X_t}{R_t}\right)^2 R_t = r_t K_t + w_t + p_t E_t$$
$$\text{and to} \qquad \dot{R}_t = X_t - E_t, \;\; \dot{S}_t = E_t \tag{18}$$

given K_0, R_0, S_0. To focus on the carbon externality, we require that households internalize that cumulative extraction.

The rest of the economy is unchanged. We omit the definition of the efficient allocation for brevity. The shifter of the exploration cost $\overline{\chi}$ is constant because we model the effect of scarcity on extraction costs explicitly through the dependence on cumulative extraction S_t.

To avoid a lengthy discussion of cases, we require two mild restrictions that are consistent with the data. First, that there is some progress in carbon intensity over time, $g_\sigma \geq 0$. Second, output growth is positive, which we show can be ensured by $\theta < 1$ and $1 + \pi\theta > 0$.

B.3.2 Exhaustible Resources with a Fixed Limit

We start with a formulation in which extraction is not possible: $X_t \equiv 0$. The partial current-value Hamiltonian (excluding the climate system) is: $\mathcal{H} = U(C_t) + \lambda_t(r_t K_t + w_t + p_t E_t - C_t) + q_t(-E_t)$. Optimality requires: $\lambda_t = u'(C_t)$, $\gamma \dot{C}_t / C_t = r_t - \rho$, $u'(C_t) p_t = q_t$, and $\rho q_t - \dot{q}_t = 0$. Combining the last two equations, we obtain: $\gamma \dot{C}_t / C_t = \dot{p}_t / p_t - \rho$.

Hence we obtain the classic Hotelling result that energy prices grow at the interest rate: $\dot{p}_t/p_t = r_t$. On a constant growth path: $r = \rho + \gamma g_Y$, so that energy prices grow at rate $g_p = \rho + \gamma g_Y$.

Using that $g_m = g_Y - g_p - g_\sigma$, we obtain: $g_m = -(\rho + (\gamma - 1)g_Y) - g_\sigma$, with $\rho + (\gamma - 1)g_Y > 0$ by the capital transversality condition. We immediately see that $g_m < 0$ if $g_\sigma < 0$: carbon and temperature stabilize in the long run. But if $g_\sigma < 0$, we can still obtain positive emissions growth. Recall that $g_E = g_m + g_\sigma = -(\rho + (\gamma - 1)g_Y) < 0$.

Case 1. $g_m < 0$. Carbon and temperature stabilizes, productivity grows at rate g. Then: $(1 + \pi)g_Y = g - \pi[\rho + (\gamma - 1)g_Y]$. Re-arranging: $g_Y = \frac{g - \pi\rho}{1 + \pi\gamma}$. We then obtain: $g_m + g_\sigma = -\frac{(1+\pi)\rho + (\gamma-1)g}{1+\pi\gamma}$. So $g_m < 0$ if and only if $g_\sigma + \frac{(1+\pi)\rho + (\gamma-1)g}{1+\pi\gamma} > 0$. This is always satisfied if $g_\sigma > 0$ and when $\gamma \geq 1$.

Case 2. $g_m > 0$. Carbon grows at g_m with a productivity drag at rate Δg_m. Therefore: $(1 + \pi)g_Y = g - \Delta(g_E - g_\sigma) + \pi g_E = g + (\pi - \Delta)g_E + \Delta g_\sigma = g - (\pi - \Delta)[\rho + (\gamma - 1)g_Y] + \Delta g_\sigma$. Re-arranging: $g_Y = \frac{g - \pi\rho + \Delta(\rho + g_\sigma)}{1 + \pi\gamma - (\gamma-1)\Delta}$, and $g_m > 0$ based on the other side of the condition from Case 1.

B.3.3 Laissez-Faire with Exploration

We now allow for exploration, but exploration costs do not depend on cumulative past extraction: $\theta = 0$.

The partial current-value Hamiltonian (excluding the climate system) is: $\mathcal{H} = U(C_t) + \lambda_t(r_t K_t + w_t + p_t E_t - C_t - \chi_t(X_t/R_t)^2 R_t/2) + q_t(X_t - E_t)$. As above, optimality requires: $\lambda_t = u'(C_t)$, $\gamma \dot{C}_t/C_t = r_t - \rho$, $u'(C_t)p_t = q_t$.

The optimality condition for exploration is, after re-expressing q_t: $X_t = \frac{p_t R_t}{\chi_t}$. The co-state equation for R_t now changes. We obtain: $\rho q_t - \dot{q}_t = u'(C_t)\frac{\chi_t}{2}\left(\frac{X_t}{R_t}\right)^2$. Substituting in the other conditions: $\rho q_t - \dot{q}_t = u'(C_t)\frac{p_t^2}{2\chi_t}$. Further re-arranging: $\gamma \dot{C}_t/C_t = \frac{\dot{p}_t}{p_t} + \frac{p_t}{2\chi_t} - \rho$.

Therefore, we now obtain: $g_p + \frac{p_t}{2\chi_t} = r = \rho + \gamma g_Y$ on a constant growth path. For this condition to hold as t grows, we need the term p_t/χ_t to remain bounded. This requires $g_p \leq g_\chi$.

Case 1. $g_p = g_\chi$. We obtain exactly the same equilibrium conditions as in our baseline with a static extraction cost, with one exception. The exception is that the level of the energy price is determined by the condition $g_\chi + \frac{p}{2\chi} = \rho + \gamma g_Y$. This condition only affects the level of the energy price, not its growth rate. Thus, Proposition 1 applies.

We need to make sure that extraction costs do not affect the ACGP. When $g_p = g_\chi$, extraction costs grow as R_t. In addition, we have: $X_t/R_t = p_t/\chi_t = 2(r - g_\chi) = 2r = 2(\rho + \gamma g_Y)$. So R_t evolves according to: $\dot{R}_t = 2rR_t - E_t$. Since $g_E = g_Y$, we can solve explicitly: $R_t = \overline{R}e^{2rt} + \frac{E_0 e^{g_Y t}}{2r - g_Y}$ for some $\overline{R}$. The reserve transversality condition is $e^{-\rho t}u'(C_t)p_t R_t \to 0$, that is, $e^{-rt}R_t \to 0$. Therefore: $\overline{R} = 0$, and reserves R_t grow at rate g_Y, which is consistent with the resource constraint.

Finally, we must check $g_Y < r = \rho + \gamma g_Y$. We have: $g_Y = \frac{g + (\Delta - \pi)g_\chi + \Delta g_\sigma}{1 + \Delta}$. A sufficient condition for $g_Y < r$ is $(\gamma - 1)g_Y \geq 0$, i.e. $(\gamma - 1)(g + (\Delta - \pi)g_\chi + \Delta g_\sigma) \geq 0$.

Case 2. $g_p < g_\chi$. We obtain $g_p = \rho + \gamma g_Y$ as in the exhaustible resource model with a hard limit. We need to check whether, indeed, $\rho + \gamma g_Y < g_\chi$. To simplify the following discussion, we impose $g_\chi = 0$ because we are already modeling scarcity directly. Hence, we would need negative output growth for this case to arise.

Case 2.1. $g_m < 0$. Then $\rho + \gamma g_Y = \frac{\rho + \gamma g}{1 + \gamma \pi} > 0$, a contradiction.

Case 2.2. $g_m > 0$. Then: $g_Y = g_m + g_\sigma > 0$ if $g_\sigma > 0$. Then: $\rho + \gamma g_Y > 0$, a contradiction.

B.3.4 Efficient Allocation with Exploration

We still allow for exploration, but exploration costs do not depend on cumulative past extraction: $\theta = 0$.

The partial current-value Hamiltonian (excluding the climate system) writes: $\mathcal{H} = U(C_t) + \lambda_t(F(Z(\mathbf{T}_t), K_t, 1, E_t) - \delta K_t - C_t - \chi_t(X_t/R_t)^2 R_t/2) + q_t(X_t - E_t) + \boldsymbol{\mu}_t'(\mathbf{AM}_t + \sigma_t E_t \mathbf{m}) + \boldsymbol{\nu}_t'(\mathbf{BT}_t + \mathbf{NF}_{eq} + \mathbf{NH}(\log \mathbf{M}_t - \log \mathbf{M}_{eq})$. Let $p_t = q_t/u'(C_t)$. The only optimality condition that differs from the laissez-faire is the one for energy: $\lambda_t \psi \frac{Y_t}{E_t} + \tau_t = p_t$. As in the laissez-faire, we obtain: $g_p + \frac{p_t}{2\chi_t} = \rho + \gamma g_Y$.

We consider the same cases as in the laissez-faire. If $g_p = g_\chi = 0$, Propositions 2 and 4 apply.

If $g_p < g_\chi < 0$, we obtain the same optimality conditions as in the planner problem. Hence, Propositions 2 and 4 apply conditional on replacing g_χ by the (endogenous) expression for g_p. We also obtain $g_p = \rho + \gamma g_Y$ as in the laissez-faire. We must now verify that these Propositions apply unconditionally to g_p.

If $g_m < 0$, growth rates from the laissez-faire apply, and we obtain the same contradiction as in the laissez-faire. If $0 < g_m$, growth rates from the laissez-faire apply and we obtain the same contradiction as in the laissez-faire.

If $g_m = \overline{g}_m > 0$ which is independent from g_p, the growth rate of p is irrelevant to the entire asymptotic growth path. Then, Propositions 2 and 4 apply directly.

B.3.5 Laissez-Faire with Exploration and Scarcity

We denote by $\eta = \frac{\theta}{1+\theta}$ the elasticity of the cost shifter. The partial current-value Hamiltonian (excluding the climate system) is:

$$\mathcal{H} = U(C_t) + \lambda_t \left(r_t K_t + w_t + p_t E_t - C_t - \frac{\chi(S_t)}{2} \left(\frac{X_t}{R_t} \right)^2 R_t \right) + q_t (X_t - E_t) + v_t E_t.$$

Define $v_t = z_t u'(C_t)$ and $\pi_t = p_t + z_t$. As above, optimality requires: $\lambda_t = u'(C_t)$, $\gamma \dot{C}_t / C_t = r_t - \rho$. Now, however, we have the energy and exploration FOCs:

$$q_t = \lambda_t \pi_t \qquad \lambda_t \chi_t \frac{X_t}{R_t} = q_t \qquad \Rightarrow \qquad \frac{X_t}{R_t} = \frac{\pi_t}{\chi_t}.$$

The co-state equations are as follows:

$$(R) \;\; \rho q_t - \dot{q}_t = \lambda_t \frac{\pi_t^2}{2\chi_t} \qquad (S) \;\; \rho v_t - \dot{v}_t = -\lambda_t \frac{\chi_t'}{2\chi_t^2} \pi_t^2 R_t$$

where $\chi_t' = \chi'(S_t)$. Using the Euler equation: $\dot{q} = \lambda((\rho - r)\pi + \dot{\pi})$, and $\dot{v} = \lambda((\rho - r)z + \dot{z})$. Therefore:

$$r_t \pi_t - \dot{\pi}_t = \frac{\pi_t^2}{2\chi_t} \qquad r_t z_t - \dot{z}_t = -\frac{\chi_t'}{2\chi_t^2} \pi_t^2 R_t$$

On a constant growth path, the first equation implies:

$$r = g_\pi + \frac{\pi_t}{2\chi_t}.$$

Now let $\chi(S) = \chi_0 S^\eta$ have a constant elasticity. Then: $g_\chi = \eta g_S = \eta g_E = \eta(g_Y - g_p)$ where the second to last equality follows from the fact that S_t grows at the growth rate of E_t, and the last equality follows from the energy FOC of the firm. The z_t equation

becomes:

$$rz_t - \dot{z}_t = -\frac{\eta}{2}\frac{\pi_t^2 R_t}{\chi_t S_t}.$$

We now distinguish cases as before.

Case 1. $g_\pi = g_\chi$. Then: $\pi/2\chi$ is a constant. We obtain: $g_\pi = g_\chi = \eta g_E$. The z_t equation then becomes: $rz_t - \dot{z}_t = -\xi\frac{\pi_t R_t}{S_t}$, with $\xi = \frac{\eta}{2}\frac{\pi}{\chi}$.

The term $\frac{\pi_t R_t}{S_t}$ grows at rate $(\eta-1)g_E + g_R$. Solving the z_t equation forward, we obtain that z_t is negative and grows at rate $g_z = (\eta-1)g_E + g_R$, with $g_E = g_Y - g_p$.

As before, we obtain that $\dot{R}_t = (2r - \eta g_E)R_t - E_t$. So R_t grows at $g_R = \max\{2r - \eta g_E, g_E\}$. The R transversality condition implies that $e^{-\rho t}q_t R_t \to 0$. Re-arranging, this implies: $e^{-rt}\pi_t R_t \to 0$. Since π_t grows at ηg_E, the TVC term grows at $\max\{r, (1+\eta)g_E - r\}$. Therefore, the component of R_t that grows at $2r - g_E$ must be zero, and so: $g_R = g_E$. We will need to verify whether, in equilibrium, $(1+\eta)g_E < r$.

Since $g_R = g_E$, we obtain that $g_z = \eta g_E = g_\chi$. Thus, π and z grow at the same rate, so that $p_t = \pi_t - z_t$ with both components positive implies: $g_p = g_\pi = g_z = g_\chi = \eta g_E$. The firm's energy FOC then implies: $g_Y = g_E - g_p = (1-\eta)g_E$, and so $g_\chi = \frac{\eta}{1-\eta}g_Y$ if $\eta \neq 1$, and $g_Y = 0$ otherwise.

We can now apply Proposition 1 conditional on $g_\chi = \frac{\eta}{1-\eta}g_Y$. To simplify the discussion, we define: $\theta = \frac{\eta}{1-\eta}$, which spans $-\infty$ to $+\infty$, except the interval $(-1, 0]$. It is positive for $\eta < 1$ and negative for $\eta > 1$. We have: $g_\chi = \theta g_Y$.

Case 1.1. $g < \omega$. Then $g_m < 0$, and case (i) applies: $g_Y = g - \pi g_\chi$, implying $g_Y = \frac{g}{1+\pi\theta}$. The condition for $g_m < 0$ becomes: $g_Y < g_\chi + g_\sigma$, i.e.: $(1-\theta)g_Y < g_\sigma$.

To avoid a lengthy discussion of cases, from now on we focus on cases in which $g_Y > 0$ in Case 1.1. This condition requires $1 + \pi\theta > 0$, which is satisfied if $\theta > -1/\pi$. This condition is satisfied if $\eta < 1$, or if $\{\eta > \frac{1}{1-\pi}$ and $\pi < 1\}$. Then, the condition for $g_m < 0$ requires $\frac{1-\theta}{1+\pi\theta}g < g_\sigma$, where both factors on the right-hand-side are positive.

We now verify whether $r = \rho + \gamma g_Y > (1+\eta)g_E = \frac{1+\eta}{1-\eta}g_Y$. This condition is met if and only if: $\rho + \left(\gamma - \frac{1+\eta}{1-\eta}\right)g_Y > 0$. Since $g_Y > 0$, a sufficient condition is $\gamma \geq \frac{1+\eta}{1-\eta} = 1 + 2\theta$, which is itself larger than 1 if $\eta < 1$, but does not bind if $\eta > 1$.

Case 1.2. $g > \omega$. Then $g_m > 0$, and case (iii) applies: $g_Y = g_\chi + g_\sigma + \frac{g-\omega}{1+\Delta} = \frac{g+(\Delta-\pi)g_\chi+\Delta g_\sigma}{1+\Delta}$, implying $g_Y = \frac{g+\Delta g_\sigma}{1+\Delta+\theta(\pi-\Delta)}$. The condition for $g_m > 0$ is the converse of the one from Case 1.1.

We obtain that $g_Y > 0$ iff either $\{\theta < \frac{1+\Delta}{\Delta-\pi}$ and $\Delta > \pi\}$, or $\{\theta > -\frac{1+\Delta}{\pi-\Delta}$ and $\Delta < \pi\}$. If $\theta < 1$ and $1 + \pi\theta > 0$, $g_Y > 0$.

We can now verify whether $r = \rho + \gamma g_Y > (1+\eta)g_E = \frac{1+\eta}{1-\eta} g_Y$. When $g_Y > 0$, a sufficient condition is $\gamma \geq \frac{1+\eta}{1-\eta}$ as above. When $g_Y < 0$, a sufficient condition is $\gamma \leq \frac{1+\eta}{1-\eta}$. Note also that given $1 + \pi\theta \geq 0$, $g_Y > 0$ if $\frac{1-2\eta}{1-\eta} \geq 0$, which requires $\eta \in (1/2, 1)$.

We summarize these conditions as: $\left(\gamma - \frac{1+\eta}{1-\eta}\right)\left(1 + \frac{\eta}{1-\eta}\frac{\pi-\Delta}{1+\Delta}\right) \geq 0$. When $\eta \to 0$ we recover $\gamma \geq 1$ similarly to above when setting $g_\chi = 0$.

Case 2. $g_\pi < g_\chi$. We then obtain $g_\pi = r = \rho + \gamma g_Y$. As above, we use the resource accumulation equation to characterize g_p. $\dot{R}_t/R + t = X_t/R_t - E_t/R_t$. Since $X_t/R_t \to 0$ by assumption in Case 2, $g_R = g_E < 0$. Transversality requires $(1+\eta)g_E < r$.

Since $r < g_\chi = \eta g_E$, we must have: $r < \eta g_E < (1+\eta)g_E < r$, a contradiction.

B.3.6 Efficient Allocation with Exploration and Scarcity

The only optimality condition that differs from the laissez-faire is energy use: $\lambda_t \psi \frac{Y_t}{E_t} + \tau_t = \pi_t$.

If $g_\pi = g_\chi$, Propositions 2 and 4 apply with the same modifications as for the laissez-faire since $\overline{g}_m$ is determined by an equation that where the only dependence on the economic module is g_Y.

If $g_\pi < g_\chi$: if $g_m < \overline{g}_m$, growth rates from the laissez-faire apply, and we obtain the same contradiction. If $g_m = \overline{g}_m$ which is independent from g_π, the growth path is independent from g_π, and Propositions 2 and 4 apply.

B.4 Proof of Corollary 3

In this section, we prove the following result.

Corollary 6 (Endogenous Technological Growth)**.** *Proposition 1, 2 and 4 apply to the endogenous growth model, with the following modifications:* $\omega^i = (1 + \Gamma^i + \pi)g_\chi + (1 + \Gamma^i)g_\sigma$, $g_Y^i = \frac{g^i + (\overline{\Delta}^i - \pi)g_\chi + \overline{\Delta} g_\sigma}{1+\Gamma^i+\pi}$, *where* $\overline{\Delta}^i = \Delta \mathbb{1}\{g^i > \omega^i\}$ *and* Γ_i *is proportional to* $\gamma - 1$, *for* $i = LF, SP$.

B.4.1 Setup

Consider a quality ladder model as in Grossman and Helpman (1991) and Aghion and Howitt (1992). There are now a continuum of intermediate varieties $j \in [0,1]$, across which households have Cobb-Douglas preferences with uniform weights. They all use the production function F, but may differ in productivity/quality. We have:

$$\log Y_t = \int_0^1 \log y_{jt} dj.$$

Demand for each variety is given by: $p_{jt} y_{jt} = Y$, where we use the aggregate price index as the numeraire. For a monopolist in variety j, the monopolistically competitive price is therefore to charge an infinite markup over marginal cost.

Each variety j is produced according to:

$$y_{jt} = z_{jt}^{(1-\alpha)(1-\psi)} F_t^* \ell_{jt},$$

where F_t^* denotes the production function evaluated at aggregate productivity of 1 and optimal input ratios $k_{jt}/\ell_{jt}, e_{jt}/\ell_{jt}$; ℓ_{jt} denotes labor demand; and z_{jt} is productivity of variety j.

There is free entry and perfect competition in each variety. In each variety, there is always a leader with a productivity advantage $z_{jt} = \lambda \widetilde{z}_{jt}$ over a competitive fringe with the old technology $\widetilde{z}_{jt}$. Let $\overline{z}_{jt} = \widetilde{z}_{jt}^{(1-\alpha)(1-\psi)}$. Given perfect competition, the leader uses limit pricing: $p_{jt} = \text{mc}_{jt} = \frac{w_t}{\overline{z}_{jt} F_t^*}$. Quantity is then: $y_{jt} = \frac{Y_t \overline{z}_{jt} F_t^*}{w_t}$. Profits are: $\pi_{jt} = \frac{\overline{\lambda}-1}{\overline{\lambda}} Y_t \equiv \varpi Y_t$, with $\overline{\lambda} = \lambda^{(1-\alpha)(1-\psi)}$.

Innovation labor n_{jt} allows to innovate on the leader by the step size λ at rate $\iota_{jt} = \eta n_{jt}$. The value of holding the patent to the leading technology satisfies:

$$r_t V_{jt} - \dot{V}_{jt} = \pi_{jt} - \iota_{jt} V_{jt},$$

where the last term represents displacement by new entrants. Free entry into innovation requires: $w_t = \eta V_{jt}$.

We focus on a symmetric equilibrium. We obtain: $(r_t + \iota_t) V_t - \dot{V}_t = \varpi Y_t$. Therefore, on a constant growth path, $g_w = g_V = g_Y$. Hence: $(r + \iota - g_Y) V_t = \varpi Y_t$, and $w_t = \eta V_t$.

Re-arranging:

$$\frac{w_t}{Y_t} = \frac{\eta\varpi}{r + \iota - g_Y} = \frac{\eta\varpi}{\rho + \iota + (\gamma - 1)g_Y}.$$

Using the production FOC w.r.t. labor, and denoting $\kappa = (1 - \alpha)(1 - \psi)$, we obtain:

$$\kappa = \frac{\eta\varpi L^Y}{\rho + \iota + (\gamma - 1)g_Y}.$$

ι is determined by the amount of labor in innovation:

$$\iota = \eta L^I = \eta(1 - L^Y).$$

Substituting into the previous equation, we pin down L^Y from:

$$\kappa = \frac{\eta\varpi L^Y}{\rho + \eta(1 - L^Y) + (\gamma - 1)g_Y}.$$

Its solution is

$$L^Y = L_0^Y + L_1^Y(\gamma - 1)g_Y,$$

where L_0^Y and L_1^Y are functions of parameters only.

Finally, since production admits constant returns, production is isomorphic to an aggregate production function with aggregate productivity Z_t:

$$\log Z_t = \int_0^1 \log z_{jt} dj.$$

For every period dt, a fraction ιdt of varieties experience a successful innovation, so that Z_t grows at exponential rate:

$$g_Z = \iota \log \lambda = \eta(1 - L^Y) \log \lambda = g - \Gamma g_Y$$

where $g = \eta(1 - L_0^Y) \log \lambda$, and $\Gamma = (\gamma - 1)\eta L_1^Y \log \lambda$. Under log utility, technology growth is entirely determined as a function of parameters.

B.4.2 Laissez-Faire

Under log utility, Proposition 1 applies directly. Away from log utility, we only have to account for the equilibrium feedback between g_Z and g_Y. Recall that $g_m = g_Y - g_\chi - g_\sigma$.

Case 1. $g_m < 0$. Then: $g_Y = g_Z - \pi g_\chi = g - \Gamma g_Y - \pi g_\chi$, so that: $g_Y = \frac{g - \pi g_\chi}{1+\Gamma}$. Then: $g_m = \frac{g - \pi g_\chi}{1+\Gamma} - g_\chi - g_\sigma$.

Case 2. $g_m > 0$. Then: $g_Y = g_Z - \pi g_\chi = g - \Gamma g_Y - \Delta(g_Y - g_\chi - g_\sigma) - \pi g_\chi$, so that: $g_Y = \frac{g + (\Delta - \pi) g_\chi + \Delta g_\sigma}{1+\Gamma+\Delta}$.

B.4.3 Efficient Allocation

Planner conditions. We set up the planning problem after aggregation. The planner solves:

$$\begin{aligned} & \max_{\{C_t, K_t, E_t, L_t^Y\}_t} \int_0^\infty e^{-\rho t} U(C_t) dt \\ \text{subject to} \quad & C_t + \dot{K}_t = F(Z_t, K_t, L_t^Y, E_t) - \chi_t E_t \\ & \frac{\dot{Z}_t}{Z_t} = (\lambda - 1)\eta(1 - L_t^Y) \\ \text{and to} \quad & \text{equations (2), (3), (6), (5), (7)} \end{aligned} \tag{19}$$

The partial current-value Hamiltonian (omitting the climate module) is:

$$\mathcal{H} = U(C_t) + \lambda_t \Big(F(Z_t, K_t, L_t^Y, E_t) - \chi_t E_t - C_t \Big) + q_t Z_t (\lambda - 1)\eta(1 - L_t^Y).$$

The optimality condition for production labor and the co-state equation for Z_t are:

$$F_{Lt} = \eta(\lambda - 1)\frac{q_t}{\lambda_t} Z_t \qquad\qquad \rho q_t - \dot{q}_t = \lambda_t F_{Zt} + q_t(\lambda - 1)\eta(1 - L_t^Y).$$

Denote $q_t = \frac{\lambda_t V_t}{Z_t}$ and $\iota_t = \eta(1 - L_t^Y)$, so that re-arranging the first equation, and combining the second equation with the Euler equation:

$$\kappa = \eta(\lambda - 1)\frac{V_t}{Y_t} L_t^Y \qquad\qquad r_t V_t - \dot{V}_t = \kappa Y_t - g_Z V_t + (\lambda - 1)\iota_t V_t.$$

where $r_t = F_K$. Now, by definition, g_Z cancels out with the last term. In addition, on a constant growth path, V_t and Y_t grow at g_Y, so that:

$$(r - g_Y)V_t = \kappa Y_t.$$

Combining with the FOC, we obtain:

$$1 = \frac{\eta(\lambda - 1)}{\rho + (\gamma - 1)g_Y} L^Y.$$

This implies:

$$g_Z = \eta(\lambda - 1) - [\rho + (\gamma - 1)g_Y].$$

Under log utility, $g_Z = \eta(\lambda - 1) - \rho$ is once more pinned down by parameters.

Emissions. Under log utility, Proposition 2 applies directly, albeit with a different $g = \eta(\lambda - 1)$ than in the decentralized equilibrium. Away from log utility, we only have to account for the equilibrium feedback between g_Z and g_Y. Recall that $g_m = g_Y - g_\chi - g_\sigma$. Define $\Gamma = \gamma - 1$ in the planner problem.

Case 1. $g_m < 0$. Then: $g_Y = g_Z - \pi g_\chi = g - \Gamma g_Y - \pi g_\chi$, so that: $g_Y = \frac{g - \pi g_\chi}{1+\Gamma}$. Then: $g_m = \frac{g - \pi g_\chi}{1+\Gamma} - g_\chi - g_\sigma$.

Case 2. $\bar{g}_m > g_m > 0$. $\bar{g}_m$ satisfies the same equation as in the baseline economy, since it is independent from g_Z. Then: $g_Y = g_Z - \pi g_\chi = g - \Gamma g_Y - \Delta(g_Y - g_\chi - g_\sigma) - \pi g_\chi$, so that: $g_Y = \frac{g + (\Delta - \pi)g_\chi + \Delta g_\sigma}{1+\Gamma+\Delta}$.

Case 3. $g_m = \bar{g}_m$. Then: $(1 + \pi)g_Y = g_Z + \pi(\bar{g}_m + g_\sigma) = g - \Gamma g_Y - \Delta \bar{g}_m + \pi(\bar{g}_m + g_\sigma)$, so that: $g_Y = \frac{g + (\pi - \Delta)\bar{g}_m + \pi g_\sigma}{1+\Gamma+\Delta}$.

Proposition 4 applies conditional on these expressions for growth rates.

B.5 Proof of Corollary 4

In this section we consider the energy bundle from Appendix A.2 and embed endogenous growth in the renewable energy sector. Recall that we then have:

$$\chi_t = \overline{\chi}_t \xi_t^{\beta} \qquad \sigma_t = \overline{\sigma}_t \xi_t^{\beta}$$
$$g_\chi = \overline{g}_\chi + \beta g_\xi \qquad g_\sigma = \overline{g}_\sigma - \beta g_\xi,$$

where ξ_t is the extraction cost of green energy, and $\overline{\chi}_t, \overline{\sigma}_t$ represent extraction costs of fossil fuel energy. β is the Cobb-Douglas energy share of green energy. Recall also that with our convention we define $\sigma_t = \sigma_0 e^{-g_\sigma t}$.

Renewable energy is produced with the final good with relative productivity $1/\xi_t$. As above, there is a unit Cobb-Douglas continuum of varieties of renewable goods, each facing a quality ladder. We can directly apply the formulas above. We thus prove the following result.

Corollary 7 (Endogenous Progress in Renewable Energy)**.** *Proposition 1, 2 and 4 apply to the model of innovation in renewables, with the following modifications:* $\omega^i = \overline{g}_\chi + \pi \widetilde{g}_\chi^i + \pi\Gamma \overline{g}_\chi + (1+\pi\Gamma^i)\overline{g}_\sigma$ *and* $g_Y^i = \frac{g + \overline{\Delta}^i \overline{g}_\chi - \pi \widetilde{g}_\chi^i + \overline{\Delta}\overline{g}_\sigma}{1+\pi\Gamma^i+\pi}$*, where* $\overline{\Delta}^i = \Delta \mathbb{1}\{g > \omega^i\}$*, for* $i = LF, SP$*.*

B.5.1 Laissez-Faire

On a growth path, we obtain:

$$\begin{aligned}
\frac{w_t}{\xi_t G_t} &= \frac{\eta \varpi}{\rho + \iota + (\gamma-1) g_G} \quad \text{iff} \quad L_t^Y \in (0,1) \\
\frac{w_t}{\xi_t G_t} &> \frac{\eta \varpi}{\rho + \iota + (\gamma-1) g_G} \quad \text{iff} \quad L_t^Y = 1 \\
\frac{w_t}{\xi_t G_t} &< \frac{\eta \varpi}{\rho + \iota + (\gamma-1) g_G} \quad \text{iff} \quad L_t^Y = 0
\end{aligned}$$

where now market size is spending on green energy $\xi_t G_t$ instead of Y_t (note that when market size was Y_t, there was implicitly a unit price of the numeraire). $\xi_t G_t$ is the total number of final good units needed to produce G_t green energy. Innovation is still paid in labor units. Using the production FOCs for labor and for energy, we obtain:

$$\kappa = \frac{w_t L_t^Y}{Y_t} \qquad \psi = \frac{\chi_t E_t}{Y_t} \qquad \beta = \frac{\xi_t G_t}{\chi_t E_t}.$$

Combining these equations, we obtain:

$$\frac{w_t}{\xi_t G_t} = \frac{\kappa}{\beta\psi}\frac{1}{L_t^Y} \qquad\qquad \beta\psi = \frac{\xi_t G_t}{Y_t},$$

with the latter equation implying $g_\xi + g_G = g_Y$.

We start by assuming an interior solution. Then:

$$\frac{\kappa}{\beta\psi} = \frac{\eta\varpi L^Y}{\rho + \eta(1 - L^Y) + (\gamma - 1)(g_Y - g_\xi)}.$$

The definition of the growth rate of productivity in the renewable sector is:

$$-g_\xi = \eta(1 - L_t^Y)\log\lambda,$$

with $\Gamma > 0$. Therefore, we obtain:

$$\frac{\kappa}{\beta\psi} = \frac{\eta\varpi L^Y}{\eta(1 + (\gamma - 1)\log\lambda)(1 - L^Y) + \rho + (\gamma - 1)g_Y}.$$

As above, the solution of this equation is:

$$L^Y = L_0^Y + L_1^Y(\gamma - 1)g_Y,$$

where L_0^Y, L_1^Y are functions of parameters only. Then:

$$g_\xi = -\eta\log\lambda\Big(1 - L_0^Y - L_1^Y(\gamma - 1)g_Y\Big) \equiv g_{\xi,0} + \Gamma_\xi g_Y \qquad \Gamma_\xi \equiv (\gamma - 1)L_1^Y\eta\log\lambda.$$

This equation then implies:

$$\begin{aligned} g_\chi &= \widetilde{g}_\chi + \Gamma g_Y & \widetilde{g}_\chi &= \overline{g}_\chi + \beta g_{\xi,0} & \Gamma &= \beta(\gamma - 1)L_1^Y\eta\log\lambda \\ g_\sigma &= \widetilde{g}_\sigma - \Gamma g_Y & \widetilde{g}_\sigma &= \overline{g}_\sigma - \beta g_{\xi,0} \end{aligned}$$

As above, with log utility, Proposition 1 applies directly with g_χ, g_σ now functions of parameters.

Away from log utility we have to incorporate the equilibrium link between g_χ, g_σ and g_Y. Recall that $g_m = g_Y - g_\chi - g_\sigma = g_Y - \widetilde{g}_\chi - \widetilde{g}_\sigma = g_Y - \overline{g}_\chi - \overline{g}_\sigma$. With a Cobb-Douglas energy bundle, technological progress in renewables exactly cancels out with the higher

implied fossil fuel demand in combined carbon savings σ_t/χ_t.

Case 1. $g_m < 0$. Then: $g_Y = g_Z - \pi g_\chi = g - \pi\widetilde{g}_\chi - \pi\Gamma g_Y$, so that:

$$g_Y = \frac{g - \pi\widetilde{g}_\chi}{1 + \pi\Gamma}.$$

Then: $g_m = \frac{g-\pi\widetilde{g}_\chi}{1+\pi\Gamma} - \overline{g}_\chi - \overline{g}_\sigma$. $g_m < 0$ then is equivalent to:

$$g < \overline{g}_\chi + \pi\widetilde{g}_\chi + \pi\Gamma\overline{g}_\chi + (1 + \pi\Gamma)\overline{g}_\sigma \equiv \omega,$$

assuming $1 + \pi\Gamma > 0$.

Case 2. $g_m > 0$. Then: $g_Y = g_Z - \Delta g_m - \pi g_\chi = g - \Delta\big(g_Y - \overline{g}_\chi - \overline{g}_\sigma\big) - \pi\widetilde{g}_\chi - \pi\Gamma g_Y$, so that:

$$g_Y = \frac{g + \Delta\overline{g}_\chi - \pi\widetilde{g}_\chi + \Delta\overline{g}_\sigma}{1 + \pi\Gamma + \Delta}.$$

B.5.2 Efficient Allocation

The partial current-value Hamiltonian (omitting the climate module) is:

$$\mathcal{H} = U(C_t) + \lambda_t\Big(F(Z_t, K_t, L_t^Y, E_t) - \overline{\chi}_t\xi_t^\beta E_t - C_t\Big) - q_t\xi_t(\lambda - 1)\eta(1 - L_t^Y),$$

where we have already optimized the choice of green vs. brown energy. The optimality condition for production labor and the co-state equation for ξ_t are:

$$F_{Lt} = -\eta(\lambda - 1)\frac{q_t}{\lambda_t}\xi_t \qquad\qquad \rho q_t - \dot{q}_t = -\beta\lambda_t\frac{\chi_t E_t}{\xi_t} - q_t(\lambda - 1)\eta(1 - L_t^Y).$$

Denote $q_t = \frac{\lambda_t V_t}{\xi_t}$ and $\iota_t = \eta(1 - L_t^Y)$, so that re-arranging the first equation, and combining the second equation with the Euler equation:

$$\kappa = -\eta(\lambda - 1)\frac{V_t}{Y_t}L_t^Y \qquad\qquad r_t V_t - \dot{V}_t = -\beta\psi Y_t - g_\xi V_t - (\lambda - 1)\iota_t V_t.$$

where $r_t = F_K$. Now, by definition, g_ξ cancels out with the last term. In addition, on a constant growth path, V_t and Y_t grow at g_Y, so that:

$$(r - g_Y)V_t = -\beta\psi Y_t.$$

Combining with the FOC, we obtain:

$$1 = \frac{\beta\psi\eta(\lambda-1)}{\rho + (\gamma-1)g_Y} L^Y.$$

This implies:

$$\begin{aligned}
g_\xi &= -\left\{\eta(\lambda-1) - \frac{\rho}{\beta\psi}\right\} + \frac{(\gamma-1)}{\beta\psi} g_Y \equiv g_{\xi,0} + g_{\xi,1} g_Y \\
g_\chi &= \overline{g}_\chi + \beta g_{\xi,0} + \frac{\gamma-1}{\psi} g_Y \equiv \widetilde{g}_\chi + \Gamma g_Y \\
g_\sigma &= \overline{g}_\sigma - \beta g_{\xi,0} - \Gamma g_Y \equiv \widetilde{g}_\sigma - \Gamma g_Y.
\end{aligned}$$

where $g_{\xi,0} = -\left\{\eta(\lambda-1) - \frac{\rho}{\beta\psi}\right\}$ and $\Gamma = \frac{\gamma-1}{\psi}$.

Emissions. Under log utility, Proposition 2 applies directly, albeit with different g_χ, g_σ than in the decentralized equilibrium. Away from log utility, we only have to account for the equilibrium feedback between g_χ, g_σ and g_Y. Recall that $g_m = g_Y - g_\chi - g_\sigma = g_Y - \overline{g}_\chi - \overline{g}_\sigma$.

The same formulas as in the laissez-faire apply for $g_m < \overline{g}_m$, conditional on changing Γ and $\widetilde{g}_\chi, \widetilde{g}_\sigma$ appropriately.

Case 1. $g_m < 0$. We obtain: $g_Y = \frac{g - \pi\widetilde{g}_\chi}{1+\pi\Gamma}$ and $g_m < 0$ iff $g < \overline{g}_\chi + \pi\widetilde{g}_\chi + \pi\Gamma\overline{g}_\chi + (1+\pi\Gamma)g_\sigma \equiv \omega$ assuming $1 + \pi\Gamma > 0$.

Case 2. $\overline{g}_m > g_m > 0$. $\overline{g}_m$ satisfies the same equation as in the baseline economy, since it is independent from g_χ, g_σ. Then the laissez-faire formula applies conditional on $\widetilde{g}_\chi, \widetilde{g}_\sigma, \Gamma$: $g_Y = \frac{g + \Delta\overline{g}_\chi - \pi\widetilde{g}_\chi + \Delta\overline{g}_\sigma}{1+\pi\Gamma+\Delta}$.

Case 3. $g_m = \overline{g}_m$. Then: $(1+\pi)g_Y = g_Z + \pi(\overline{g}_m + g_\sigma) = g - \Delta\overline{g}_m + \pi\overline{g}_m + \pi\widetilde{g}_\sigma - \pi\Gamma g_Y$, so that: $g_Y = \frac{g + (\pi-\Delta)\overline{g}_m + \pi\widetilde{g}_\sigma}{1+\Gamma\pi+\Delta}$.

Proposition 4 applies conditional on these expressions for growth rates.

B.6 Proof of Proposition 3

We consider a possibly nonlinear damage function $D(T_t)$ such that: $\log Z_t = \log Z_0 + gt - D(T_t)$. For brevity, we consider a unidimensional climate system, but our proof extends immediately to a multidimensional climate system.

B.6.1 Laissez-faire

The asymptotic behavior of temperature conditional on emissions is independent from the damage function. We thus recall:

- If $g_m < 0$, temperature T_t stabilizes.
- If $g_m = 0$, temperature grows log-linearly: $T_t = \theta \log t + \mathcal{O}(1)$
- If $g_m > 0$, temperature grows linearly: $T_t = t g_m \theta + \mathcal{O}(1)$.

We start from the accounting identities that hold away from a growth path: $g_Y = g_Z - \pi g_\chi$ and $g_Y = g_m + g_\chi + g_\sigma$, where we omit time subscripts on growth rates when unambiguous. Together, they imply: $g_m = g_Z - \omega$. In addition, we have: $g_Z = g - D'(T_t)\dot{T}_t$.

Case 1. $D'(T) \to 0$ as $T \to \infty$. If $g_m < 0$, $g_Z = g$. If $g_m = 0$, $|g_Z - g| = |D'(T_t)|\theta/t \to 0$. If $g_m > 0$, $|g_Z - g| = |D'(T_t)|\theta g_m| \to 0$. In all cases, technological growth dominates in the long run. In that case, climate damages have no long-run effect on growth rates, and the expressions from Proposition 1(i) apply regardless of the comparison between g and ω.

Case 2. $D'(T) \to +\infty$ as $T \to \infty$. We start with a few restrictions when $g > \omega$. Start from $g_m = g - \omega - D'(T_t)\dot{T}_t$. Then T_t must go to infinity. Indeed, otherwise if T_t is bounded above (and long-run dynamics are monotone), $\dot{T}_t = 0$ and $D'(T_t)$ converges to a constant, so that $g_m = g - \omega > 0$, a contradiction.

Case 2.1. $g_m > 0$. Then: $g_Z = g - D'(T_t)\theta g_m \to -\infty$. Hence $g_Y \to -\infty$, and so $g_m \to -\infty$, a contradiction. Thus, this case can never arise.

In addition, it emissions growth is not necessarily exponential but bounded below by a positive constant $g_{mt} > 0$, then we obtain the same contradiction as just above. Hence, emissions growth must be weakly negative (including zero) asymptotically. However, there can be positive growth at finite t, as long as the growth rate converges to zero. By the same token, we cannot have $g_{Mt} > 0$ bounded below, for the carbon stock.

Case 2.2. $g_m < 0$. Temperatures stabilize. Therefore: $g_Z = g - D'(T_t)\dot{T}_t$. Hence $g_Z = g$ in the long run, and so $g_m = g - \omega$. If $g - \omega < 0$, the equilibrium is compatible with Proposition 1(i), which therefore is the equilibrium. If $g > \omega$, we obtain a contradiction. Hence, $g > \omega$ is incompatible with $g_m < 0$ and with $g_m > 0$.

Thus, we now focus on the parametric case $g > \omega$. We must have strictly increasing temperature T_t that does not converge. We allow the emissions growth rate g_{mt} to depend on time. In the unidimensional climate system: $F_t = \overline{F} + h \log M_t$ and $\dot{T}_t = F_t - \overline{\lambda} T_t$. Therefore:

$$\dot{T}_t = \overline{F} + nh \log M_t - \overline{\lambda} T_t.$$

Since we operate under the case $\dot{M}_t / M_t = g_{Mt} \to 0$ from above, we guess and verify that, to leading order, the solution:

$$T_t = \frac{nh}{\overline{\lambda}} \log M_t \equiv a \log M_t,$$

is indeed compatible with $\dot{T}_t \to 0$. Let $a = \frac{\overline{\lambda}}{nh} = \frac{\lambda}{h}$ and $b = g - \omega > 0$. Then, to leading order: $a\dot{T}_t = \frac{\dot{M}_t}{M_t} = g_{mt}$. We thus have:

$$a\dot{T}_t = g_{mt} = b - D'(T_t)\dot{T}_t, \qquad \text{and so} \qquad (a + D'(T_t))\dot{T}_t = b.$$

Hence, to leading order:

$$aT_t + D(T_t) = bt.$$

Let $\overline{T}_t$ be such that $D(\overline{T}_t) = bt$. And let $T_t = \overline{T}_t + \widehat{T}_t$, with $\widehat{T}_t \ll \overline{T}_t$. Expanding the T_t equation, we obtain to leading order: $a\overline{T}_t + a\widehat{T}_t + D'(\overline{T}_t)\widehat{T}_t = 0$, and so:

$$\widehat{T}_t = -\frac{a\overline{T}_t}{a + D'(\overline{T}_t)} \qquad\qquad T_t = \overline{T}_t - \frac{a\overline{T}_t}{a + D'(\overline{T}_t)}.$$

We then obtain, to leading order:

$$g_{mt} = a\dot{T}_t = \frac{ab}{a + D'(T_t)} = \frac{ab}{a + D'(\overline{T}_t)} \to 0.$$

Thus, to leading order:

$$g_{Yt} = g_\chi + g_\sigma + g_{mt} = g_\chi + g_\sigma + \frac{ab}{a + D'(\overline{T}_t)} \to g_\chi + g_\sigma.$$

When $D(T) = \zeta T^{1+d}$, we obtain: $\overline{T}_t = \left(\frac{bt}{\zeta}\right)^{\frac{1}{1+d}}$. When $D(T) = \zeta e^{dT}$, we obtain to leading order: $\overline{T}_t = \frac{1}{d}\log t$.

B.6.2 Efficient Allocation

We start from the accounting identity that holds away from a growth path: $g_Y = g_Z - \pi g_\chi$.

Case 1. $D'(T) \to 0$ as $T \to \infty$. If $g_m < 0$, $g_Z = g$. If $g_m = 0$, $|g_Z - g| = |D'(T_t)|\theta/t \to 0$. If $g_m > 0$, $|g_Z - g| = |D'(T_t)|\theta g_m| \to 0$. In all cases, technological growth dominates in the long run. In that case, climate damages have no long-run effect on growth rates, and the expressions from the low emissions regime from Propositions 2 and 4 apply for all values of g, g_χ, g_σ.

Case 2. $D'(T) \to +\infty$ as $T \to \infty$.

Social cost of energy with growing emissions. We must now characterize the social cost of energy. Denote by $\overline{\zeta}_t = (1-\alpha)(1-\psi)D'(T_t)$ which is weakly rising over time. Our calculation holds regardless of the sign of g_m.

Then:

$$(\rho + \overline{\lambda} - g_\nu)\nu_t = -u'(C_t)Y_t\overline{\zeta}_t \qquad (\rho - g_\mu)\mu_t = \frac{nh\nu_t}{M_t} = -\frac{nhY_t\overline{\zeta}_t}{(\rho + \overline{\lambda} - g_\nu)C_t^\gamma M_t}.$$

We then obtain: $g_\nu = (1-\gamma)g_Y + g_\zeta$ and $g_\mu = (1-\gamma)g_Y + g_\zeta - g_M$, and so:

$$\mu_t = -\frac{nh}{(\rho + \overline{\lambda} - (1-\gamma)g_Y - g_\zeta)(\rho - (1-\gamma)g_Y - g_\zeta + g_M)}\frac{Y_t\overline{\zeta}_t}{C_t^\gamma M_t} \equiv -\frac{nh}{\mathcal{M}(g_Y, g_M, g_\zeta)}\frac{Y_t\overline{\zeta}_t}{C_t^\gamma M_t}$$

Recall the energy FOC: $\psi = \frac{\chi_t E_t}{Y_t} - \frac{E_t^m C_t^\gamma \mu_t}{Y_t}$. Then:

$$\frac{E_t^m C_t^\gamma \mu_t}{Y_t} = -\frac{nh}{\mathcal{M}(g_Y, g_M, g_\zeta)}\overline{\zeta}_t\frac{E_t^m}{M_t} = -\frac{nh\max\{g_m, 0\}}{\mathcal{M}(g_Y, g_m, g_\zeta)}\overline{\zeta}_t,$$

where the second equality uses the relationship between E_t^m and M_t when $g_m > 0$. Hence, the energy FOC becomes:

$$\left\{\psi - \frac{nh\max\{g_m,0\}}{\mathcal{M}(g_Y,g_m,g_\zeta)}\overline{\zeta}_t\right\}\frac{Y_t}{\chi_t E_t} = 1.$$

We denote $\Psi_t = \frac{nh\max\{g_m,0\}}{\mathcal{M}(g_Y,g_m,g_\zeta)}\overline{\zeta}_t$.

Case 2.1. $g_m > 0$. Then: $g_Z = g - D'(T_t)\theta g_m \to -\infty$. Hence $g_Y \to -\infty$.

If $\psi > \Psi_t$ at all times, then $g_m = g_Y + g_\chi + g_\sigma \to -\infty$ and we obtain a contradiction. If $\psi = \Psi_t$ after some time, then $g_m = \overline{g}_m$ and $g_Y = \overline{g}_m - g_\chi - g_\sigma$ is constant, a contradiction. Therefore, this case can never arise.

Case 2.2. $g_m < 0$. Temperatures stabilize. Therefore: $g_Z = g - D'(T_t)\dot{T}_t$. Hence $g_Z = g$ in the long run. As before, we are in low emissions regime, and so $g_m = g - \omega$. If $g - \omega < 0$, the equilibrium is compatible with the expressions from the low emissions regime from Propositions 2 and 4. If $g > \omega$, we obtain a contradiction. Hence, $g > \omega$ is incompatible with $g_m < 0$ and with $g_m > 0$.

We now focus on $g > \omega$. If $\psi > \Psi_t$ at all large times, the formulas from the laissez-faire apply and $g_{mt} \to 0$, $g_{Yt} \to g_\chi + g_\sigma$, and T_t grows to infinity. We must verify whether these conditions are compatible with the long run behavior of Ψ_t. We have to leading order:

$$\begin{aligned}
\Psi_t &= \frac{nh}{\mathcal{M}(g_{Yt},g_{mt},g_{\zeta t})}g_{mt}\overline{\zeta}_t \\
&= \frac{nh}{\mathcal{M}(g_\chi+g_\sigma,0,g_{\zeta t})}\frac{abD'(\overline{T}_t)}{a+D'(\overline{T}_t)} \\
&= \frac{anh}{\mathcal{M}(g_\chi+g_\sigma,0,g_{\zeta t})}(g-\omega) \\
&= \frac{n\lambda}{\mathcal{M}(g_\chi+g_\sigma,0,0)}(g-\omega)
\end{aligned}$$

with $g_{\zeta t} = \frac{D''(\overline{T}_t)}{D'(\overline{T}_t)}\dot{\overline{T}}_t = \frac{D''(\overline{T}_t)}{D'(\overline{T}_t)}\frac{b}{a+D'(\overline{T}_t)} = \frac{bD''(\overline{T}_t)}{\left(D'(\overline{T}_t)\right)^2} \to 0$, since, for damage functions that remain finite at all T we must have $D''(T)/(D'(T))^2 \to 0$.[9]

[9] If the limit is positive, solve the associated differential equation to obtain that D', and hence D, diverges

Let $\overline{\mathcal{M}} = \mathcal{M}(g_\chi + g_\sigma, 0, 0) = (\rho + \overline{\lambda} + (\gamma - 1)(g_\chi + g_\sigma))(\rho + (\gamma - 1)(g_\chi + g_\sigma))$. Then:

$$\Psi_t \to \overline{\Psi} \equiv \frac{n\lambda(g - \omega)}{\overline{\mathcal{M}}}.$$

So if $\psi > \overline{\Psi}$, we are in the laissez-faire regime. This condition becomes:

$$g - \omega < \frac{\psi\overline{\mathcal{M}}}{n\lambda} = \frac{\psi\rho(\rho + \lambda n)}{n\lambda}$$

If $\psi < \overline{\Psi}$, then the planner chooses g_{mt} so that $\psi = \Psi_t$ at large times. For brevity, we characterize it when $\gamma = 1$ so that $\mathcal{M}$ does not depend on g_Y.

We have $a\dot{T}_t = g_{mt}$. Thus, we have:

$$\psi\mathcal{M}\left(a\dot{T}_t, \frac{D''(T_t)}{D'(T_t)}\dot{T}_t\right) = anh\dot{T}_t D'(T_t).$$

Therefore:

$$\frac{anh}{\psi}D'(T_t)\dot{T}_t = \left(\widetilde{\rho} - \frac{D''(T_t)}{D'(T_t)}\dot{T}_t\right)\left(\rho - \left[\frac{D''(T_t)}{D'(T_t)} - a\right]\dot{T}_t\right).$$

with $\widetilde{\rho} = \rho + \overline{\lambda}$, and $anh = \overline{\lambda}$. We guess and verify that $\frac{D''(T_t)}{D'(T_t)}\dot{T}_t \to 0$. Under this guess, we have to leading order:

$$\left(\frac{\overline{\lambda}}{\psi}D'(T_t) - \widetilde{\rho}a\right)\dot{T}_t = \rho\widetilde{\rho}.$$

Thus, to leading order:

$$D'(T_t)\dot{T}_t = \frac{\psi\rho\widetilde{\rho}}{\overline{\lambda}} = \frac{\psi\rho(\rho + \overline{\lambda})}{\overline{\lambda}}.$$

This result then implies: $\frac{D''(T_t)}{D'(T_t)}\dot{T}_t \sim \frac{D''(T_t)}{(D'(T_t))^2} \to 0$ as T_t grows, and the guess is verified. Thus, to leading order we obtain:

$$g_{mt} = a\dot{T}_t = \frac{\psi\rho(\rho + \overline{\lambda})}{nh}\frac{1}{D'(T_t)} \to 0.$$

on a finite support.

From the production function and the definition of emissions, we obtain:

$$\begin{aligned}(1+\pi)g_{Yt} &= g - D'(T_t)\dot{T}_t + \pi(g_{mt} + g_\sigma) \\ &= g - \frac{\psi\rho(\rho+\overline{\lambda})}{\overline{\lambda}} + \pi(g_{mt} + g_\sigma) \\ &\to g - \frac{\psi\rho(\rho+\overline{\lambda})}{\overline{\lambda}} + \pi g_\sigma.\end{aligned}$$

Under our case $g > \omega$, we obtain in the long run:

$$\begin{aligned}(1+\pi)g_Y &= g - \omega + (1+\pi)g_\chi + g_\sigma - \frac{\psi\rho(\rho+\overline{\lambda})}{\overline{\lambda}} + \pi g_\sigma \\ &= g - \omega + (1+\pi)(g_\chi + g_\sigma) - \frac{\psi\rho(\rho+\overline{\lambda})}{\overline{\lambda}} \\ &= g - \omega - \frac{\psi\rho(\rho+\overline{\lambda})}{\overline{\lambda}} + (1+\pi)g_Y^{\mathrm{DE}}.\end{aligned}$$

Therefore:

$$g_Y^{\mathrm{SP}} = g_Y^{\mathrm{DE}} + \frac{g - \omega - \frac{\psi\rho(\rho+\overline{\lambda})}{\overline{\lambda}}}{1+\pi}.$$

In our calibration, $\frac{\psi\rho(\rho+\overline{\lambda})}{\overline{\lambda}} = 0.001$. Hence, as soon as $g > \omega + 0.001$, the planner achieves a strictly higher output growth rate than the laissez-faire.